

Silicification in the Ocean: from molecular pathways to silicifiers' ecology and biogeochemical cycles

Ivia Closset^{1,2}, J. Jotautas Baronas³, Fiorenza Torricella^{4,5}, Félix de Tombeur^{6,7}, Bianca T.P. Liguori⁸, Alessandra Petrucciani^{9,10}, Natasha Bryan¹¹, María López-Acosta^{12,*}, Yelena Churakova¹³, Antonia U. Thielecke^{11,*}, Zhouling Zhang⁸, Natalia Llopis Monferrer^{14,15}, Rebecca A. Pickering¹⁶, Mathis Guyomard¹⁷, Dongdong Zhu¹⁸

¹Finnish Meteorological Institute, Dynamicum Erik Palménin aukio 1, 00560 Helsinki, Finland

²Marine Science Institute, University of California Santa Barbara, Santa Barbara, CA, USA

³Department of Earth Sciences, Durham University, UK

⁴Department of Mathematics, Informatics and Geosciences, MIGe, University of Trieste

⁵Instituto of Polar Sciences, ISP-CNR, Bologna

⁶CEFE, Univ Montpellier, CNRS, EPHE, IRD, Montpellier, France

⁷School of Biological Sciences and Institute of Agriculture, The University of Western Australia, Perth, WA, Australia

⁸GEOMAR, Helmholtz Centre for Ocean Research, Kiel, Germany

⁹Dipartimento di scienze della vita e dell'ambiente, Università Politecnica delle Marche, Ancona, Italy

¹⁰CIRCC, Consorzio Interuniversitario Reattività Chimica e Catalisi, Italy

¹¹Alfred Wegener Institute Helmholtz Centre for polar and marine research, Germany

¹²Instituto de Investigaciones Marinas (IIM), CSIC, C/Eduardo Cabello 6, 36208 Vigo, Spain

¹³Centre for Ecology and Evolution in Microbial Model Systems (EEMiS), Linnaeus University, Kalmar, Sweden

¹⁴Sorbonne University, CNRS, UMR7144 Adaptation and Diversity in Marine Environment (AD2M) Laboratory, Ecology of Marine Plankton team, Station Biologique de Roscoff, Roscoff, France

¹⁵Monterey Bay Aquarium Research Institute, Moss Landing, CA, United States

¹⁶Department of Geological Sciences, Stockholm University, Stockholm, Sweden

¹⁷LOCEAN-IPSL, Sorbonne Université (SU, CNRS, IRD, MNHN), Paris 75005, France

¹⁸Key Laboratory of Marine Chemistry Theory and Technology, Ministry of Education, Ocean University of China, Qingdao 266100, China

Correspondence to: María López-Acosta (lopezacosta@iim.csic.es) and Antonia U. Thielecke (antonia.thielecke@awi.de)

Abstract. The oceanic silicon ([Si](#)) cycle has undergone a profound transformation from an abiotic system in the Precambrian to a biologically regulated cycle driven by siliceous organisms such as diatoms, Rhizaria, and sponges. These organisms actively uptake [siliconSi](#) using specialized proteins to transport and polymerize it into amorphous silica through the process of [biosilicification-biosilicification](#). This biological control varies depending on environmental conditions, influencing both the rate of silicification and its ecological function, including structural support, defence, and stress mitigation. Evidence suggests that silicification has evolved multiple times independently across different taxa, each developing distinct molecular mechanisms for [siliconSi](#) handling. This review identifies major gaps in our understanding of biosilicification, particularly among lesser-known silicifiers beyond traditional model organisms like diatoms. It emphasizes the ecological significance of these underexplored taxa and synthesizes current knowledge of molecular pathways involved in [siliconSi](#) uptake and polymerization. By comparing biosilicification strategies across taxa, this review calls for expanding the repertoire of model organisms and leveraging new advanced tools to uncover [siliconSi](#) transport mechanisms, efflux regulation, and environmental responses. It also emphasizes the need to integrate biological and geological perspectives, both to refine palaeoceanographic proxies and to improve the interpretation of microfossil records and present-day biogeochemical models. On a global scale, [siliconSi](#) enters the ocean primarily via terrestrial weathering and is removed through burial in sediments and/or authigenic clay formation. While open-ocean processes are relatively well studied, dynamic boundary zones – where land, sediments, and ice interact with seawater – are [nowadaysincreasingly](#) recognized as key [regulators-of-siliconinterfaces regulating global Si](#) fluxes, though they remain poorly understood. Therefore, special attention is given to the role of dynamic boundary zones such as the interfaces between land and ocean, the benthic zone, and the cryosphere, which are often overlooked yet play critical roles in controlling [siliconSi](#) cycling. By bringing together cross-discipline insights, this review proposes a new integrated framework for understanding the complex biological and biogeochemical dimensions of the oceanic [siliconSi](#) cycle. This integrated perspective is essential for improving global [siliconSi](#) budget estimates, predicting climate-driven changes in marine productivity, and assessing the role of [siliconSi](#) in modulating Earth’s long-term carbon balance.

1 Introduction

Silicon (Si) is the second most abundant element in the Earth’s crust after oxygen and plays a crucial role in a variety of biological and biogeochemical processes (Struyf et al., 2009; Tréguer et al., 2021). It is [an-essentiala](#) nutrient used by various terrestrial organisms, including plants and mammals, as well as a diverse range of marine life, such as unicellular diatoms and multicellular sponges (DeMaster, 2003; Farooq and Dietz, 2015). These organisms, collectively referred to as silicifiers, produce siliceous structures (also known as biogenic silica, bSi, or opal) through a biologically controlled process known as biosilicification- [\(in the context of this paper biosilicification and silicification are used interchangeably\)](#). These silicifiers modulate Si cycling in the ocean through Si uptake and [act](#) as vessels of Si sedimentation and burial. While diatoms have received [the](#) most attention in biosilicification research due to their ecological importance, abundance, and relative ease to maintain in culture, they are not the only marine silicifiers. Recent studies have highlighted the importance of other key groups

such as Rhizaria and sponges (Llopis Monferrer et al., 2020; López-Acosta et al., 2018; Maldonado et al., 2020). Silicon also contributes to other forms of biomineralization beyond siliceous structures made by silicifiers. It plays a role in the calcification of some coccolithophores (Durak et al., 2016; Ratcliffe et al., 2023a) and in the formation of silicified mouthparts in copepods (Naumova et al., 2015). In plants, Si is found at a wide range of concentrations and silicification contributes to the regulation of numerous biotic and abiotic stresses (Currie and Perry, 2007). Furthermore, the use of Si extends beyond eukaryotes, and it has been demonstrated that marine picocyanobacteria are able to accumulate important quantities of bSi (Baines et al., 2012). This growing body of work reveals that biosilicification is a widespread and evolutionary diverse phenomenon. Broadening our focus beyond diatoms is therefore essential to fully capture the complexity and global significance of biosilicification and its influence on the Si cycle in the ocean.

Particularly among non-model taxa such as protists, sponges, and picocyanobacteria, the physiological mechanisms underlying Si uptake, transport, and polymerization are still unknown, limiting our ability to generalize across taxa or predict functional responses to environmental change. Moreover, the role of silicifiers in shaping Si dynamics in the modern ocean and over geological timescales remains difficult to quantify. This is due to limited in situ measurements, unknown isotopic fractionation pathways, and the insufficient integration of biological diversity into global biogeochemical models. This includes a limited representation of how silicifiers influence other biogeochemical cycles, particularly the carbon (C) cycle, despite their major role in trapping ~~carbon~~C in surface waters and contributing to its long-term sequestration into the deep ocean via the biological pump (Laget et al., 2024; Ragueneau et al., 2006; Tréguer et al., 2018). Together, these knowledge gaps hinder our ability to assess how the Si cycle may respond to ongoing environmental changes, including global warming, ocean acidification, and shifts in nutrient availability.

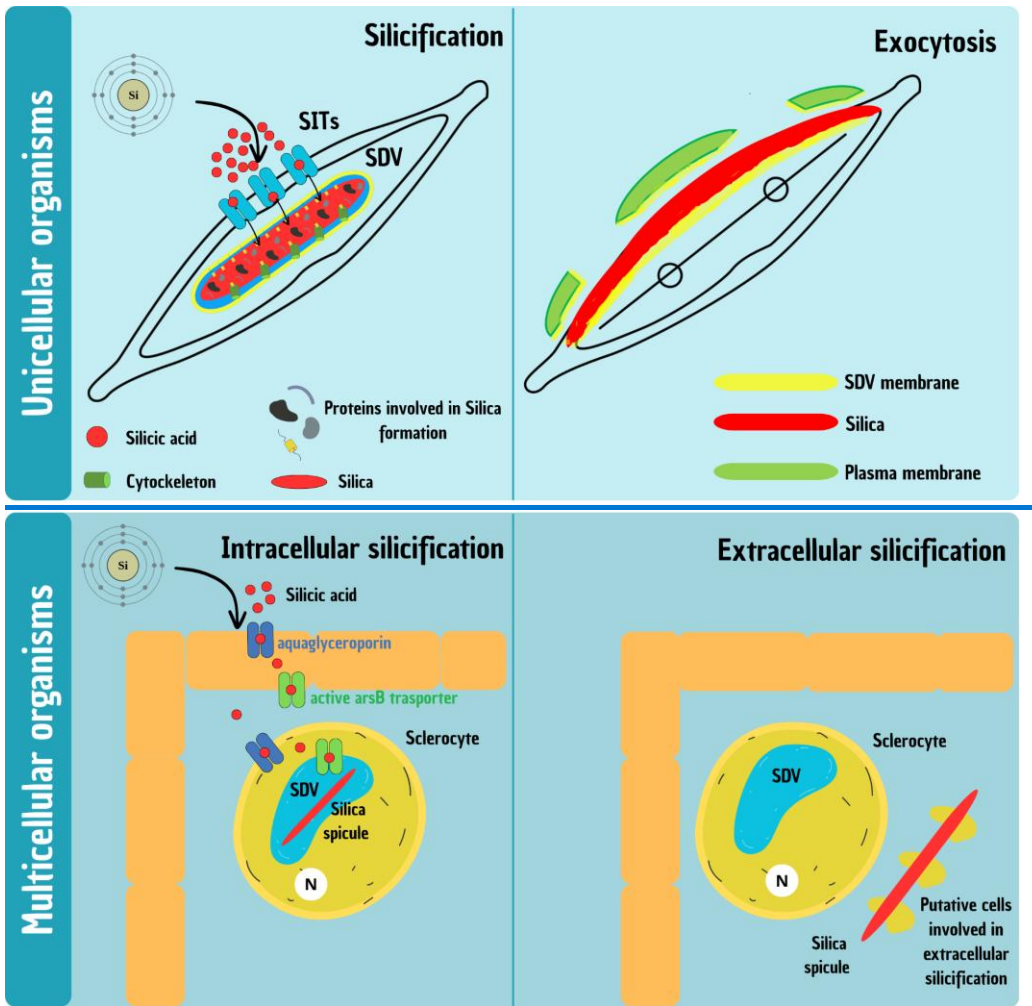
In celebration of the Ocean Science Jubilee, we — a group of early-career researchers specializing in biosilicification and Si cycling — have collaborated to produce this review, which synthesizes current understanding of biosilicification across diverse organisms and its influence on the global marine Si cycle. We summarize existing knowledge on Si transport and polymerization at the cellular and molecular levels, the biological functions of bSi, and the environmental and ecological factors that regulate biosilicification. We also explore the taxonomic diversity of marine silicifiers and assess their roles in Si cycling across geological timescales and the modern ocean. Where relevant, we include examples from terrestrial ecosystems to highlight similarities and differences with marine silicifiers and identify opportunities for cross-system knowledge exchange. In addition, we examine key marine Si cycling processes in the different Earth interface zones (i.e., land-ocean, sediment-ocean, and ice-ocean), which are often underrepresented in global models but play a pivotal role in Si transformation and fluxes. In doing so, we highlight how stable (^{29}Si and ^{30}Si) and radioactive (^{32}Si) isotopic tools have been instrumental in uncovering the contributions of these interfaces, as well as the broader biogeochemical impacts of silicifiers across time and space. Finally, we identify major knowledge gaps and unknowns across taxonomic, physiological, ecological, and biogeochemical domains, and propose a framework for future interdisciplinary research to address these challenges and advance our understanding of biosilicification and the global marine Si cycle.

2. Silicification: a widespread yet enigmatic process

Silicification involves the incorporation of inorganic Si, ~~primarily as orthosilicates~~, into living organisms to form silica structures. This form of biomineralization represents a remarkable feat of biological engineering, characterized by the precise precipitation of amorphous silica within specialized cellular compartments. In the ocean, Si is found in dissolved form as silicic acid, which is readily available for biological uptake by organisms. The silicification process in marine environments occurs at relatively low temperatures, typically ranging from a few degrees Celsius in deep waters or high latitudes to around 30°C in tropical surface waters. In contrast, synthetic silica formation in industrial or laboratory settings generally requires significantly higher temperatures and controlled conditions to facilitate precipitation and structural formation (De Tommasi et al., 2017). This stark difference highlights the efficiency of biological silicification, which occurs under ambient environmental conditions without the need for high temperatures or external catalysts (Livage, 2018).

Understanding ~~this process~~ silicification reveals the mechanisms by which organisms ~~control silica formation at the nanoscale, leading to the production of~~ produce highly intricate and functionally optimized structures (see **Box 1** for tools used to study biosilicification and Si uptake). Studying biological silicification not only deepens our knowledge of biomineralization and evolutionary adaptations but also has potential applications in biomimetic materials, nanotechnology, and sustainable engineering. Despite its broad distribution among marine lineages and the well-recognized benefits, such as protection from predation, light regulation, and enhanced structural support (Ghobara et al., 2019; Pančić et al., 2019; Petrucciani et al., 2022a), the specific requirements for Si and the mechanisms underlying its metabolism remains poorly defined in most living groups.

In marine environments, most work on silicification processes has focused on diatoms, admittedly due to their abundance and the relative ease of culturing them. In these organisms, silicification begins with the intracellular accumulation of ~~silicate~~ Si, which must reach a sufficiently high concentration (19–340 mM) for deposition (Kumar et al., 2020a). Dissolved silica (dSi) from the environment is transported across the plasma membrane into the cell and concentrated in specialized intracellular compartments called silica deposition vesicles (SDVs, **Fig 1**; Martin-Jézéquel et al., 2000) (~~Fig. 1~~), where controlled amorphous silica deposition occurs. Given the limited availability of dSi in modern oceans (ranging from under 2 µM in the surface water of central gyres to around 100 µM in polar regions; Tréguer et al., 1995) (~~ranging from under 2 µM in the surface water of central gyres to around 100 µM in polar regions~~), its uptake is considered the key step in silicification. While most studies have focused on dSi influx, an often-overlooked but crucial process is Si efflux from the cell, which helps prevent excessive intracellular Si accumulation that could lead to auto-polymerization and disrupt cellular function (Petrucciani et al., 2022b). Efflux has been proposed to operate through a mechanism similar to that of the influx but in reverse, although the role of sodium in this process remains unclear (Thamatrakoln et al., 2006).



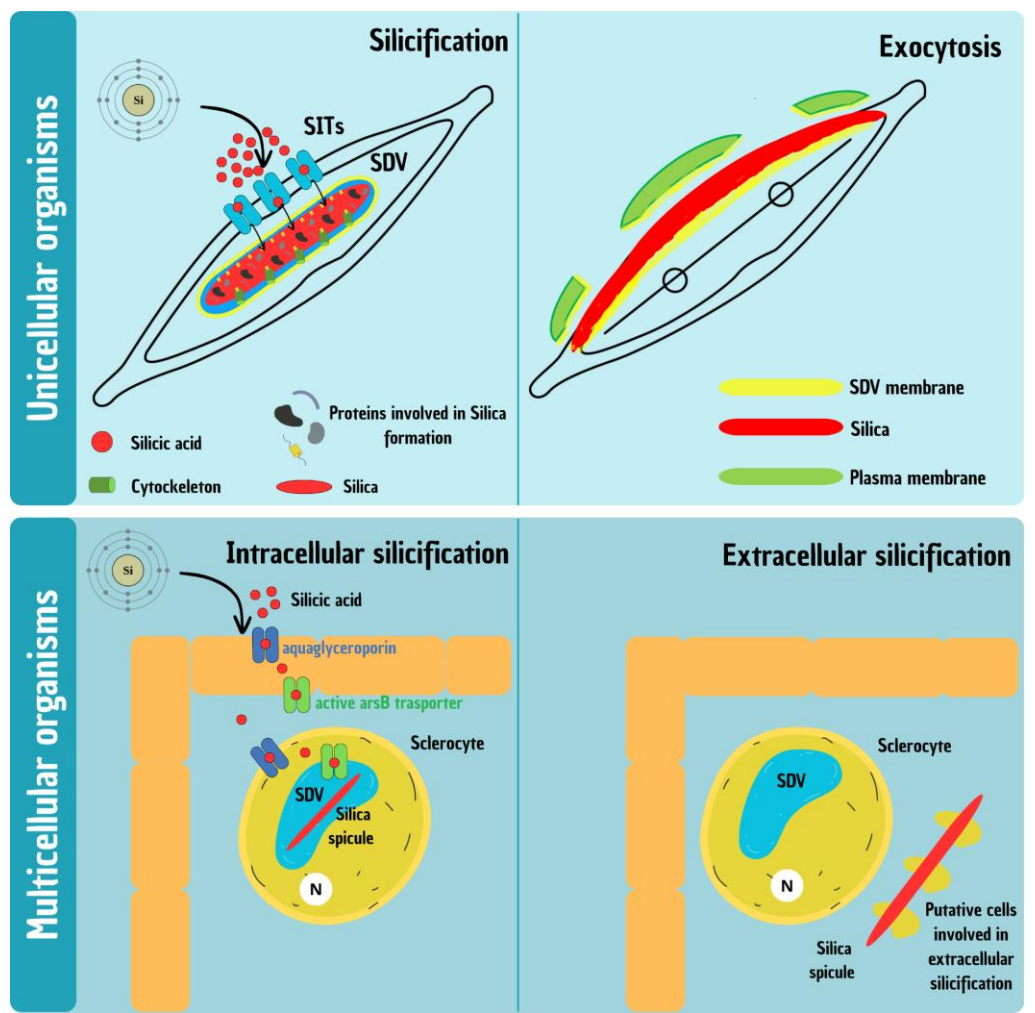


Figure 1. Schematic representation of the silicification process in unicellular and multicellular organisms. (Top) Silicification in unicellular organisms, illustrated with a model diatom. Two main phases are shown: intracellular formation (left) and exocytosis (right) of the silica-based cell wall. In the first phase, dSi is transported [via Si transporters \(SITs\)](#) into the membrane-bound silica deposition vesicle (SDV), where polymerization forms the intricate valve structure. In the second phase, the mature silica element is exocytosed: the distal SDV membrane and plasma membrane gradually detach from the newly formed silica and disintegrate in the extracellular space, while the proximal SDV membrane remains and functions as the new plasma membrane, forming the interface between the cell and its environment. (Bottom) Silicification in multicellular organisms, illustrated using Hexactinellid sponges. Two phases are also depicted: intracellular formation (left) and extracellular elongation (right). During the first phase, dSi is transported to the silica deposition vesicle (SDV) inside specialized cells called sclerocytes, where proteins and enzymes regulate silica polymerization to form spicules. Once spicules outgrow the cell, formation continues extracellularly, though the molecular and cytological mechanisms governing this phase remain largely unresolved.

While silicification in unicellular organisms like diatoms is relatively well understood, the process becomes significantly more complex in multicellular organisms. Unlike single-celled organisms, where dSi is directly taken up from the environment, in multicellular systems, it must traverse multiple cellular barriers before reaching the site for silica deposition (**Fig. 1**). For

example, in sponges, Si uptake and deposition involve several sequential steps. Sponges take up dSi from seawater through their outer epithelial cells and transport it internally across multiple cell layers to specialized silica-secreting cells called sclerocytes. Within sclerocytes, dSi is concentrated in [silica deposition vesicles \(SDV\), SDVs](#), where polymerization occurs to form silica spicules, the structural elements of the sponge skeleton (Maldonado et al., 2020). [The formation of long spicules, known as megascleres, is completed outside the cell, where silica is deposited externally.](#)

2.1 Silicon transport

Silicic acid, a small and uncharged molecule, can diffuse freely across membranes at environmentally relevant concentrations, making diffusion the main mode of uptake in diatoms (Thametrakoln and Hildebrand, 2008). However, the average surface seawater silicic acid concentration in marine environments is $10 \mu\text{mol L}^{-1}$ (Conley et al., 2017; Frings et al., 2016), which is relatively low compared to the amounts required for biomineralization. To overcome this limitation, diatoms rely on specialized protein-mediated active transport systems to efficiently take up and concentrate Si within the diatom cell, ensuring the formation of silica-based structures. This process is tightly regulated, with specific proteins preventing premature silica polymerization during the initial stages of silicification.

The first Si transporters (SITs) were identified in the pennate diatom *Cylindrotheca fusiformis* (Hildebrand et al., 1997). These sodium-coupled active transporters facilitate silicic acid uptake from the environment and exhibit variations in cellular localization, binding affinity and transport rates. Diatoms possess multiple SITs (Durkin et al., 2016) with distinct gene expression patterns, potentially corresponding to different silicification roles (Thametrakoln et al., 2006). Structurally, SITs typically contain 10 transmembrane domain segments (TMDs), arranged as two symmetrical 5 TMDs, and operate through a proposed transport model based on well-conserved [amino acid motif pairs](#): EGXQ and GRQ-~~motif pairs~~ (Thametrakoln et al., 2006), which are ~~short amino acid sequences~~ believed to play key roles in substrate recognition and translocation across the membrane. The hydroxyl group of silicic acid binds to the carbonyl group of the glutamine ~~belonging to a conserved GXQ in the EGXQ~~ motif in the SIT proteins, triggering a conformational change that allows silicic acid to pass through the membrane (Knight et al., 2016).

SITs have been identified in many eukaryotic supergroups, such as chrysophytes (Likhoshway et al., 2006) and choanoflagellates (Marron et al., 2013). These SITs, along with those from diatoms, are proposed to have evolved from SIT-like (SIT-L) proteins through duplication and fusion events (Knight et al., 2023; Marron et al., 2016). SIT-L proteins resemble half-completed variations of SITs, containing only 5 TMDs and a single EGXQ-GRQ motif pair, and likely originated in bacteria (Marron et al., 2016). Although SIT-Ls share structural similarities with SITs, their role in silicic acid uptake remains uncertain. This uncertainty is reinforced by the observation that eukaryotic lineages containing SIT-Ls tend to be less silicified than those with SITs (Hendry et al., 2018; Marron et al., 2016; Ratcliffe et al., 2023b). Recently, a SIT-L protein from the coccolithophore *Coccolithus braarudii* was confirmed to actively drawdown silicic acid in a heterologous system (Ratcliffe et al., 2023b). However, this study also suggests that SIT-Ls are less efficient transporters than conventional SITs, as their silicic

acid uptake remained undetectable even when using highly sensitive radioisotopic methods (^{32}Si) typically used to measure uptake of silicic acid in diatoms and Rhizaria (see **Box 1**).

While SITs and SIT-Ls play a crucial role in Si transport in unicellular silicifiers, the mechanisms governing this process in multicellular organisms appear to be fundamentally different, suggesting independent evolutionary pathways for silicification. In sponges, Si transport involves both passive and active transport mechanisms. Passive transport occurs via aquaglyceroporins, facilitating Si diffusion along its concentration gradient. Active transport is mediated by Na^+ -coupled co-transporters, enabling Si accumulation against its gradient. This dual transport system allows sponges to acquire dSi from seawater and transport it through the various cell barriers to the sites of spicule formation, where ~~dSi is concentrated to initiate silicification~~ polymerization is initiated (Maldonado et al., 2020).

Research on Si transport in marine macrophytes is rather limited, despite recent evidence that they may play a key role in marine Si biogeochemistry (e.g. macroalgae; Yacano et al., 2021)~~(e.g. macroalgae;~~. In seagrasses, a protein called Siliplant1 has been associated with the vesicular transport of silica into the apoplast, the network of cell walls and intracellular spaces outside the plasma membrane, facilitating its incorporation into the extracellular matrix (Kumar et al., 2020b; Nawaz et al., 2020). For example, in *Zostera marina*, this mechanism likely facilitates the deposition of amorphous silica within cell walls and intercellular spaces that can persist even after harsh chemical treatments like alkaline digestion (Roth et al., 2025). Despite such evidence of “active Si transport”, more research is needed to better understand and characterize Si accumulation in marine macrophytes. In this respect, research on terrestrial plant species may provide valuable information. In particular, the tremendous variation in plant Si accumulation between terrestrial plant species (e.g. in leaves, Si concentration ranges from negligible amounts to over 10% of dry weight; de Tombour et al., 2023b)~~(e.g. in leaves, Si concentration ranges from negligible amounts to over 10% of dry weight;~~ is classically attributed to the relative importance of passive and active transport (Liang et al., 2006). In short, the presence of specific influx and efflux channels encoded by specific genes would allow silicic acid uptake from the soil solution. Notably, a gene coding for cell-specific silica deposition has been recently identified in rice (Mitani-Ueno et al., 2023), shedding light on why certain taxa accumulate significantly more Si than others (Deshmukh et al., 2020; Hodson et al., 2005). However, such gene-based mechanisms remain poorly explored in marine plants. For instance, only a few proteins, such as Siliplant1, have been tentatively linked to Si transport in seagrasses (Kumar et al., 2020b; Nawaz et al., 2020), with homologues of other known Si transporter genes in plants yet to be found.

2.2 Silica polymerization

Extensive research has sought to understand how silicic acid is internalized by silicifying organisms. ~~However, the core of the silicification process lies in the polymerization of soluble silicic acid into amorphous silica, a transformation tightly regulated by biological mechanisms.~~ This process is still being actively studied to better understand its details, even though a lot of research has already been done in model diatoms (Hildebrand et al., 2018; Mayzel et al., 2021; McCutchin et al., 2025), as well as ~~more recently~~ in sponges (Shimizu et al., 2015, 2024; Wang et al., 2012), and plants (Kumar et al., 2017a, b, 2021;

Zexer et al., 2023). Silicification can occur intracellularly or extracellularly, but in all cases, specialized proteins guide the formation of silica into intricate nanoscale shapes.

Diatoms are characterised by their ability to exploit silicic acid to build a siliceous external cell wall, called a frustule. In diatoms, silica polymerization and ~~cell wall~~frustule synthesis occur within ~~specialized intracellular compartments known as silica deposition vesicles (SDVs), which are enclosed by a membrane called silicalemma.~~ These vesicles have been visualized using transmission electron microscopy but have yet to be biochemically isolated (Hildebrand et al., 2018; Hildebrand and Lerch, 2015). The internal environment of the SDVs is slightly acidic, facilitating the polymerization of silicic acid into a gel-like silica network (Iler, 1979). Once inside the cells, yet unidentified binding components –potentially ligands or proteins– are thought to maintain silicic acid in solution and prevent premature autopolymerisation, which occurs at concentrations exceeding 2 mM (Martin-Jézéquel et al., 2000). Although polymerization was long assumed to be restricted to SDVs, recent discoveries in certain diatom species with elaborate silica appendages suggest that silicification may also occur extracellularly (Mayzel et al., 2021).

Silicon polymerization in diatoms is finely controlled by specialized proteins, with silaffins being the most extensively studied. These small, lysine- and serine-rich peptides catalyse silica polymerization, and the morphology of the resulting silica structure depends on their concentration and specific combination (Kröger et al., 1999, 2002). Other key proteins include long-chain polyamines (LCPAs), which catalyse silica polymerization in the presence of polyanions, and silacidins, proteins rich in serine and acidic amino acids that catalyse silica formation in the presence of LCPAs (Wenzl et al., 2008). Additional proteins contribute to specific steps in the process: 1) Cingulins, which are rich in tryptophan and tyrosine, localize to the girdle bands of diatom frustules; 2) Ammonium fluoride insoluble proteins (AFIM) are hypothesized to serve as pattern-forming base layers, and 3) silicalemma associated proteins (SAPs), including Silicanin-1, probably function as intermediaries between the cytoskeleton and the SDV (Görlich et al., 2019; Kotzsch et al., 2017; Tesson et al., 2017).

Silica polymerization in sponges is also biologically regulated and occurs both intracellularly and extracellularly. Generally, intracellularly polymerization occurs within SDVs located in sclerocytes, ~~the specialized silica-secreting cells.~~ For : The formation of longer spicules ~~longer than ca. (i.e. 250-300 μm), known as megascleres, is completed outside the cell,~~ where silica is deposited externally (Schröder et al., 2007), ~~Initial formation begins inside the sclerocyte but continues extracellularly, beingis~~ transported out of the cell for further elongation, although the mechanisms underlying extracellular silicification remain poorly understood. Some studies suggest that sclerocytes may either release exosome-like, silica-rich vesicles (silicasomes) or physically migrate along the growing spicule, depositing silica directly without the need for protein mediation (Müller et al., 2013; Schröder et al., 2007; Wang et al., 2012). More recently, specific enzymes involved in extracellular silica deposition have been identified in hexactinellid sponges (Shimizu et al., 2024), suggesting a more complex and regulated process than previously assumed. However, some evidence also indicates that not all large hexactinellid spicules are completed extracellularly, challenging the assumption that size alone determines the transition from intra- to extracellular silicification (Mackie and Singla, 1997).

Most research on the enzymatic control of silica polymerization in sponges is relatively recent. The first enzyme identified in this process, silicatein, was described by Shimizu et al. (1998). Silicateins are cathepsin-like proteins that catalyze the hydrolysis and condensation of silicic acid, facilitating controlled silica polymerization (Müller et al., 2007; Riesgo et al., 2015; Wang et al., 2012). These enzymes regulate polymerization through their surface hydroxyl groups and exhibit species-specific variants that influence spicule morphology (Shimizu et al., 2015). Sponges also produce silicase, an enzyme that hydrolyzes silica under specific physiological conditions, potentially regulating silica solubility and remodeling during spicule growth (Ehrlich et al., 2010). Recent findings have identified additional proteins involved in silica polymerization, including silicatein-interacting proteins that modulate polymerization efficiency and structural integrity (Shimizu et al., 2024). Furthermore, collagen-like and lectin-like proteins may play auxiliary roles in silica deposition by modulating silica-protein interactions (Shimizu et al., 2024; Wang et al., 2012).

These biomineralization mechanisms evolved independently across the three classes of siliceous sponges. Demosponges rely on silicateins for silica deposition, whereas hexactinellid sponges lack silicateins and instead use hexaxilin for intracellular polymerization, along with glassin and perisilin for extracellular silica deposition that thickens spicules (Shimizu et al., 2015, 2024). Homoscleromorph sponges also display unique silica polymerization mechanisms, though the enzymes involved remain unidentified. The presence of unrelated enzymes in the Class Demospongiae and Hexactinellida, along with the distinct mechanisms observed in Homoscleromorpha, suggests that silicification has evolved multiple times independently in sponges (Shimizu et al., 2024). This convergent evolution underscores the adaptive significance of silica biomineralization in marine environments and highlights the diverse molecular strategies underpinning sponge silicification.

In plants, it is increasingly accepted that ~~beyond the simple effect of monosilicic acid concentration beyond saturation levels after water loss with transpiration,~~ some cell wall polymers and proteins can initiate and control silicification (Zexer et al., 2023). ~~Essentially, polymers carrying hydroxyl groups, such as hemicellulose, callose or lignin, may stabilize silicic acid, concentrate it, and favor its precipitation as amorphous silica. Beyond cell wall type silica, it seems that proteins can also favor silica deposits in cell lumens.~~ For instance, the deposits of silica in the so-called silica cells found in many grass species are thought to be controlled by a protein named Siliplant1 (Kumar et al., 2020b; Zexer et al., 2023). These works have been pivotal to further understanding plant silicification and its potential links to other silicifying organisms (Kumar et al., 2020a).

2.3. Environmental and ecological influences on silicification

While the regulated flow of silica ions ~~and precursors~~ is crucial for biomineralization, it is not the only factor determining this process. Biomineralization is influenced by a complex interplay of environmental and ecological conditions. Although most studies have again focused on diatoms, similar mechanisms likely occur in other silicifying organisms. Silica deposition depends directly on dSi availability, with its limitation resulting in reduced silicification (Brzezinski et al., 1990; McNair et al., 2018; Shrestha et al., 2012). Lower temperatures have also been associated with increased silicification in diatoms (Durbin, 1977). Additionally, under replete silica conditions, silicification tends to be inversely correlated with growth rate, suggesting that other growth-limiting factors, such as the availability of iron ($\text{Fe}^{2+}/\text{Fe}^{3+}$) and zinc (Zn^{2+}), may indirectly regulate frustule

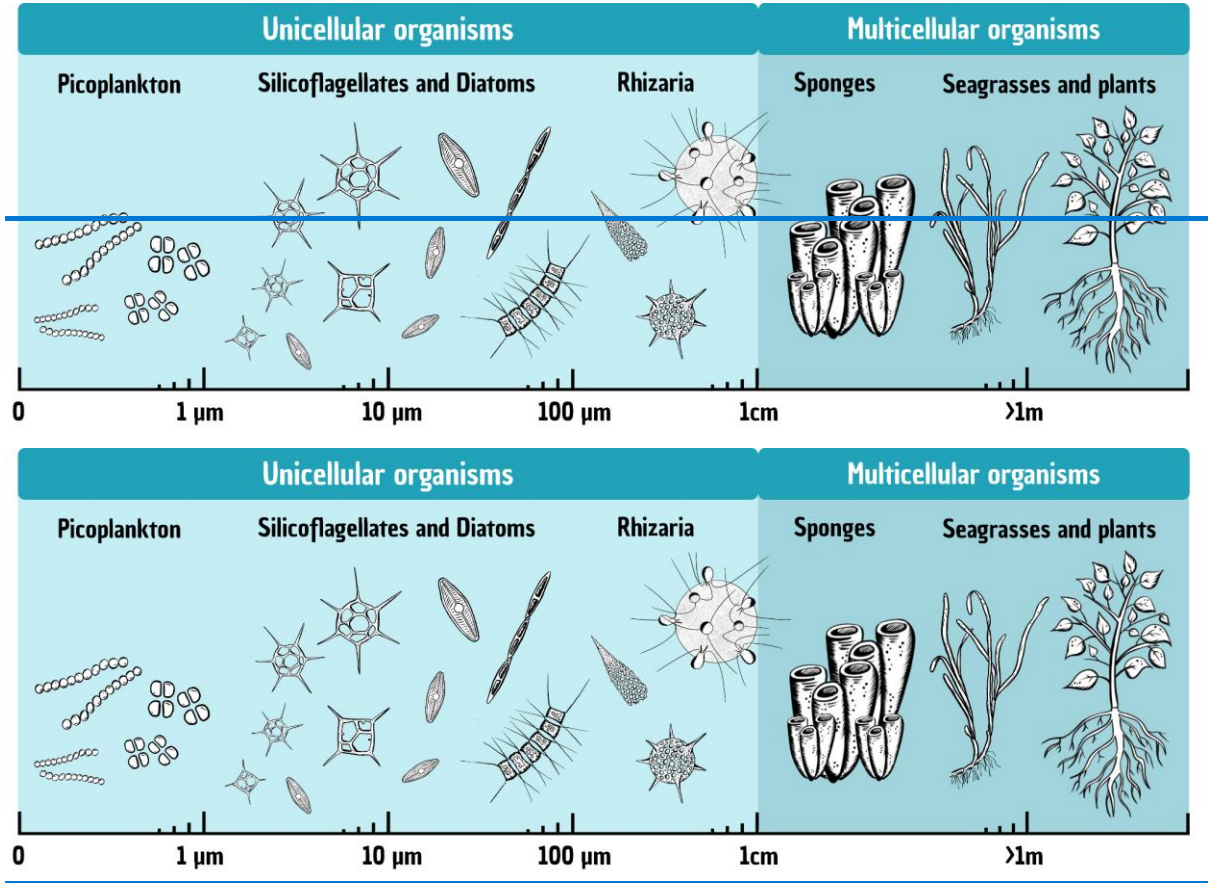
formation (Flynn and Martin-Jézéquel, 2000; Martin-Jézéquel et al., 2000). Light intensity further influences silicification in a complex manner, with increased silicification observed under both low (15 $\mu\text{mol photons m}^{-2} \text{ s}^{-1}$) and high (300 $\mu\text{mol photons m}^{-2} \text{ s}^{-1}$) light conditions (Petruciani et al., 2023; Su et al., 2018; Xu et al., 2021). Other environmental factors, such as salinity (Vrieling et al., 2007) and pH (Hervé et al., 2012), can also modulate silicification, emphasizing the intricate interplay between environmental conditions and biomineralization.

Beyond its biochemical and environmental determinants, silicification plays a fundamental ecological role for silicifying organisms contributing to their overall fitness. In diatoms, frustules act as protection against predators ~~thanks due~~ to high mechanical strength (Hamm et al., 2003). More heavily silicified diatoms are often rejected as food sources by copepods (Ryderheim et al., 2022), and increased silicification has been observed in response to predator presence (Petruciani et al., 2022a; Pondaven et al., 2007). This suggests that the trophic chain can influence biomineralization processes and affect Si bioavailability. Similarly, some sponge species allocate more resources to skeleton formation as a ~~defensed~~~~defence~~ strategy against predation, thereby enhancing their chances of survival (Ferguson and Davis, 2008; Rohde and Schupp, 2011). In terrestrial plants, silica deposition enhances resistance to herbivory by making leaves more abrasive and harder to digest (Hartley and DeGabriel, 2016; Massey et al., 2006). However, studies on silica-based ~~defenses~~~~defences~~ in seagrasses are currently lacking, and it remains unclear whether these marine plants use similar strategies.

3. Diversity of Marine Silicifiers

Over the past decade, research has transformed our understanding of the marine Si cycle by revealing that multiple groups of organisms contribute to silica dynamics, challenging the long-standing paradigm that diatoms were the sole important silicifiers. Historically, diatoms have been considered the primary drivers of bSi production and recycling in the ocean (Nelson et al., 1995; Tréguer et al., 1995; Tréguer and De La Rocha, 2013). However, recent studies have highlighted the significant role of other groups, such as Rhizaria and sponges (e.g. Laget et al., 2024; Llopis Monferrer et al., 2020; Maldonado et al., 2019)(~~e.g., while. Additionally,~~ many ~~additional~~~~other~~ taxa have been identified as interacting with Si (Baines et al., 2012; Churakova et al., 2023; **Fig. 2**;~~Fig. 2~~), however, their contributions to Si cycling have yet to be quantified on regional and global scales. Beyond their contributions to Si cycling, the ecophysiological functioning of these groups is often poorly understood. Understanding the taxonomic and functional diversity of silicifiers is not only crucial for ecological and evolutionary perspectives, but also provides essential inputs for functional trait models that incorporate silicic acid cycling and silicifying organisms (see also Box 3), thereby improving the predictive power of global biogeochemical models. For example, Naidoo-Bagwell et al. (2024) recently demonstrated this by extending the Earth system model cGEnIE with a diatom functional group, therefore requiring dSi, which improved the model's ability to reproduce observed nutrient fields, export production, and global distributions of diatoms. This expanding knowledge emphasizes the need to integrate multiple biological contributors

302 into the Si biogeochemical cycle to better understand its functioning and enhance our ability to predict the effects of climate
303 change and anthropogenic impacts (Tréguer et al., 2021).



304
305
306 **Figure 2. Total size range of silicifiers, from the smallest unicellular organisms (picoplankton) up to multicellular terrestrial plants.**

307
308 The following paragraphs provide an overview of the main groups of silicifiers, ordered by their average size ranges [and the](#)
309 [current state of the art regarding their ecology and contributions to Si and C cycling](#).

310
311 **3.1. Picoplankton**

312 Picoplankton is a broad size category encompassing all planktonic or floating organisms measuring under 2 μm, though this
313 is often extended to 3 μm due to the filter sizes used in field studies (Vaulot et al., 2008). The three main groups of picoplankton
314 include heterotrophic bacteria, autotrophic bacteria (picocyanobacteria from the genera *Prochlorococcus* and *Synechococcus*),
315 and autotrophic eukaryotes (picoeukaryotes), [with](#). Picocyanobacteria and picoeukaryotes [are](#) typically grouped together
316 under the moniker picophytoplankton. The discovery of large abundances of heterotrophic bacteria in the oceans, larger than

317 previously estimated, first put these tiny unicellular organisms on the map (Hobbie et al., 1977). Since then, picoplankton have
318 been discovered to be the base of the microbial food web, and their significant contributions in terms of biomass and
319 productivity make them influential players in global biogeochemical cycling (Azam et al., 1983; Falkowski et al., 2008; Le
320 Quéré et al., 2005).

321 Picoplankton are distributed widely in ~~oceans~~oceanic and freshwater environments, often described as ubiquitous or
322 cosmopolitan. However, different picoplankton groups fill different environmental niches. For example, *Synechococcus* and
323 picoeukaryotes prefer lower temperatures, while *Prochlorococcus* thrives in higher temperatures and lower latitudes
324 (Buitenhuis et al., 2012; Flombaum et al., 2020; Visintini et al., 2021). *Prochlorococcus* abundances are notoriously high in
325 oligotrophic (low nutrient) areas of the ocean, which can be explained by their competitive advantages (e.g. extremely small
326 size, high diversity; Biller et al., 2015)~~(e.g. extremely small size, high diversity;~~. Meanwhile, in nutrient-replete upwelling
327 areas picoeukaryote growth is favoured (Li et al., 2023; Painting et al., 1993). Additional environmental factors that can affect
328 picoplankton distribution patterns are light intensity and water mass events, as well as biological factors~~like;~~ such as the
329 presence of predatory microplankton and viruses (Fuhrman, 1999; Otero-Ferrer et al., 2018; Sieradzki et al., 2019). Models
330 predicting the impact of climate change on picoplankton suggest a global increase in picophytoplankton abundances,
331 particularly in areas like the Arctic ~~Ocean~~ and Indian ~~Ocean~~Oceans (Flombaum et al., 2020). In contrast, heterotrophic bacterial
332 biomass in surface waters is expected to slightly decline, though this decrease is minor compared to the predicted reductions
333 in microplankton and larger organisms (Heneghan et al., 2024; Kim et al., 2023). Overall, these findings indicate that future
334 oceans will be ~~dominated~~ increasingly dominated by picoplankton.

335 Picoplankton generally lack structural cellular components made of Si. However, some exceptions exist, such as *Triparma*
336 *laevis* from the class Bolidophyceae, a close relative of diatoms that can measure less than 3 µm in size (Booth and Marchant,
337 1987; Kuwata et al., 2018; Yamada et al., 2014). Nevertheless, there is strong evidence that picoplankton interact with dSi in
338 their environments regardless of whether or not they possess siliceous structures. Both extracellular and intracellular
339 incorporation of dSi has been observed in heterotrophic bacteria. In some species of the bacterium *Bacillus*, dSi uptake occurs
340 during an early stationary phase and is used for spore formation (Hirota et al., 2010). Environments where dSi is saturated,
341 particularly geothermal hot springs, are sites of extracellular silica polymerization in different bacterial species (Inagaki et al.,
342 2003; Lalonde et al., 2005; Phoenix et al., 2000). In the marine environment, *Synechococcus* cells from the Sargasso Sea were
343 found to harbour highly concentrated quantities of bSi (Baines et al., 2012). bSi accumulation and/or dSi uptake has been
344 demonstrated by marine *Synechococcus* strains in both the natural environment and in laboratory experiments (Aguilera et al.,
345 2025; Krause et al., 2017; Ohnemus et al., 2016).

346 The effect of dSi on picoplankton has generally been considered neutral, as *Synechococcus* growth rates do not change
347 when cultured in a wide range of dSi concentrations, though a new study demonstrates that high silicic acid concentrations can
348 have negative effects on cell physiology (Ou et al., 2025). bSi accumulation has also been demonstrated by cultures of marine
349 and brackish picoeukaryotes, including the smallest known marine eukaryote *Ostreococcus tauri* (Churakova et al., 2023).
350 Curiously, in freshwater, *Synechococcus* bSi accumulation was not observed, suggesting that *Synechococcus* strains in this

environment lack the same mechanism for dSi uptake or do not utilize dSi in ways similar to marine or brackish *Synechococcus* (Aguilera et al., 2025). A mechanistic explanation for Si uptake in these non-silicifying organisms can partially be explained by the SIT-Ls found in a limited number of bacterial and picocyanobacterial genomes (see **Section 2** and Marron et al., 2016)(~~see Section 2 and~~. However, in the majority of species and strains studied, the mechanisms by which picoplankton uptake and utilize dSi need further investigation and more relevant methodologies for studying picoplankton need development.

3.2 Silicoflagellates

Silicoflagellates are marine planktonic organisms belonging to the class Dictyochophyceae (Silva, 1982), order Dictyochales (Haeckel, 1887), which are characterised by a distinctive star-shaped silica skeleton (mostly 20–100 µm). They are exclusively marine unicellular protists; and mostly being considered photosynthetic, however, studies also show mixotrophic behaviour or non-photosynthetic bacteriivory (Eckford-Soper and Daughjerg, 2016; Gereá et al., 2016; Sekiguchi et al., 2002). They have chromatophores for photosynthesis, but also possess pseudopodia, a typical feature of zooplankton, further complicating their classification (Sheath and Wehr, 2003).

Almost all of their protoplasm is located inside the skeleton, which is composed of hollow tubular elements joined at triple junctions to create a tridimensional star-shaped structure constructed outside of the cytoplasm. They have a single flagellum situated at the anterior end of the cell, which extends outside the skeleton itself (Chang et al., 2017a). In culture, they have occasionally been observed to shed their skeletons, especially at high cell abundances, and continue swimming either as swimming-flagellated cells or as unflagellated; amoeboid cells. These cells can divide without cytokinesis and develop into multinucleate organisms (Henriksen et al., 1993; Van Valkenburg and Norris, 1970). This naked stage has since been described in nature and has been found to occasionally occur in significant blooms (Jochem and Babenerd, 1989; Moestrup and Thomsen, 1990). Reproduction occurs through binary fission (Van Valkenburg and Norris, 1970). In rare cases, the formation of double skeletons has been observed with the two skeletons joined at the basal ring (McCartney et al., 2014). Though other modes of reproduction have not been observed, the possibility of a sexual reproduction phase — similar to that of other phytoplanktonic organisms (e.g. diatoms) — cannot be ruled out. Silicoflagellate cell physiology remains largely understudied (Sancetta, 1990), partially due to challenges in maintaining them in culture. Despite the first successful culture in 1970 (Van Valkenburg and Norris, 1970), few cultures exist today, so individuals must be isolated from field samples for physiological experiments (Chang and Gall, 2016; Taguchi and Laws, 1985a).

Silicoflagellates first appeared in the Early Cretaceous (115 million years ago; McCartney et al., 2014)(~~115 million years ago;~~ and showed great diversification throughout the Cenozoic (<66 Ma) (McCartney et al., 1995, 2018). Their distinct skeleton structure and morphology are the basis for taxonomic identification (Malinverno, 2010) and due to their high abundance in sediments, they are used in micropalaeontology as proxies for palaeotemperature reconstructions (see **Box 2** for further details). In the modern ocean, silicoflagellates are thought to be composed of four extant genera (~~the~~ *Dictyocha* (Ehrenberg, 1837), *Octactism* (Schiller, 1925), *Vicicitus* (Chang et al., 2012), and *Stephanocha* (Jordan and McCartney, 2015).

However, as there is strong variability and plasticity in the skeleton (Dumitrica, 2014; McCartney et al., 2014; Van Valkenburg and Norris, 1970), in addition to the presence of the naked stage, this has led to considerable controversy regarding the number of species and genera (Chang et al., 2012, 2017a; Jordan and McCartney, 2015).

The abundances of different silicoflagellate species are influenced by variations in temperature and salinity, both in cultures (Henriksen et al., 1993; Van Valkenburg and Norris, 1970) and natural environments (Hernández-Becerril and Bravo-Sierra, 2001; Ignatiades, 1970; Rigual-Hernández et al., 2016; Sancetta, 1990). However, the responses of individual species to these environmental factors are not always consistent (Sancetta, 1990). Additionally, Maliverno et al. (2010) demonstrated that the same species, *Stephanocha speculum*, can present different varieties linked to their precise ecological niches, with some varieties (*S. speculum* var. *monospicata*, var. *bispicata*, and var. *speculum*) being found in open ocean conditions, while *S. speculum* var. *coronata* is associated with sea ice cover.

Silicoflagellates are most abundant in nutrient-rich areas of the ocean at high latitudes (Fagerness, 1984; Henriksen et al., 1993; Onodera et al., 2016; Takahashi et al., 2009) and in upwelling systems (e.g. Hernández-Becerril and Bravo-Sierra, 2001; Murray and Schrader, 1983; Sancetta, 1990). Their [carbonC](#) uptake rates have been shown to be comparable to other phototrophic phytoplankton (e.g. for *Dictyocha perlaevis*; Taguchi and Laws, 1985b), though there are no studies to date comparing different species of silicoflagellates or changes in environmental conditions. Despite occasional high abundances, they are mostly considered insignificant contributors to primary production, planktic dynamics, and export fluxes. For example, in the Arctic Ocean, [while](#) they have been shown to contribute less than 1% of the flux of particulate organic [carbonC](#) (Onodera et al., 2016). ~~However,~~ they are regionally important prey for different copepod and krill species (Nakagawa et al., 2002; Passmore et al., 2006; Pasternak and Schnack-Schiel, 2001) as well as gelatinous grazers (Hiebert et al., 2025). Some species of silicoflagellates (e.g. *Dictyocha* spp.) have additional ecological significance through their role as harmful algae bloom (HAB) species with significant ichthyotoxicity (Esenkulova et al., 2020; Henriksen et al., 1993).

While the ecological relevance of silicoflagellates has been recognised, their mechanisms of silicic acid uptake remain unexplored, and their contribution to the Si and [carbonC](#) cycles has yet to be quantified. While [some previous](#) studies focused on quantifying the regional contribution of silicoflagellates to Si export (Takahashi, 1989), their role in global Si cycling is entirely unconstrained (Tréguer et al., 2021).

3.3. Diatoms

Diatoms are a greatly diversified group of eukaryotic phytoplankton (Bacillariophyceae) belonging to the supergroup Stramenopiles (Bowler et al., 2010). They were first observed in 1703 (Round et al., 1990) and, since then, have attracted scientific interest across multiple disciplines, from taxonomists, oceanographers, [and](#) geologists, [to more recently](#) engineers, and chemists, establishing them as the by far best-studied group of marine silicifiers. [To date around 18,000 species of diatoms have been described, while their total diversity is estimated between 100,000 to 200,000 genera](#) (Jeong and Lee, 2024; Mann and Vanormelingen, 2013). These photoautotrophic unicellular microorganisms are ubiquitous and can be found in all aquatic

environments, including in sea ice ~~and in~~ soils, lichens, biofilms, and airborne; denoting their extensive adaptive capabilities (Lohman, 1960).

~~Diatoms are characterised by their ability to exploit silicic acid to build a siliceous shell called a frustule.~~ Diatom taxonomy is based on frustule morphological traits and categorizes the species in two groups based on cellular symmetry: centric diatoms, with a radial symmetry, and pennate diatoms, with an elongated and bilateral symmetry (Round et al., 1990). Diatoms are thought to be secondary endosymbionts (Gentil et al., 2017; Morozov and Galachyants, 2019), meaning that their precursor was a eukaryote that phagocytized another eukaryote (which became an organelle), resulting in chloroplasts surrounded by 4 membranes. The earliest known fossil record of diatoms is still widely debated (Brylka et al., 2023)~~(Brylka et al., 2023),~~ but molecular clock and sedimentary evidence suggest an ~~earlier~~ origin, near the Triassic-Jurassic boundary (Nakov et al., 2018)~~(Nakov et al., 2018),~~ when a greater availability of niches occurred. The gap in fossil records during this period has been hypothesized to relate to non-silicified or lightly silicified diatoms (Armbrust, 2009).

Diatoms are key primary producers in ~~the oceans~~ nowadays ~~oceans~~ and their ability to adapt to different environmental conditions allows them to outcompete other phytoplanktonic groups during blooms. They are highly efficient primary producers constituting 40% of marine primary production or 20–25% of global Earth's primary production, despite representing only 1% of Earth's photosynthetic organic biomass (Falkowski et al., 2004; Field et al., 1998). ~~The~~ Their intricate frustules provide improve ~~diatom~~ fitness compared to other microorganisms (Martin-Jézéquel et al., 2000) including but not limited to providing mechanical protection, allowing hydrodynamic control of particle diffusion and advection, or increasing photosynthetic efficiency.

Nutrient uptake in diatoms is facilitated by their large vacuoles, which store essential elements like nitrogen (N) and Si. This storage capacity supports rapid growth during favourable conditions, contributing to their ecological success (Behrenfeld et al., 2021). Diatoms reproduce asexually through mitotic division, which progressively reduces cell size due to the constraints of their rigid siliceous frustules. During each division, the daughter ~~cells inherit~~ cell inherits one parental valve and ~~form~~ forms a new, smaller valve within it, leading to a gradual decrease in cell dimensions over successive generations (Jewson, 1997). When cells approach a critical minimum size threshold, sexual reproduction is triggered to restore maximal cell dimensions. This process involves the formation of auxospores, specialized zygotic cells that expand and produce the initial large vegetative cells for the next cycle (Chepurnov et al., 2002). Auxospore formation is influenced by environmental factors such as light, nutrient availability, and cell density, as well as endogenous chemical signals (Assmy et al., 2006; Mouget et al., 2009). The interplay between asexual size reduction and sexual size restoration ensures diatom populations maintain their ecological and evolutionary success. This unique life cycle strategy contributes to their adaptability and widespread distribution in aquatic ecosystems.

~~Their ecological success marks diatoms as important contributors of biogeochemical cycles. Globally, diatoms produce approximately 255 Tmol Si yr⁻¹ of bSi, with regional variations influenced by nutrient availability and oceanic regimes. Coastal areas exhibit silica production rates 3–12 times higher than the global average, while oligotrophic gyres show rates 2–4 times lower. Nutrient limitation, particularly of Si, iron, and nitrogen~~ Nutrient limitation, particularly of Si, Fe, and N, is a

key driver of diatom growth and silica production. In oligotrophic gyres, low dSi concentrations (0.9–3.0 μM) limit silica production, despite rapid diatom growth rates. In nutrient-rich zones, diatom blooms significantly enhance silica and [carbonC](#) export, with Si:C ratios ranging from 0.09 to 0.15 depending on species and environmental conditions (Brzezinski, 1985). Their regionally high abundance and ubiquitous distribution make them a key source of organic [carbonC](#) for higher trophic levels, including zooplankton and fish larvae. Moreover, diatoms are an important vector for [carbonC](#) export (~20-40%; Jin et al., 2006) ~~(~20-40%)~~ due to their ability to form aggregates and their dense frustule, which improves sinking. As they sink, they rapidly transport organic matter to deeper ocean layers, and eventually are sequestered in sediments over geological time scales thanks to their siliceous frustules that enhance their preservation within the sedimentary records. Due to the well-defined ecological niches occupied by individual diatom species, their fossil assemblages serve as a reliable proxy for reconstructing past environmental conditions and tracking climate evolution (see **Box 2** and e.g. Crosta et al., 2021; Torricella et al., 2025) ~~(see Box 2 and e.g.~~.

3.4 Siliceous Rhizaria

Rhizaria, a diverse ‘supergroup’ of unicellular eukaryotes, represents a fascinating and largely unexplored realm of biodiversity (Burki and Keeling, 2014). This supergroup is subdivided in three phyla: Endomyxa, Cercozoa, and Retaria. A key unifying morphological feature within these phyla is the production of very fine pseudopodia, often numerous, and typically supported by microtubules called filopodia (Adl, 2024). The major taxa of siliceous Rhizaria are represented by organisms belonging to the Cercozoa and Retaria phyla. Among Cercozoans with skeletons, those belonging to the Thecofilosaria, especially the Phaeodaria, possess skeletons that take the form of spicules or bars, which vary in size and shape. Although Phaeodaria were traditionally classified as Radiolaria due to morphological similarities, molecular phylogenetic analyses have demonstrated that they are not closely related to Radiolaria and are instead affiliated with the Cercozoa (Nikolaev et al., 2004). The phylum Retaria includes organisms with skeletons of various compositions, and is divided into Foraminifera and Radiolaria. The skeletons of Foraminifera are primarily made of calcium carbonate, while Radiolaria exhibit skeletons of various nature, including strontium sulfate (exclusive to the Acantharia class) or opaline silica (found in the Polycystine and Sticholonche classes).

Phaeodaria and Radiolaria, both characterized by an intricate siliceous skeleton, exhibit a remarkable range of lifestyles (solitary and colonial) and trophic diversity (heterotrophic or mixotrophic with photosynthetic symbionts). They also present great morphological variability, with sizes spanning from a few tens of micrometres to several millimetres, [a gigantic sizessize](#) for protists. A key structural distinction lies in their skeletons. While Radiolaria skeletons are composed of robust, solid amorphous silica, Phaeodaria skeletons are hollow (Takahashi, 1983). Among the Polycystine Radiolaria, Spumellaria and Nassellaria are the most extensively studied groups, largely due to their robust skeletons and continuous fossil record dating back to the early Cambrian (De Wever et al., 2001). Spumellaria are characterized by concentric, generally spherical skeletons and were the first to appear in the Cambrian period. In contrast, Nassellaria display bilateral symmetry and possess conical skeletal structures with a limited number of spicules, first emerging in the Early Triassic (Anderson, 2001). Nassellaria are

also known for their ability to form colonies, such as those seen in Collodaria, or large solitary skeletons, such as those of Orodaria (Nakamura et al., 2021).

Siliceous Rhizaria are widely distributed across the world's oceans, from tropical to polar regions, and are especially abundant in open-ocean environments. These protists are commonly found in the upper layers of the ocean, where sunlight supports the photosynthetic symbionts hosted by many Rhizaria species (Decelle et al., 2021). However, they are also well represented in deeper zones, including the mesopelagic (Biard and Ohman, 2020). Global assessments indicate that Rhizaria play a substantial role in zooplankton abundance, contributing up to 33% (Biard et al., 2016). More recent studies, also using advanced imaging techniques to quantify large Rhizaria, indicate that they represent up to 1.7% of mesozooplankton ~~carbon~~^C biomass within the upper 500 m of the water column (Laget et al., 2024). Interestingly, Rhizaria biomass, particularly that of Phaeodaria, is more than twice as high in the mesopelagic than in the epipelagic layer (Laget et al., 2024). In marine ecosystems, Rhizaria have also been shown to dominate the eukaryotic community captured in sediment trap samples collected below the euphotic zone, as revealed by metabarcoding analyses (Gutierrez-Rodriguez et al., 2019; Preston et al., 2020).

The reproductive biology of Rhizaria remains poorly understood, primarily due to the challenges of maintaining most species under laboratory conditions. Although various life stages and lineage-specific cellular innovations have been observed in natural environments, their functional roles, as well as their physiological and ecological significance, remain largely uncharacterized (Rizos et al., 2024). Evidence suggests that both sexual and asexual reproduction occur across different Rhizaria lineages. Sexual reproduction involves the production and release of haploid gametes, which fuse to form a zygote with genetic material from both parent organisms. Asexual reproduction occurs by cell division during mitosis, resulting in two identical organisms. In colonial forms, asexual growth may occur through fission of the central capsules, contributing to colony expansion or fragmentation into multiple new colonies. In several species, reproduction involves the release of numerous flagellated swarmer cells that are considered to be gametes, produced via multiple nuclear divisions within the parent cell. These swarmers are released simultaneously and are presumed to fuse into zygotes, although the exact mechanisms of gamete fusion and early development remain poorly understood (Suzuki and Not, 2015). While the early ontogenetic stages are still not fully documented, the process of skeletal formation during growth has been extensively studied in several species under laboratory conditions (Anderson, 2001).

The widespread distribution of siliceous Rhizaria across marine ecosystems underpins their ecological importance in both food web dynamics and biogeochemical cycles. As basal components of planktonic communities, they serve as essential food sources and can act as vectors for energy transfer to higher trophic levels. Many Rhizaria host photosynthetic symbionts, enhancing primary production in oligotrophic waters (e.g. Llopis Monferrer et al., 2025)~~(e.g.~~. For instance, Collodaria are particularly abundant in nutrient-poor, tropical epipelagic zones and contribute significantly to zooplankton biomass (Faure et al., 2019). In deeper waters, Rhizaria play an important role in transforming sinking particles and serve as a key source of organic ~~carbon~~^C in the mesopelagic zone (Laget et al., 2024; Lampitt et al., 2023). Their ecological significance extends to the Si cycle, as many Rhizaria species take up silicic acid from seawater to build their intricate skeleton (Llopis Monferrer et al., 2020) contributing ^{up} to approximately 20% of the bSi production in the global ocean (Tréguer et al., 2021). Through both

biological uptake and export, Rhizaria facilitate the vertical transport of silica and [carbon](#) to the deep ocean, reinforcing their role in long-term elemental cycling (Biard et al., 2018; Stukel et al., 2018). The opaline silica skeletons they produce also contribute to a rich and continuous fossil record since the Cambrian, more than 500 million years ago (**Box 2**; De Wever et al., 2001).

3.5 Sponges

Sponges belong to the phylum Porifera, which comprises approximately [9,750](#) species classified into four distinct classes: Demospongiae, Calcarea, Hexactinellida, and Homoscleromorpha (Hooper and Van Soest, 2002; de Voogd et al., 2025). The largest and most diverse class, Demospongiae, accounts for nearly 84% of all known sponge species. The remaining species are distributed among the classes Calcarea (8%), Hexactinellida (7%), and Homoscleromorpha (1%; Van Soest et al., 2012). Sponges have been part of marine fauna since the late Precambrian (890-[540 Ma](#)) and are among the earliest known multicellular organisms on Earth (Wörheide et al., 2012). Since the Early Cambrian, many sponges have evolved siliceous skeletons, a trait present in over 80% of extant species (Neuweiler et al., 2014). These sessile filter feeders inhabit a vast range of marine habitats, from intertidal zones to the deep sea, across all latitudes (Maldonado et al., 2017; Van Soest et al., 2012). While some species have broad distributions, others are highly specialized, restricted to specific substrates or environmental conditions such as deep-sea sponge reefs, coral-associated habitats, or high-silica environments.

Due to their ubiquity and substantial biomass, sponges are increasingly recognized as key functional components of ocean ecosystems (Bell, 2008; Bell et al., 2023; Folkers and Rombouts, 2020). Their complex body structures provide habitat for a diverse array of sessile and mobile organisms, making sponge-dominant communities biodiversity hotspots (Beazley et al., 2013; Klitgaard, 1995). Additionally, sponges contribute significantly to biogeochemical cycling by filtering and recycling dissolved organic and inorganic matter and nutrients, thereby influencing the fluxes of essential elements such as [carbon](#), [nitrogen](#), [phosphorus](#), [N](#), [P](#), and Si (Busch et al., 2022; De Goeij et al., 2013; Maldonado et al., 2012).

Sponges reproduce both sexually and asexually. In sexual reproduction, gametes are released into the water column for external fertilization, although some species exhibit internal fertilization (Maldonado and Riesgo, 2008). Asexual reproduction occurs through budding, fragmentation, or gemmule formation, contributing to their resilience in dynamic environments (Battershill and Bergquist, 1990). Sponges exhibit a biphasic life cycle, alternating between a pelagic larval stage and a sessile adult stage. Larvae are typically short-lived, ranging from hours to a few days, and rely on passive dispersal by ocean currents (Maldonado and Abdul Wahab, 2025). Upon settlement, larvae undergo metamorphosis into juvenile sponges, attaching to a substrate where they develop into mature, filter-feeding adults. Sponges generally live for several years to decades, with some species known to survive even for centuries (Leys and Lauzon, 1998; McGrath et al., 2018; McMurray et al., 2008).

For decades, the role of sponges in Si cycling was considered negligible. However, recent research has demonstrated their significant contribution at both regional and global scales (López-Acosta et al., 2022; Maldonado et al., 2019, 2021). Siliceous sponges actively assimilate large amounts of dSi, transforming it into bSi for skeletal formation. Upon their death, this silica can either dissolve back into the water column, sustaining other silicifiers, or be buried in sediments, influencing long-term

silica sequestration. This process is particularly relevant in deep-sea sponge grounds and continental shelf ecosystems, where sponges are particularly abundant and act as major reservoirs facilitating benthic-pelagic coupling of the Si cycle (Tréguer et al., 2021). Furthermore, sponge-mediated Si cycling interacts with other major biogeochemical cycles such as those of [carbonC](#) and [nitrogenN](#), as sponge excretion and microbial symbionts further contribute to matter and nutrient transformations (Busch et al., 2022; Maldonado et al., 2012).

3.6 Plants

In the last two decades, an important number of functions has been assigned to leaf silicification (Cooke and Leishman, 2016; Johnson et al., 2024; de Tombeur et al., 2023b), including for wetland and aquatic plants (Schoelynck et al., 2012; Schoelynck and Struyf, 2016). ~~Concentrations of Si in wetland and aquatic plant species are highly variable, and can sometimes reach very high values. For instance, concentrations of Si in yellow water lily (*Nuphar lutea*) can go up to 8% in some individuals.~~ Interestingly, species that are emergent (only basal stem parts in the water) and submerged tend to accumulate more Si compared with species that mostly have floating organs (Schoelynck and Struyf, 2016). ~~Such difference has been interpreted as resulting from the structural role of silicification.~~ In emergent and submerged species, silicification could be used to increase strength in order to overcome different physical stresses (gravity, horizontal force, etc.; Schoelynck and Struyf, 2016). ~~(gravity, horizontal force, etc.).~~ In floating species, on the contrary, silicification ~~would be considered~~ less important because they are less impacted by hydrodynamics forces (Schoelynck and Struyf, 2016). ~~Such link between silicification and physical stress is supported by evidence of trade-offs with others C-based structural components, such as cellulose and lignin, and by links between wind speed and Si accumulation in terrestrial herbaceous species.~~ Beyond the structural role of Si in wetland and aquatic species, Si is also used for [better](#)-resisting herbivory. For instance, the bSi concentration of different *N. lutea* individuals is negatively correlated with the damages caused by *Galerucella nymphaeae* (Schoelynck and Struyf, 2016). Whether silicification is an adaptation or exaptation to grazing is, however, still debated (de Tombeur et al., 2023b). While trait-based approaches have recently advanced our understanding of silicification strategies in plants, applying similar frameworks to other marine silicifiers such as diatoms remains challenging due to fundamental differences in morphology and silica utilization patterns (see **Box 3**).

In coastal systems, seagrass meadows provide vital ecological services, including nutrient cycling and climate regulation, and may influence Si dynamics in estuarine and marine environments. Despite their ecological importance and proximity to riverine Si inputs, the role of seagrasses in the Si cycle remains understudied. While the elemental composition of seagrass leaves has been widely analysed for macronutrients like [nitrogenN](#) and phosphorus, only a few studies have quantified Si concentration in seagrass (see Herman et al., 1996; Roth et al., 2025; Vonk et al., 2018) ~~(see~~, leaving an important gap in understanding their role in biogeochemical Si cycling. The mechanisms of Si accumulation in seagrasses are not yet fully understood, but recent research in *Zostera marina* has identified phytoliths in its roots, stems, and leaves (Rong et al., 2024) and suggests a functional dSi uptake pathway involving the Slp1 protein and vesicular transport (Kumar et al., 2020b; Nawaz et al., 2020). By measuring bSi in four families of seagrass species, Vonk et al. (2018) showed that *Z. marina* tends to

584 accumulate more silica than other seagrasses, though still less than freshwater vegetation. This species displays a relatively
585 low bSi content but may still play a significant role in coastal Si cycling, especially since some of its Si resists dissolution and
586 could buffer the transport of dSi to the ocean (Roth et al., 2025).

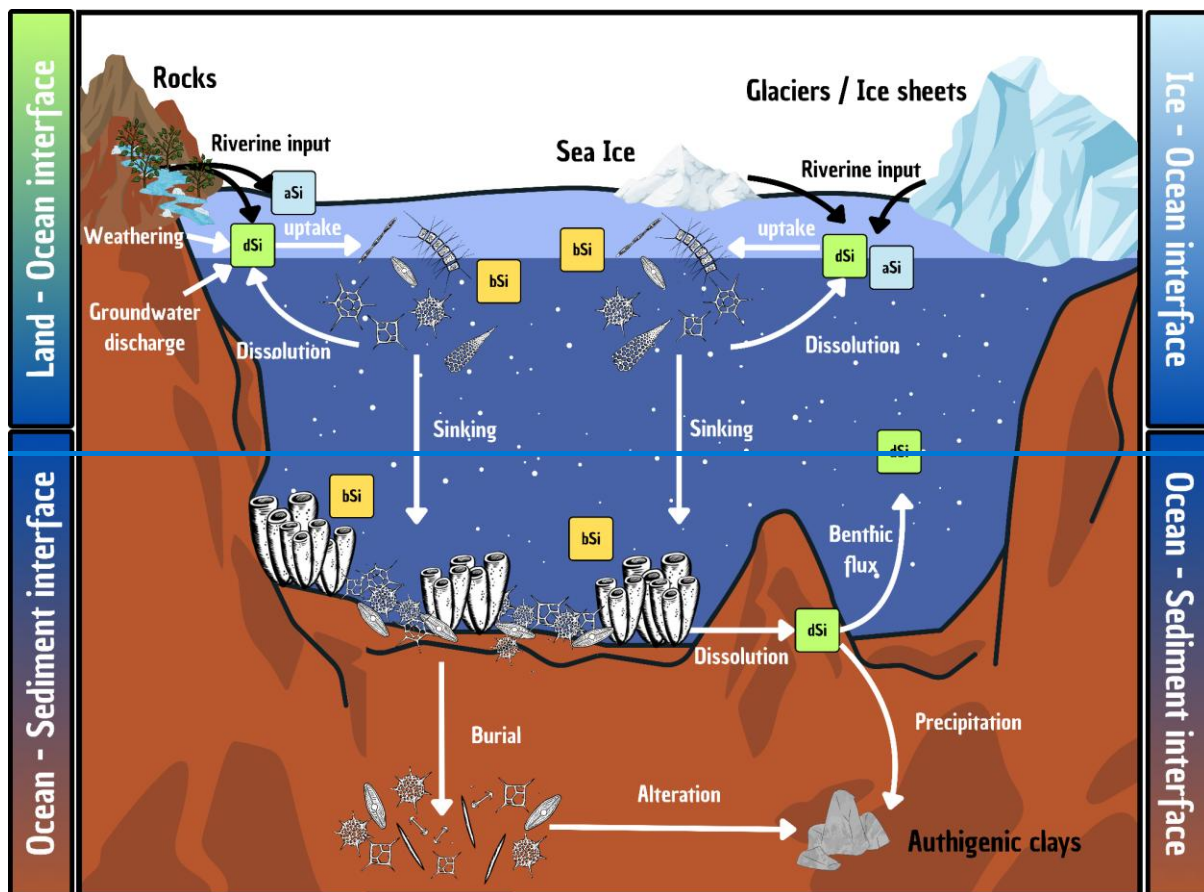
587 **4. Impact of living organisms on marine silicon cycling**

588 Understanding the diversity, biology, and ecological roles of silicifying organisms is essential to contextualize their broader
589 influence on Earth system processes. ~~These organisms not only construct siliceous structures but also actively shape the marine~~
590 ~~and terrestrial Si cycles through uptake, recycling, and burial of bSi. Their evolutionary emergence and ecological expansion~~
591 ~~have fundamentally altered the distribution and availability of dSi in aquatic environments over geological timescales.~~ In the
592 following section, we examine how the biogeochemical cycle of Si has evolved from abiotic to biologically mediated control,
593 highlighting the role of silicifying taxa in transforming Si fluxes, sedimentation patterns, and ocean chemistry across Earth's
594 history and into the modern era.

595 **4.1. Evolution of the silicon cycle across geologic time**

596 Researchers began trying to better understand the evolution of the oceanic Si cycle just over three and a half decades ago
597 (Maliva et al., 1989; Siever, 1991, 1992), with considerable effort since then focused on standing stocks and how the current
598 cycle evolved (Conley et al., 2017; Trower et al., 2021). The modern oceanic Si cycle is relatively well studied (Tréguer et al.,
599 2021), with Si mainly occurring in the marine environment in the form of dSi. The amount of dSi available in the ocean is a
600 balance between inputs (e.g. rivers, aeolian, submarine groundwater, glaciers, and hydrothermal activity), biological
601 circulation via silicifiers (e.g. diatoms, sponges, and Rhizaria), and removal (e.g. burial, biogenic uptake, and secondary
602 formation; see **Fig. 3**). Overall, modern oceanic dSi concentrations are low, averaging less than 10 μM at the surface and
603 around 70 μM in the deep ocean (Gouretski and Koltermann, 2004; Tréguer et al., 1995), primarily regulated by biological
604 activity, but this has not always been the case. In the absence of silicifiers, the oceans must have had higher dSi concentrations
605 in the Precambrian compared to the Phanerozoic (Maliva et al., 2005). Understanding the evolution of silicifiers is therefore
606 crucial to understanding the geologic history of the oceanic Si cycle.

607



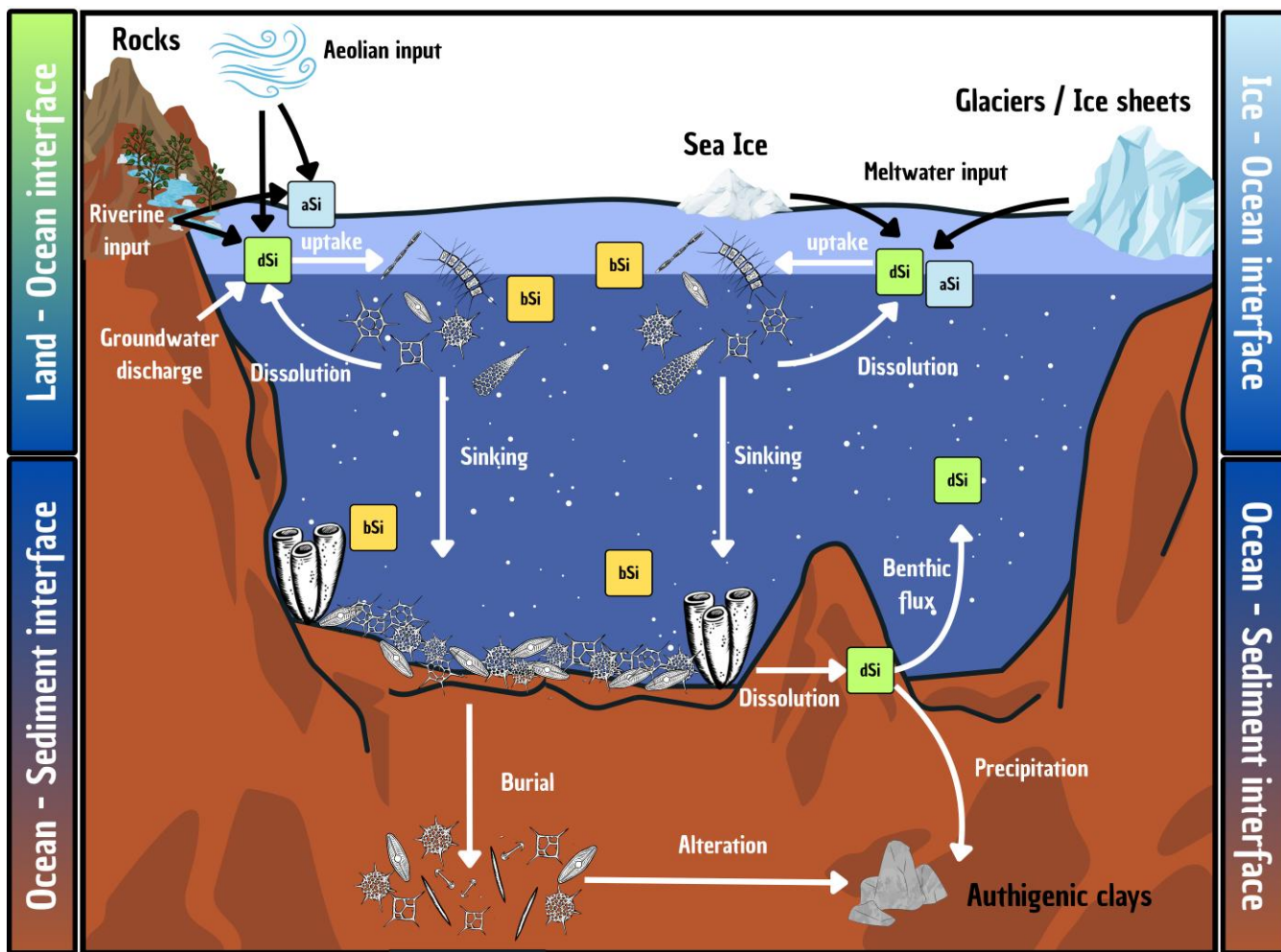


Figure 3. Schematic representation of the Si cycle in the modern global ocean, illustrating key processes occurring at the interface between the ocean and other environments (e.g. sediments, land, ice). Particular attention is given to the transformations and transfers of [silicon](#) in both dissolved (dSi; green boxes) and particulate forms (e.g. biogenic silica, bSi - yellow boxes - and amorphous silica, aSi - blue boxes) as it moves between the surface and deep ocean. Details are given in section 4.3 and quantification of the fluxes are presented in Table 1.

The Precambrian era (>540 Ma) covers most of the Earth's history with little to no complex life forms in the oceans and is characterized by its widespread abiotic silica-rich chert formations. Precambrian cherts are chemically precipitated sedimentary rocks that formed in peritidal and shallow shelf environments mainly during the Proterozoic (2500 – 540 Ma) (Perry and Lefticariu, 2007). Due to continental weathering, volcanism, and hydrothermal activity, the oceans were saturated with respect to dSi, and the Si cycle was mainly controlled by the solubility of mineral phases precipitating out of the seawater (Siever, 1991, 1992). For this reason, there is one main difference between the Precambrian and the Phanerozoic (<540 Ma): bSi precipitation. Silicifiers had not yet fully evolved in an abundance to efficiently remove dSi from the oceans and influence

the Si cycle as they do today. Pinpointing the exact evolutionary timeline of dSi utilizing organisms is tricky, as fossil evidence for early biogenic silicification is viewed as controversial (Chang et al., 2017b; Porter and Knoll, 2000; Sperling et al., 2010). There are some Neoproterozoic (1000 – 540 Ma) protists which had scales that were probably siliceous (Morais et al., 2017), and Ediacaran (635 – 540 Ma) sponges with siliceous spicules (Chang et al., 2019; Chen et al., 2023), but the full extent of their influence on the Si cycle is still unknown.

The appearance of biogenic tools used during silicification challenges the idea that dSi in the Precambrian oceans was only controlled by inorganic reactions, and suggests that oceanic dSi could have been influenced by biology before the Phanerozoic began. The Precambrian Si cycle may therefore not only be abiotically controlled by inorganic reactions, volcanism, hydrothermal activity, and reverse weathering (Isson and Planavsky, 2018; Jurkowska and Świerczewska-Gładysz, 2024; Maliva et al., 1989, 2005), but potentially [by](#) the appearance of organisms capable of using Si (Conley et al., 2017; Marron et al., 2016). While the exact timeline and quantity is widely debated in the literature (e.g. Conley et al., 2017; Grenne and Slack, 2003; Maliva et al., 2005; Trower et al., 2021), following the Precambrian, a decrease in oceanic dSi concentrations (~500 – 1000 μ M) occurred with the widespread evolution of large-scale skeletal marine silicification and the appearance and radiation of siliceous sponges.

The expansion of silica biomineralization via sponges at the beginning of the Paleozoic (540 – 420 Ma) (Chang et al., 2019) lowered dSi concentrations below saturation and changed the oceanic Si cycle to a biologically dominated system, which we continue to see today (Tréguer et al., 2021; Trower et al., 2021). Fossil evidence confirms this biological switch as it was observed that, as sponge populations began to increase, the thick layers of shallow abiotic silica-rich chert became less common and were replaced by deep ocean patchy hydrothermally influenced biogenic chert formations (Chang et al., 2019). Just after the appearance of sponges, a siliceous zooplankton group, Radiolaria, emerged and quickly expanded worldwide during the Ordovician (485 Ma) (Fortey and Holdsworth, 1971; Kidder and Tomescu, 2016), resulting in an additional parallel drop in oceanic dSi concentrations. From there, sponges and radiolarians regulated dSi in the oceans for several million years via biomineralization and the uptake and burial of bSi.

The Mesozoic Era (250 – 145 Ma) saw a massive change in the oceanic ecosystem, with a significant decrease in dSi concentrations. It is believed that the Mesozoic Si cycle was closer to modern day values due to the radiation of diatoms (Harper and Knoll, 1975; Maliva et al., 1989; Siever, 1991). The exact timeline of this major dSi drawdown is largely questioned (Conley et al., 2017; Trower et al., 2021; Yager et al., 2025), as the evolution and worldwide radiation of diatoms is still widely debated (Brylka et al., 2023). Molecular clocks suggest that diatoms originated 200 million years ago near the Triassic-Jurassic boundary (Nakov et al., 2018), but the first widespread fossil deposits were found in the Lower Cretaceous (121 Ma) (Brylka et al., 2024), causing uncertainty in when their abundance took control of the global oceanic Si cycle.

While the major players remain the same, the current oceans differ from those of the Mesozoic in many aspects including sea level, tectonic seafloor spreading and a lack of epicontinental seas. Our present-day marine Si cycle, as presented in the next section, is likely the result of not only biological evolution but also tectonic and palaeoenvironmental conditions

established in the Eocene (33.9 Ma), with low dSi concentrations and biological control of uptake, circulation and burial (Jurkowska and Świerczewska-Gładysz, 2024).

4.2 The modern ocean Si cycle and its fluxes

4.2.1 Biogenic silica production of different silicifiers

Silicic acid levels in modern oceans are largely regulated by diatoms (Krause et al., 2011; Kristiansen et al., 2000; Ng et al., 2024), ~~with the biological activities of silicifiers playing a key role in shaping the marine geochemical cycle of Si. Direct measurements of bSi production by diatoms have often relied on radioisotope tracer methods using ^{32}Si , which allow precise quantification of Si uptake and bSi production rates in natural assemblages.~~ In the modern ocean, pelagic diatoms consume Si more efficiently and produce bSi at a rate of $255 \pm 52 \text{ Tmol-Si yr}^{-1}$ (Tréguer et al., 2021), which is higher than the annual production rate of picocyanobacteria ($<20 \text{ Tmol-Si yr}^{-1}$; Brzezinski et al., 2017; Krause et al., 2017), rhizarians ($2\text{--}58 \text{ Tmol-Si yr}^{-1}$; Llopis Monferrer et al., 2020), siliceous sponges ($6.2 \pm 5.9 \text{ Tmol-Si yr}^{-1}$; Tréguer et al., 2021), benthic diatoms ($6.1 \pm 0.7 \text{ Tmol-Si yr}^{-1}$; Tréguer et al., 2021), and macroalgae ($0.27\text{--}1.33 \text{ Tmol-Si yr}^{-1}$; Yacano et al., 2021). As the bSi production of non-diatom silicifiers is minor and falls within margin of error for pelagic diatom production, Tréguer et al. (2021) set the preferred estimate for global pelagic bSi production at $255 \pm 52 \text{ Tmol-Si yr}^{-1}$.

Although pelagic diatoms are the primary producers of bSi in the global ocean, the contributions of other silicifiers to the marine bSi production are also important at both regional and global scales when considering their role in the marine food web and the export of [carbonC](#) to depth via the biological Si pump. For instance, the accumulation of Si by picocyanobacteria accounts for around 10% of the bSi produced in the mid-latitude ocean gyres and oligotrophic oceans (Baines et al., 2012; Krause et al., 2017; Wei et al., 2023). A recent estimate based on the Si:C ratio and picocyanobacteria cell abundances found that Si accumulation by picocyanobacteria may account for 12% of the global Si inventory and 45% of the global annual bSi production (Wei et al., 2023). However, it should be noted that Wei et al. (2023) applied the Si:C ratio of *Synechococcus* to *Prochlorococcus* (the most abundant species) in nutrient-depleted waters, where competition for dSi by diatoms is undermined, to the global ocean, which likely overestimates the role of picocyanobacteria in the marine Si cycle.

Benthic diatoms are another important group of silicifiers living in the coastal photic zone (Cahoon, 1999). The first estimate of global benthic diatom production was calculated based on: 1) a normalised production rate of benthic diatoms ($1 \text{ mol-Si m}^{-2} \text{ yr}^{-1}$ applied to the global coastal photic zone, yielding $6.8 \text{ Tmol-Si yr}^{-1}$) and 2) global benthic microalgal primary production and the Si:C ratio of the diatom cells (i.e. $(0.13 \text{ mol-Si mol-C}^{-1} \times 514 \times 10^{12} \text{ g-C yr}^{-1})/12 \text{ g-C mol}^{-1} = 5.4 \text{ Tmol-Si yr}^{-1}$; see Tréguer et al., 2021) ~~(i.e. $(0.13 \text{ mol-Si mol-C}^{-1} \times 514 \times 10^{12} \text{ g-C yr}^{-1})/12 \text{ g-C mol}^{-1} = 5.4 \text{ Tmol-Si yr}^{-1}$; see.~~

Due to their long lifespans and low dissolution rate, siliceous sponges store a considerable amount of Si within their skeletons (Chu et al., 2011; López-Acosta et al., 2022; Maldonado et al., 2019). ~~They are widely distributed in the world's oceans and comprise a diverse range of species. Dense sponge reefs have been found in the Strait of Georgia, while sponge spicules have been found in mats exceeding 1 m in thickness in the Antarctic.~~ However, the quantification of the sponge bSi

688 production on the global scale remains highly uncertain (DeMaster, 2019; Tréguer et al., 2021) because of the large variations
689 in Si consumption among sponge species at different growth stages and in different regions (López-Acosta et al., 2016; López-
690 Acosta et al., 2018; Maldonado et al., 2011), and the poorly constrained standing crop of siliceous sponges on the seafloor.
691 Thus, Tréguer et al. (2021) estimated the sponge bSi production by assuming the deposition rate of sponge bSi was equal to
692 the sponge production rate, a method that does not require information on the sponge standing crop.

693 ~~Furthermore,~~ Marine macroalgae and seagrasses also contain Si ~~in their biomass, therefore, they, and~~ may contribute
694 significantly to bSi production in the global neritic zone. By analysing the Si content of various macroalgae genera, Yacano et
695 al. (2021) found large variability in the Si content (ranging from 0.13% to 39.4% by dry weight). By scaling the global net
696 primary production of macroalgae ($80 - 210 \text{ Tmol-C yr}^{-1}$; see Raven, 2018) ~~($80 - 210 \text{ Tmol-C yr}^{-1}$, see~~ by the mean C:Si ratio
697 of macroalgae (295.6) and the median C:Si ratio of macroalgae (157.4), Yacano et al. (2021) estimated the global macroalgae
698 bSi production to be $0.27 - 1.33 \text{ Tmol-Si yr}^{-1}$. This is similar in magnitude to the global bSi production of sponges and
699 benthic diatoms.

700 The area of seagrasses in the global ocean was estimated using field survey data ($160,387 - 266,562 \text{ km}^2$; McKenzie et al.,
701 2020) ~~($160,387 - 266,562 \text{ km}^2$;~~ and modelling results ($917,169 \text{ km}^2$; Gouvêa et al., 2024) ~~($917,169 \text{ km}^2$;~~, yielding large variations
702 in the estimated seagrass meadow area. Based on the previously reported global seagrass shoot production rate (0.34 g DW
703 $\text{m}^{-2} \text{ d}^{-1}$; Strydom et al., 2023) ~~($0.34 \text{ g DW m}^{-2} \text{ d}^{-1}$;~~, the Si content of seagrass leaves ($0.082\% \text{ DW}$; Vonk et al., 2018) ~~(0.082%
704 DW ;~~, and the Si reservoir in seagrass meadows (0.18 g-Si m^{-2} ; Roth et al., 2025) ~~(0.18 g-Si m^{-2} ;~~ of the North Atlantic, ~~we~~
705 ~~made~~ a conservative estimation of the annual global seagrass bSi production ~~(would range from $0.58 - 3.33 \times 10^{-3} \text{ Tmol-Si}$~~
706 ~~yr^{-1})~~ and the ~~resulting~~ seagrass bSi reservoir ~~(would range from $0.33 - 1.86 \times 10^{-3} \text{ Tmol-Si}$)~~. This represents a lower limit of
707 the global seagrass bSi production due to the low seagrass Si content (Vonk et al., 2018) used in the calculation and the low
708 production rate in the North Atlantic compared to other regions such as the temperate North Pacific and the temperate Southern
709 Hemisphere (Strydom et al., 2023). ~~Previous studies had not considered the production of bSi by marine macroalgae and~~
710 ~~seagrasses. However, these marine organisms may produce an important amount of bSi in the neritic zone; and this study).~~
711 Further research is necessary to understand the bSi production of these silicifiers at different seasonal and regional scales.

712 4.2.2 Fluxes and budget of Si in the modern ocean

713 Silicon, which is ultimately derived from the weathering of the Earth's crust, is transported to the ocean via various pathways
714 ~~(Fig. 3 and Table 1)~~. It is then removed from the ocean through the burial of bSi (Tréguer et al., 2021) and the formation of
715 authigenic clays (Aller and Wehrmann, 2025; Rahman et al., 2017). Accurately quantifying the different fluxes of the marine
716 Si budget is important for understanding how it evolves in response to global warming ~~and~~ ocean acidification, and ~~other~~
717 anthropogenic impacts (e.g. river damming and changes in land use).

718 The first Si budget was evaluated by Calvert (1968) and considered river and seafloor basalt weathering to be major marine
719 Si sources. The burial of bSi on the seafloor was identified as the only ocean Si sink (**Table 1**). However, further research has
720 identified several additional significant sources of Si, including hydrothermal activity (DeMaster, 1981), aeolian input (Tréguer

et al., 1995), submarine groundwater discharge (Tréguer and De La Rocha, 2013) and glacial meltwater in the polar regions (Tréguer et al., 2021), and the release of Si from sandy beaches (Aparicio et al., 2025). Several important sinks were also identified, including siliceous sponges (Maldonado et al., 2019; Tréguer and De La Rocha, 2013) and authigenic clay formation (Michalopoulos and Aller, 1995; Tréguer et al., 2021; Tréguer and De La Rocha, 2013) (see **Table 1** and Section 4.3.3).

Table 1. Si sources and sinks of the global ocean accessed during the past 60 years. The unit of the flux is expressed as Tmol-Si yr⁻¹ (10¹² mol-Si yr⁻¹). The numbers marked with “*” represent values calculated in this study, and values in parentheses are fractions of the total Si source or sink.

| Marine Si Sources | Calvert (1968) | DeMaster (1981) | Tréguer et al. (1995) | DeMaster (2002) | Tréguer and De La Rocha (2013) | Frings et al. (2016) | DeMaster (2019) | Tréguer et al. (2021) | Aparicio et al. (2025) |
|---------------------------------|----------------|-----------------|-----------------------|-----------------|--------------------------------|----------------------|---------------------|-----------------------|------------------------|
| River | 7.2 (99%) | 5.6 (90%) | 5.0±1.1 (82%) | 5.6 (84%) | 7.3±2.0 (67%) | 6.33±0.36 (62%) | 6.3±0.4 (53-81%) | 8.1±2.0 (55%) | 8.1±2.8 (38%) |
| Riverine amorphous Si | - | - | - | - | - | 1.90±1.00 (19%) | 0.2±0.5 (2-3%) | - | - |
| Hydrothermal sources | - | 0.6 (10%) | 0.2±0.1 (3%) | 0.6 (9%) | 0.6±0.4 (6%) | 0.60±0.40 (6%) | 0.4±0.2 (3-5%) | 1.7±0.8 (11%) | 1.7±0.9 (8%) |
| Basalt weathering | 0.1 (1%) | - | 0.4±0.3 (7%) | - | 1.9±1.7 (17%) | 0.40±0.30 (4%) | 0.1±0.2 (1%) | 1.9±0.7 (13%) | 1.9±0.7 (9%) |
| Aeolian input | - | - | 0.5±0.5 (8%) | 0.5 (7%) | 0.5±0.5 (5%) | 0.30±0.20 (3%) | 0.2- (3-8%) | 0.5±0.5 (3%) | 0.5±0.5 (2%) |
| Submarine ground water | - | - | - | - | 0.6±0.6 (6%) | 0.65±0.54 (6%) | 0.6- (3-8%) | 2.3±1.1 (16%) | 0.4±0.3 (2%) |
| Glacial meltwater in polar area | - | - | - | - | - | - | - | 0.3±0.3 (2%) | 0.3±0.3 (1%) |
| Sandy beaches | - | - | - | - | - | - | - | - | 8.3±3.0 (39%) |
| Total Si input flux | 7.3 (100%) | 6.2 (100%) | 6.1±2.0 (100%) | 6.7 (100%) | 10.9±4.7 (100%) | 10.20±1.3 (100%) | 7.8- (100%) | 14.8±2.6 (100%) | 21.3±8.5 (100%) |

| | | | | | | | | | |
|--------------------|-------|---------|---------|---------|---------|--------|---------|---------|----------|
| | | | | | (100%) | | | | |
| | | | | | * | | | | |
| Marine Si | | | | | | | | | |
| Sinks | | | | | | | | | |
| Diatom | 6.0 | 5.5-7.5 | 7.1±1.8 | 6.5-7.4 | 6.3±3.6 | - | 7.4- | 9.2±1.6 | 9.2±2.8 |
| | (100% | (100%) | (100%) | (100%) | (55%) | | 8.8±1.5 | (59%) | (59%) |
| |) | | | | | | (91- | | |
| | | | | | | | 100%) | | |
| Sponges | - | - | - | - | 3.6±3.7 | - | 0.04- | 1.7±1.6 | 1.7±1.6 |
| | | | | | (32%) | | 0.9±0.9 | (11%) | (11%) |
| | | | | | | | (0-9%) | | |
| Reverse | - | - | - | - | 1.5±0.5 | - | 0 (0%) | 4.7±2.3 | 4.7±2.3 |
| weathering | | | | | (13%) | | | (30%) | (30%) |
| <i>Total Si</i> | 6.0 | 5.5-7.5 | 7.1±1.8 | 6.5-7.4 | 11.4±7. | - | 7.4- | 15.6±2. | 15.6±6.7 |
| <i>output flux</i> | (100% | (100%) | (100%) | (100%) | 6 | | 9.7±1.8 | 3 | (100%) |
| |) | | | | (100%) | | (100%) | (100%) | |
| Total marine | 97000 | 97000* | 97000 | 97000* | 97000 | 112000 | 112000 | 120000 | 90000 |
| dSi reservoir | * | | | | | | | | |
| (Tmol Si) | | | | | | | | | |
| <i>Marine</i> | 15000 | 15400* | 15000 | 14000* | 10000 | 12000 | 9500- | 7700 | 4200- |
| <i>geological</i> | * | | | | | | 14400 | | 7000 |
| <i>residence</i> | | | | | | | | | |
| <i>time of Si</i> | | | | | | | | | |
| <i>(yrs)</i> | | | | | | | | | |

Based on the evaluations of marine Si sources and sinks, the modern marine Si cycle was long considered to be in a steady state, with an equal input and output flux of Si (see **Table 1** and references therein). However, ~~some~~ recent studies suggest that the dissolution of Si from sandy beaches in the intertidal surf zones contributes a significant flux of dSi to the ocean (Aparicio et al., 2025; Fabre et al., 2019). This leads to an imbalanced global ocean Si budget (Si input flux: 21.3 Tmol-Si yr⁻¹, Si output flux: 15.6 Tmol-Si yr⁻¹; see **Table 1**). However, Tréguer et al. (2021) found that Fabre et al. (2019) overvalued the dSi from sandy beaches due to the complex composition of world ocean beaches, variable sand and seawater mixing conditions at both spatial and temporal scales, and the likely overestimation of coastal water dSi concentration (85.4 µmol L⁻¹). Furthermore, Si

efflux from sandy beaches was included in the submarine groundwater discharge by Cho et al. (2018). Thus, the potential double counting of the coastal zone's Si input flux may lead to an overestimation of the world ocean's Si sources.

Due to the identification of new pathways and processes, as well as important bSi sinks (e.g., siliceous sponges), the estimation of Si input and output fluxes has doubled since the study by Calvert (1968) (**Table 1**). This has resulted in a shorter residence time of Si in the ocean, from ~~45,000~~15,000 years to approximately ~~7,000~~7,000 years. Ultimately, more accurate estimates of the biotic and abiotic fluxes and processes that drive the global Si cycle are needed to assess whether it is in a steady state or if the ocean is becoming more enriched or gradually depleted of dSi. However, this task is challenging, ~~if not impossible~~, given the complexity of the large number of interconnected processes, coupled with both natural variability and anthropogenic perturbation.

4.3 Interfaces in the oceanic silicon cycle: processes, pathways, and perturbations

Beyond the open ocean, the global Si cycle is shaped by dynamic exchange zones — interfaces where land, sediments, and ice meet the sea. These interfaces host complex physical, chemical, and biological processes that modulate the pathways and reactivity of Si entering or leaving the ocean. Exploring these often-overlooked boundaries reveals critical controls on Si availability and ecosystem function and is essential to constrain the spatial heterogeneity and long-term evolution of the marine Si cycle.

4.3.1 Land–ocean interface: biogeochemical filters and emerging pathways in the silicon cycle

The land-ocean interface plays a critical role in the global Si cycle, serving as a dynamic transition zone where terrestrial inputs, biological transformations, and sedimentary processes interact to modulate Si fluxes to the coastal and open ocean. Rivers, the primary source of Si to the ocean, transport Si derived from continental weathering, with an increasing number of studies using germanium (Ge)/Si ratios, and Si and Ge isotopes to understand Si cycling during weathering and Critical Zone processes on land (Baronas et al., 2018; Fernandez et al., 2022; Frings et al., 2016, 2021). Recent studies have identified a number of previously overlooked Si sources, including submarine groundwater (Cho et al., 2018; Rahman et al., 2019; Santos et al., 2021; Zhu et al., 2025), salt marshes (Williams et al., 2022), and sandy beaches (Aparicio et al., 2025). These new sources challenge the ~~conventional~~ view that land-ocean inputs are dominated by silicifier-modulated riverine fluxes, suggesting that physical processes may play a larger role than previously assumed. The effect of submarine groundwater discharge and beach sand dissolution on the productivity of silicifiers is yet to be investigated.

Silicifying organisms exert substantial control over Si retention, recycling, and export from land. For example, diatoms play a key role in Si cycling in large estuaries, making them effective Si filters that sequester a significant fraction of terrestrial Si before it reaches the ocean (Baronas et al., 2016; Chong et al., 2014; Zhang et al., 2020a). Similarly, plant Si accumulation exerts a major control on the terrestrial Si cycle (Alexandre et al., 1997; de Tombeur et al., 2020), with probable consequences for the land-to-ocean transfer of dSi (Conley, 2002; Conley and Carey, 2015). In fact, the annual soil-plant systems recycle much more Si (global annual Si uptake by vegetation ranges from 60 to 200 Tmol Si yr⁻¹; Conley, 2002) ~~(global annual Si~~

uptake by vegetation ranges from 60 to 200 Tmol Si yr⁻¹; compared to what is transferred from land to oceans through rivers (Table 1). Ge and Si isotope mass balances also indicate 12–54% of all Si released during terrestrial weathering is taken up by terrestrial vegetation (Baronas et al., 2018; Frings et al., 2021). Such phenomena are often referred to as the “terrestrial ecosystem silica filter” (Struyf and Conley, 2012). In addition to retaining and enhancing the formation of secondary weathering products on land (Baronas et al., 2020; Cornelis and Delvaux, 2016), plants also increase silicate weathering rates through a wide range of processes (i.e. bio-weathering; Wild et al., 2022)(i.e. bio-weathering;. In contrast to the numerous studies on marine and terrestrial silicifiers, there have been relatively few studies of lacustrine Si cycle, with most studies focusing on bSi oxygen isotope analyses or palaeoproductivity reconstructions (Frings et al., 2024; Meister et al., 2024). As a result, the impact of freshwater bSi cycling on the land-to-ocean Si flux is relatively unconstrained.

Anthropogenic activities, including land use change, eutrophication, and damming, are reshaping Si fluxes at the land-ocean interface, with implications for diatom productivity and coastal ecosystem health (Laruelle et al., 2009; Maavara et al., 2014). New evidence continues to demonstrate the effects of eutrophication and damming on Si trapping in both river channels and reservoir systems (Ran et al., 2022). Zhang et al. (2020b) showed that damming and eutrophication have altered the Si isotopic signature in the Baltic Sea due to shifts in diatom-driven Si utilization and sedimentary Si regeneration. Additionally, research has shown that coastal Si cycling is amplified by oyster aquaculture, which drives rapid recycling of dSi to the water column (Ray et al., 2021). Climate change also impacts Si dynamics at the land-ocean interface. Palaeo-records from Chesapeake Bay, the largest estuary in the US, indicate that estuarine Si cycling is sensitive to changes in sedimentation rate over the Holocene, influenced by both climatic shifts (e.g. sea level rise, runoff changes) and human activities (e.g. deforestation) (Nantke et al., 2019). Geilert et al. (2023) demonstrated how climatic events such as coastal El Niño can accelerate marine silicate alteration, driving rapid authigenic clay formation that modifies Si availability in continental margin sediments. This underscores the sensitivity of coastal Si cycling to episodic disturbances, which are becoming more frequent due to climate change.

4.3.2 Benthic interface: silicon recycling and burial at the seawater–sediment boundary

The flux and efficiency of bSi burial in marine sediments primarily depends on 1) the bSi delivery rate to the sediment (itself a function of productivity and pelagic recycling rates; Van Cappellen et al., 2002)(itself a function of productivity and pelagic recycling rates; 2) the type of bSi (e.g. diatom, Rhizaria, sponges, etc.) and its inherent solubility, surface area, and dissolution rates (Aller and Wehrmann, 2025; Maldonado et al., 2019, 2022); 3) detrital sediment supply and overall sediment accumulation (Loucaides et al., 2010; Presti and Michalopoulos, 2008); and 4) diagenetic and redox conditions in marine sediments (McManus et al., 1995; Van Cappellen and Qiu, 1997; Zhu et al., 2024). Regarding the contribution of different organisms to the benthic bSi burial flux, the long-term general consensus of diatom dominance has recently been challenged by a number of studies on other silicifying organisms, notably rhizarians and sponges. Maldonado et al. (2019) have shown that, due to the high preservation efficiency ($45.2 \pm 27.4\%$), sponge spicules could contribute a burial flux of 1.71 ± 1.61 Tmol

Si yr^{-1} globally, more than an order of magnitude higher than previously estimated. While dissolution rates can vary significantly between different sponge types, bSi of the dominant demosponges is orders of magnitude more resistant to dissolution compared to diatom bSi under seafloor-like conditions, although the cause is yet to be identified (Maldonado et al., 2022). While rhizarians have a much lower preservation efficiency of $6.8 \pm 10.1\%$ (Maldonado et al., 2019), a recent study has significantly revised their global productivity upwards to $2\text{--}58 \text{ Tmol-Si yr}^{-1}$ (Llopis Monferrer et al., 2020). Assuming a similar benthic export efficiency to diatoms (33%), rhizarian bSi could thus theoretically contribute $0.1\text{--}3.4 \text{ Tmol-Si yr}^{-1}$ to the benthic bSi burial flux. The lower end of this range is consistent with the $0.09 \pm 0.05 \text{ Tmol-Si yr}^{-1}$ estimated by Maldonado et al. (2019)(2019), using direct observations of rhizarian skeletons in marine sediments from across the global ocean.

Once deposited, bSi undergoes (partial) dissolution, often coupled with diagenetic alteration (see the recent review by Aller and Wehrmann (2025) and Fig. 3)(see the recent review by (Aller and Wehrmann, 2025 and Fig. 3)). The latter includes the direct alteration of bSi and/or the formation of authigenic silicate (clay) phases, frequently as coatings and partial replacement of the initial bSi phases. Recent studies have attempted to quantify the relative contribution of these different processes by investigating the Si and Ge isotopic signature of both sediments and pore waters (Baronas et al., 2019; Cassarino et al., 2020; Closset et al., 2022; Ward et al., 2022). Indeed, unique isotopic fractionation during these processes could lead to predictable shifts in the Si isotopic composition ($\delta^{30}\text{Si}$) of pore water values, helping decipher the complex Si cycle in surface sediments (see Box 4). Most of the studies targeted the Southern Ocean or upwelling areas that are known to play a dominant role in the global marine Si cycle, hosting abundant diatom populations and exporting large quantities of bSi. For example, the Southern Ocean produces ~30% of global silica and ~~act~~acts as the largest sedimentary sink (~~2 Tmol of Si~~ $\sim 2 \text{ Tmol-Si yr}^{-1}$; Tréguer, 2014)~~-yr⁻¹~~.

The main output of these studies is that most settling bSi dissolves within the upper few centimetres of the sediment directly below the sediment-water interface, regulating pore water dSi concentrations and deep ocean Si fluxes. For example, in the Southern Ocean, diffusive Si fluxes from the sediment show a zonal trend, peaking near the Polar Front and correlating with sediment bSi content likely reflecting diatom productivity in the overlying water column (Closset et al., 2022). However, isotopic compositions of both pore water and bSi preserved in the sediment indicate that secondary processes such as the formation of authigenic aluminosilicates from the dissolving bSi, dissolution of reactive lithogenic silica, and adsorption onto particles can play a significant role in both shallow and deep benthic marine environments (Frings et al., 2024; Luo et al., 2022; Ward et al., 2022)~~but differ between regions~~.

When authigenic silicate clay formation incorporates major cations, it lowers the pH of surrounding pore waters and therefore reduces seawater alkalinity, which is termed “reverse weathering” (Mackenzie and Garrels, 1966). It is important to recognize that not all authigenic mineral formation results in reverse weathering, but only that which consumes alkalinity and therefore drives an increase in atmosphere-ocean pCO_2 (Hong et al., 2025). While there is ample evidence that clay authigenesis is a major sink of Si and some trace elements (Baronas et al., 2019; Lauchli et al., 2025; Rahman et al., 2017), only a few studies have directly evidenced the associated consumption of cations (Michalopoulos and Aller, 1995, 2004; Wu

et al., 2025). Nevertheless, it has recently been proposed that reverse weathering has played a crucial role in stabilizing marine pH and regulating climate over geological timescales (Isson and Planavsky, 2018).

Despite its importance, the formation of authigenic (newly precipitated) clays is difficult to detect in sediments dominated by detrital clays but it can occur relatively quickly (less than one year; Michalopoulos et al., 2000). However, a re-estimate of both forward and reverse weathering rates in marine sediments has suggested that there is no net alkalinity flux in marine sediments, and both processes must be tightly coupled to enable each other (Wallmann et al., 2023). Furthermore, forward and reverse silicate weathering exhibits only a secondary role, and is strongly influenced by organic matter degradation and carbonate mineral reactions in marine sediments (Hong et al., 2025; Luo et al., 2025). Therefore, the role that bSi diagenesis-enabled reverse weathering plays in controlling Earth's long-term carbon cycle balance is still open for debate.

4.3.3 Cryospheric interface: the role of glacial and sea-ice systems in silicon cycling

The cryosphere includes all of Earth's frozen systems, both on land and in the ocean. This encompasses snow, glaciers, ice sheets, icebergs, sea ice, frozen rivers and lakes, permafrost, and seasonal frozen grounds. While the role of each of these systems on the Si cycle is not yet fully understood, significant progress has been made in studying glaciers, ice sheets, sea ice and permafrost (Alfredsson et al., 2015; Hatton et al., 2019b; Hawkings et al., 2017; Pokrovsky et al., 2013).

Glaciers and ice sheets cover up to 30% of Earth's land during glacial cycles, releasing significant amounts of freshwater and sediment impacting downstream ecosystems (Hopwood et al., 2025; Tréguer, 2014). This discharge can limit light penetration into the water column (Halbach et al., 2019) but it also supplies essential nutrients to marine environments, increasing primary production (Hawkings et al., 2017). Recent studies highlighted the significant contribution of glaciers and ice sheets to the global Si cycle, supplying both dSi and amorphous silica (aSi) to marine environments (Hawkings et al., 2017; Meire et al., 2016; Tréguer et al., 2021). These contributions rival other inputs such as dust deposition, groundwater discharge and hydrothermal input (Hawkings et al., 2017). The magnitude and reactivity of glacial Si fluxes have a direct influence on the dissolution rates and availability of bioavailable dSi, potentially enhancing primary production in coastal and shelf seas (Hatton et al., 2023; Ng et al., 2024).

Pro-glacial rivers are characterized by a lighter isotopic signature in both dSi and aSi, lower than the average of non-glacial rivers, from 0.16‰ to 1.38‰ respectively for the dissolved fraction (Hatton et al., 2019b) and lower than the surrounding sediment and bedrock (Hawkings et al., 2018). Under glacial conditions, enhanced chemical weathering — driven by processes such as dissolution–reprecipitation and the leaching of freshly abraded mineral surfaces — produces highly reactive inorganic aSi. Long water residence times and intense erosion further promote silicate dissolution, even at low temperatures (Hatton et al., 2021). Additionally, suspended fine particulate matter from intense erosion carries a substantial fraction of dissolvable aSi (Baronas et al., 2021; Hatton et al., 2019a; Hawkings et al., 2017). This highly soluble aSi can represent up to 95% of total potentially bioavailable silica dSi and aSi in areas receiving glacial meltwaters. Up to 20% of this aSi can dissolve rapidly after two weeks in low-nutrient seawater ($dSi < 1\mu M$) at 18°C (Hawkings et al., 2017; Hendry et al., 2025). An even less

studied and potentially highly bioavailable, colloidal-nanoparticulate size Si-~~(CNSi)~~ seems to represent a significant fraction of total bioavailable Si, only present in pro-glacial rivers, which may be a similar order of magnitude to the concentration of dSi and aSi (Pryer et al., 2020). Dissolution, precipitation, sedimentation, resuspension and uptake are key processes in glacial estuary environments controlling the fate of glacial dSi and aSi inputs to the coastal environment (Hendry et al., 2025). In addition, complex, heterogeneous and still poorly understood processes in pro-glacial environments and fjords lead to lower dSi concentrations in interstitial fluids near glacial outputs than in coastal shelf sediments, which may impact the dSi cycle in the water column and its offshore dynamics (Hendry et al., 2025; Ng et al., 2020, 2022).

Sea ice consists of frozen seawater floating on the ocean's surface, and it can be formed seasonally or be perennial. During its formation, small pockets of brine are formed due to salt expulsion (Eicken, 2003). As the expulsion of brine increases the salinity of the mixing layer, it can enhance sea water circulation (Wang and Danilov, 2022), therefore promoting the upwelling of deep water and affecting the nutrient supply to surface waters. Furthermore, sea ice supports diverse communities, including diatoms, inhabiting these brine pockets, as well as the sea ice surface and attached underneath the sea ice (Arrigo, 2017). [The recycling of bSi within these habitats directly sustains the growth of such silicifying organisms under extreme polar conditions.](#) For example, by focusing on the distribution of natural Si isotopes within the Antarctic pack ice, Fripiat et al. (2014) found that bSi dissolution contributes significantly to silica production, with a dissolution-to-production ratio between 0.4 and 0.9. This suggests that there is considerable regeneration of Si within the brine network, which fuels new bSi production. This study was crucial in filling a gap in the understanding of sea ice Si cycling, a topic that is still poorly studied due to the difficulty of measuring rates in such environments.

The role of permafrost in the polar regions and their influence on the Si cycle remains uncertain, particularly in the context of a warming climate. Seasonal isotopic variations observed in the Lena River (Russian Siberia) suggest that Si sources shift throughout the year—clay minerals dominate in winter, while summer brings increased dissolution of silicate minerals and phytoliths from the upper active layer (Sun et al., 2018). These findings imply that permafrost thawing, driven by climate change, could significantly alter Si fluxes and isotopic compositions in high-latitude rivers. However, a study by Mavromatis et al. (2016) in the Yenisey River and its tributaries found that mineral dissolution in the watershed plays a crucial role in defining the riverine dissolved $\delta^{30}\text{Si}$, regardless of permafrost coverage. Their findings highlight the influence of suspended particles (e.g. clays), plant material decomposition (both contributing lower $\delta^{30}\text{Si}$), and groundwater discharge enriched in heavier isotopes due to secondary silicate formation. These contrasting findings underscore the complexity of Si cycling in regions covered by permafrost where multiple processes occur, [with potential downstream implications for the availability and isotopic composition of silica supplied to silicifying organisms in Arctic rivers and coastal zones.](#) Further studies are essential for predicting how ongoing climate change might reshape the Si export to the ocean and how these signals can be interpreted in palaeorecords.

In a recent study, Opfergelt et al. (2024) investigated how winter river ice formation in the Lena River affects the biogeochemical cycling of key nutrients like [nitrogen](#) and Si, and their transport to the Arctic Ocean. During very cold periods, *frazil ice* forms microzones that slow water flow and create favourable conditions for microbial activity. These zones

allow organic matter recycling and alter nutrient processing. The formation of ice crystals leads to the precipitation of aSi, which changes $\delta^{30}\text{Si}$ and the Ge/Si ratio in the remaining water. Through isotope mass balance, Opfergelt et al. (2024) estimate that about 39% of Lena River water passes through this ice-induced filter during winter, leading to notable silica loss and a shift in river biogeochemistry.

These cryosphere–Si interactions are particularly relevant for silicifying organisms. For instance, the input of highly soluble amorphous silica and colloidal-nanoparticulate Si from glaciers and pro-glacial rivers provides an important source of bioavailable silica that can stimulate diatom blooms in coastal and shelf seas. Similarly, brine pockets in sea ice sustain diverse diatom communities, where rapid recycling of bSi supports continued growth under extreme conditions. Changes in the magnitude, timing, and isotopic composition of these fluxes therefore have direct consequences for the ecology and distribution of silicifiers, as well as for the interpretation of palaeoceanographic records based on their silica remains. For example, climate change is accelerating the melting of glaciers, permafrost and sea ice, reducing ice-covered areas and increasing open-water regions. ~~These shifts alter,~~ altering habitats, species distributions, and nutrient dynamics. The melting of sea ice, glaciers and ice sheets also releases previously trapped trace metals and nutrients into seawater, further influencing marine productivity and biogeochemical cycles (Hopwood et al., 2020). Given their vast size and prolonged melting periods, ice sheets may have a more significant global impact on Si input compared to smaller glaciers with more seasonal contributions. While glacial retreat and melting are expected to increase Si fluxes to the ocean, the long-term effects remain uncertain, as they could reshape marine ecosystems and biogeochemical cycles (Hatton et al., 2019b; Pryer et al., 2020). Palaeorecords of $\delta^{30}\text{Si}$ and Ge/Si signatures in sedimentary bSi are emerging as a useful tool to reconstruct and quantify the effects of glaciation on the Si cycle and weathering (Hou et al., 2025). Understanding the role of glaciers in the Si cycle — particularly how their contributions interact with other sources and evolve under future climate scenarios — remains a key area of research.

5. Perspectives and conclusions

Despite major advances in our understanding of silicification, ~~silicifiers~~ silicifiers' diversity, and the global Si cycle, critical knowledge gaps persist across taxonomic, physiological, ecological, and geochemical dimensions. To move the field forward, we outline key research priorities that we believe will be pivotal in developing a more integrated and predictive understanding of biosilicification and its role in the marine Si cycle. Addressing these challenges will require integrative and interdisciplinary research approaches that bridge molecular biology, ecology, biogeochemistry, (palae)oceanography, and Earth system science.

1. Expand taxonomic and functional knowledge across silicifiers: Research remains heavily biased toward a few model organisms such as diatoms and terrestrial plants. Many other silicifying taxa, including Rhizaria, silicoflagellates, sponges, macrophytes, and even some prokaryotes, are understudied despite their potential significant contributions to the Si cycle. Broader taxonomic coverage, including the development of new model systems and comparative studies, will be essential to capture the evolutionary, functional, and ecological diversity of silicification strategies across domains of life.

2. Elucidate cellular mechanisms and physiological regulation: Much remains to be understood about how organisms control Si uptake, intra- and intercellular transport, polymerization, and efflux. For instance, the mechanisms of Si efflux, crucial for homeostasis in diatoms, are poorly characterized in most groups. Investigating the molecular basis of silicification — including gene expression, transporter function, and nanoscale silica assembly — will benefit from the use of high-resolution imaging, omics technologies, and experimental manipulation under variable environmental conditions.

3. Integrate silicifiers into ecosystem and global models: Current biogeochemical models often overlook key silicifiers such as sponges and Rhizaria. Their omission limits our ability to predict Si fluxes and understand how Si cycling interacts with other elemental cycles like [carbonC](#) and [nitrogenN](#). Incorporating a broader range of silicifiers into these models is essential, particularly under changing climate regimes.

4. Clarify interactions between biotic and abiotic Si processes: The interplay between biological silicification, [biogenic silicabSi](#) dissolution, silicate weathering, and authigenic clay formation remains insufficiently understood. This is especially true in transitional environments like estuaries and coastal margins, where complex feedbacks occur. Further research is needed to disentangle the contributions and temporal dynamics of biotic versus abiotic Si pathways.

5. Assess environmental and climatic influences on silicification and Si fluxes: While the environmental drivers of silicification are well studied in diatoms, their effects on other silicifiers are largely unknown. Additionally, how climate-related stressors — such as warming, acidification, altered precipitation, and sea-level rise — affect Si cycling and silicifiers distribution is not well constrained. These processes may reshape the ecological roles of silicifiers and the fate of Si at critical interfaces such as the land–ocean boundary.

6. Foster cross-disciplinary integration: Bridging disciplinary divides — between marine and terrestrial science, biology and geochemistry — will enhance our understanding of the Si cycle. Cross-comparisons (e.g. between plant and algal silicification), training in diverse analytical techniques, and collaboration across fields will enable more holistic interpretations of both modern processes and palaeoenvironmental records.

Silicon plays a pivotal yet still underappreciated role in shaping biological and geochemical processes across marine and terrestrial systems. This review highlights the remarkable diversity of silicifying organisms and their crucial, but often overlooked, roles in shaping the global marine Si cycle. From unicellular diatoms to multicellular sponges, and from well-studied phytoplankton to enigmatic protists and prokaryotes, silicifiers contribute to a wide array of ecological functions and influence biogeochemical feedbacks across spatial and temporal scales. As research expands beyond classical models, a more nuanced and integrative picture of the Si cycle is emerging — one that includes diverse silicifiers, complex environmental feedbacks, and deep-time dynamics. Despite significant progress over the last decade, major uncertainties persist regarding the cellular machinery of silicification, the environmental controls of Si fluxes and the integration of silicifiers into predictive models. These gaps are especially pressing in the context of global change, where shifts in climate and nutrient regimes are

likely to affect the distribution, abundance and ecological function of silicifiers in ways that are still poorly understood. Addressing these challenges will require coordinated, cross-disciplinary efforts that link biological, ecological and geochemical research. Leveraging recent advances in molecular biology, high-resolution imaging, in situ monitoring, and Earth system ~~modeling~~modelling will be key to ~~unraveling~~unravelling the complexity of Si cycling. Advancing our understanding of biosilicification is not only essential for reconstructing past marine environments but also for predicting the future of ocean biogeochemistry in an era of rapid planetary change.

References

- Abelmann, A., Gersonde, R., Knorr, G., Zhang, X., Chaplign, B., Maier, E., Esper, O., Friedrichsen, H., Lohmann, G., Meyer, H., and Tiedemann, R.: The seasonal sea-ice zone in the glacial Southern Ocean as a carbon sink, *Nat. Commun.*, 6, 8136, <https://doi.org/10.1038/ncomms9136>, 2015.
- Abramson, J., Adler, J., Dunger, J., Evans, R., Green, T., Pritzel, A., Ronneberger, O., Willmore, L., Ballard, A. J., Bambrick, J., Bodenstein, S. W., Evans, D. A., Hung, C.-C., O'Neill, M., Reiman, D., Tunyasuvunakool, K., Wu, Z., Žemgulytė, A., Arvaniti, E., Beattie, C., Bertolli, O., Bridgland, A., Cherepanov, A., Congreve, M., Cowen-Rivers, A. I., Cowie, A., Figurnov, M., Fuchs, F. B., Gladman, H., Jain, R., Khan, Y. A., Low, C. M. R., Perlin, K., Potapenko, A., Savy, P., Singh, S., Stecula, A., Thillaisundaram, A., Tong, C., Yakneen, S., Zhong, E. D., Zielinski, M., Židek, A., Bapst, V., Kohli, P., Jaderberg, M., Hassabis, D., and Jumper, J. M.: Accurate structure prediction of biomolecular interactions with AlphaFold 3, *Nature*, 630, 493–500, <https://doi.org/10.1038/s41586-024-07487-w>, 2024.
- Ács, É., Földi, A., Vad, C. F., Trábert, Z., Kiss, K. T., Duleba, M., Borics, G., Grigorszky, I., and Botta-Dukát, Z.: Trait-based community assembly of epiphytic diatoms in saline astatic ponds: a test of the stress-dominance hypothesis, *Sci. Rep.*, 9, 15749, <https://doi.org/10.1038/s41598-019-52304-4>, 2019.
- Adl, S.: *Rhizoa*, Protistol. Elsevier, 2024.
- Aguilera, A., Lundin, D., Charalampous, E., Churakova, Y., Tellgren-Roth, C., Śliwińska-Wilczewska, S., Conley, D. J., Farnelid, H., and Pinhassi, J.: The evaluation of biogenic silica in brackish and freshwater strains reveals links between phylogeny and silica accumulation in picocyanobacteria, *Appl. Environ. Microbiol.*, 91, <https://doi.org/10.1128/aem.02527-24>, 2025.
- Alexandre, A., Meunier, J.-D., Colin, F., and Koud, J.-M.: Plant impact on the biogeochemical cycle of silicon and related weathering processes, *Geochim. Cosmochim. Acta*, 61, 677–682, [https://doi.org/10.1016/s0016-7037\(97\)00001-x](https://doi.org/10.1016/s0016-7037(97)00001-x), 1997.
- Alfredsson, H., Hugelius, G., Clymans, W., Stadmark, J., Kuhry, P., and Conley, D. J.: Amorphous silica pools in permafrost soils of the Central Canadian Arctic and the potential impact of climate change, *Biogeochemistry*, 124, 441–459, <https://doi.org/10.1007/s10533-015-0108-1>, 2015.
- Aller, R. C. and Wehrmann, L. M.: Sedimentary diagenesis, depositional environments, and benthic fluxes, in: *Treatise on Geochemistry*, vol. 4, edited by: Anbar, A. and Weis, D., Elsevier, 573–629, <https://doi.org/10.1016/b978-0-323-99762-1.00095-4>, 2025.
- Alley, K., Patacca, K., Pike, J., Dunbar, R., and Leventer, A.: Iceberg Alley, East Antarctic Margin: Continuously laminated diatomaceous sediments from the late Holocene, *Mar. Micropaleontol.*, 140, 56–68, <https://doi.org/10.1016/j.marmicro.2017.12.002>, 2018.

1001 Anderson, O. R.: Protozoa, Radiolarians, in: Encyclopedia of Ocean Sciences, edited by: Steele, J. H., Thorpe, S. A., and
1002 Turekian, K. K., Academic Press, Oxford, 2315–2320, 2001.

1003 Aparicio, M., Le Bihan, A., Jeandel, C., Fabre, S., Almar, R., and Mingo, I. M.: Contribution of sandy beaches to the global
1004 marine silicon cycle, *Nat. Geosci.*, 18, 154–159, <https://doi.org/10.1038/s41561-024-01628-6>, 2025.

1005 Armbrust, E. V.: The life of diatoms in the world’s oceans, *Nature*, 459, 185–192, <https://doi.org/10.1038/nature08057>, 2009.

1006 Arrigo, K. R.: Sea ice as a habitat for primary producers, in: *Sea Ice*, edited by: Thomas, D. N., Wiley, 352–369,
1007 <https://doi.org/10.1002/9781118778371.ch14>, 2017.

1008 Assmy, P., Henjes, J., Smetacek, V., and Montresor, M.: Auxospore formation by the silica-sinking, oceanic diatom
1009 *Fragilariopsis kerguelensis* (*Bacillariophyceae*), *J. Phycol.*, 42, 1002–1006, [https://doi.org/10.1111/j.1529-](https://doi.org/10.1111/j.1529-8817.2006.00260.x)
1010 8817.2006.00260.x, 2006.

1011 Azam, F., Fenchel, T., Field, J. G., Gray, J. S., Meyer-Reil, L. A., and Thingstad, F.: The Ecological Role of Water-Column
1012 Microbes in the Sea, *Mar. Ecol. Prog. Ser.*, 10, 257–263, <https://doi.org/10.3354/meps010257>, 1983.

1013 Baines, S. B., Twining, B. S., Brzezinski, M. A., Krause, J. W., Vogt, S., Assael, D., and McDaniel, H.: Significant silicon
1014 accumulation by marine picocyanobacteria, *Nat. Geosci.*, 5, 886–891, <https://doi.org/10.1038/ngeo1641>, 2012.

1015 Bárcena, M. A., Cacho, I., Abrantes, F., Sierro, F. J., Grimalt, J. O., and Flores, J. A.: Paleoproductivity variations related to
1016 climatic conditions in the Alboran Sea (western Mediterranean) during the last glacial–interglacial transition: the diatom
1017 record, *Palaeogeogr. Palaeoclimatol. Palaeoecol.*, 167, 337–357, [https://doi.org/10.1016/S0031-0182\(00\)00246-7](https://doi.org/10.1016/S0031-0182(00)00246-7), 2001.

1018 Baronas, J. J., Hammond, D. E., Berelson, W. M., McManus, J., and Severmann, S.: Germanium–silicon fractionation in a
1019 river-influenced continental margin: The Northern Gulf of Mexico, *Geochim. Cosmochim. Acta*, 178, 124–142,
1020 <https://doi.org/10.1016/j.gca.2016.01.028>, 2016.

1021 Baronas, J. J., Torres, M. A., West, A. J., Rouxel, O., Georg, B., Bouchez, J., Gaillardet, J., and Hammond, D. E.: Ge and Si
1022 isotope signatures in rivers: A quantitative multi-proxy approach, *Earth Planet. Sci. Lett.*, 503, 194–215,
1023 <https://doi.org/10.1016/j.epsl.2018.09.022>, 2018.

1024 Baronas, J. J., Hammond, D. E., Rouxel, O. J., and Monteverde, D. R.: A First Look at Dissolved Ge Isotopes in Marine
1025 Sediments, *Front. Earth Sci.*, 7, <https://doi.org/10.3389/feart.2019.00162>, 2019.

1026 Baronas, J. J., West, A. J., Burton, K. W., Hammond, D. E., Opfergelt, S., Pogge Von Strandmann, P. A. E., James, R. H., and
1027 Rouxel, O. J.: Ge and Si Isotope Behavior During Intense Tropical Weathering and Ecosystem Cycling, *Glob. Biogeochem.*
1028 *Cycles*, 34, <https://doi.org/10.1029/2019gb006522>, 2020.

1029 Baronas, J. J., Hammond, D. E., Bennett, M. M., Rouxel, O., Pitcher, L. H., and Smith, L. C.: Ge/Si and Ge Isotope
1030 Fractionation During Glacial and Non-glacial Weathering: Field and Experimental Data From West Greenland, *Front. Earth*
1031 *Sci.*, 9, <https://doi.org/10.3389/feart.2021.551900>, 2021.

1032 Barrio-Hernandez, I., Yeo, J., Jänes, J., Mirdita, M., Gilchrist, C. L. M., Wein, T., Varadi, M., Velankar, S., Beltrao, P., and
1033 Steinegger, M.: Clustering predicted structures at the scale of the known protein universe, *Nature*, 622, 637–645,
1034 <https://doi.org/10.1038/s41586-023-06510-w>, 2023.

1035 Barron, J. A., Bukry, D. B., and Gersonde, R.: Diatom and silicoflagellate biostratigraphy for the late Eocene: ODP 1090 (sub-
1036 Antarctic Atlantic), in: *Diatom research over time and space Morphology, taxonomy, ecology and distribution of diatoms -*

1037 from fossil to recent, marine to freshwater, established species and genera to new ones, edited by: Kociolek, J., Kulikovskiy,
1038 M., Witkowski, J., and Harwood, D., Nova Hedwigia, Stuttgart, 1–32, 2014.

1039 Battershill, C. and Bergquist, P.: The influence of storms on asexual reproduction, recruitment, and survivorship of sponges.,
1040 in: New perspectives in sponge biology, edited by: Rutzler, K., Smithsonian Institution Press, Washington, DC, 397–403,
1041 1990.

1042 Beazley, L. I., Kenchington, E. L., Murillo, F. J., and Sacau, M. D. M.: Deep-sea sponge grounds enhance diversity and
1043 abundance of epibenthic megafauna in the Northwest Atlantic, ICES J. Mar. Sci., 70, 1471–1490,
1044 <https://doi.org/10.1093/icesjms/fst124>, 2013.

1045 Behrenfeld, M. J., Halsey, K. H., Boss, E., Karp-Boss, L., Milligan, A. J., and Peers, G.: Thoughts on the evolution and
1046 ecological niche of diatoms, Ecol. Monogr., 91, <https://doi.org/10.1002/ecm.1457>, 2021.

1047 Bell, J. J.: The functional roles of marine sponges, Estuar. Coast. Shelf Sci., 79, 341–353,
1048 <https://doi.org/10.1016/j.ecss.2008.05.002>, 2008.

1049 Bell, J. J., Strano, F., Broadribb, M., Wood, G., Harris, B., Resende, A. C., Novak, E., and Micaroni, V.: Chapter Two - Sponge
1050 functional roles in a changing world, in: Advances in Marine Biology, vol. 95, edited by: Sheppard, C., Academic Press, 27–
1051 89, <https://doi.org/10.1016/bs.amb.2023.07.002>, 2023.

1052 Biard, T. and Ohman, M. D.: Vertical niche definition of test-bearing protists (Rhizaria) into the twilight zone revealed by in
1053 situ imaging, Limnol. Oceanogr., 65, 2583–2602, <https://doi.org/10.1002/lno.11472>, 2020.

1054 Biard, T., Stemmann, L., Picheral, M., Mayot, N., Vandromme, P., Hauss, H., Gorsky, G., Guidi, L., Kiko, R., and Not, F.: In
1055 situ imaging reveals the biomass of giant protists in the global ocean, Nature, 532, 504–507,
1056 <https://doi.org/10.1038/nature17652>, 2016.

1057 Biard, T., Krause, J. W., Stukel, M. R., and Ohman, M. D.: The Significance of Giant Phaeodarians (Rhizaria) to Biogenic
1058 Silica Export in the California Current Ecosystem, Glob. Biogeochem. Cycles, 32, 987–1004,
1059 <https://doi.org/10.1029/2018GB005877>, 2018.

1060 Biller, S. J., Berube, P. M., Lindell, D., and Chisholm, S. W.: Prochlorococcus: the structure and function of collective
1061 diversity, Nat. Rev. Microbiol., 13, 13–27, <https://doi.org/10.1038/nrmicro3378>, 2015.

1062 Booth, B. C. and Marchant, H. J.: Parmales, a New Order of Marine Chrysophytes, with Descriptions of Three New Genera
1063 and Seven New Species, J. Phycol., 23, 245–260, <https://doi.org/10.1111/j.1529-8817.1987.tb04132.x>, 1987.

1064 Bowler, C., De Martino, A., and Falciatore, A.: Diatom cell division in an environmental context, Curr. Opin. Plant Biol., 13,
1065 623–630, <https://doi.org/10.1016/j.pbi.2010.09.014>, 2010.

1066 Brylka, K., Alverson, A. J., Pickering, R. A., Richoz, S., and Conley, D. J.: Uncertainties surrounding the oldest fossil record
1067 of diatoms, Sci. Rep., 13, <https://doi.org/10.1038/s41598-023-35078-8>, 2023.

1068 Brylka, K., Ashworth, M. P., Alverson, A. J., and Conley, D. J.: The Cretaceous Diatom Database: A tool for investigating
1069 early diatom evolution, J. Phycol., 60, 1090–1104, <https://doi.org/10.1111/jpy.13499>, 2024.

1070 Brzezinski, M., Olson, R., and Chisholm, S.: Silicon availability and cell-cycle progression in marine diatoms, Mar. Ecol.
1071 Prog. Ser., 67, 83–96, <https://doi.org/10.3354/meps067083>, 1990.

1072 Brzezinski, M. A.: THE Si:C:N RATIO OF MARINE DIATOMS: INTERSPECIFIC VARIABILITY AND THE EFFECT
1073 OF SOME ENVIRONMENTAL VARIABLES, *J. Phycol.*, 21, 347–357, <https://doi.org/10.1111/j.0022-3646.1985.00347.x>,
1074 1985.

1075 Brzezinski, M. A., Villareal, T. A., and Lipschultz, F.: Silica production and the contribution of diatoms to new and primary
1076 production in the central North Pacific, *Mar. Ecol. Prog. Ser.*, 167, 89–104, <https://doi.org/10.3354/meps167089>, 1998.

1077 Brzezinski, M. A., Krause, J. W., Baines, S. B., Collier, J. L., Ohnemus, D. C., and Twining, B. S.: Patterns and regulation of
1078 silicon accumulation in *Synechococcus* spp., *J. Phycol.*, 53, 746–761, <https://doi.org/10.1111/jpy.12545>, 2017.

1079 Buitenhuis, E. T., Li, W. K. W., Vault, D., Lomas, M. W., Landry, M. R., Partensky, F., Karl, D. M., Ulloa, O., Campbell,
1080 L., Jacquet, S., Lantoin, F., Chavez, F., Macias, D., Gosselin, M., and McManus, G. B.: Picophytoplankton biomass
1081 distribution in the global ocean, *Earth Syst. Sci. Data*, 4, 37–46, <https://doi.org/10.5194/essd-4-37-2012>, 2012.

1082 Burki, F. and Keeling, P. J.: Rhizaria, *Curr. Biol.*, 24, R103–R107, <https://doi.org/10.1016/j.cub.2013.12.025>, 2014.

1083 Busch, K., Slaby, B. M., Bach, W., Boetius, A., Clefsen, I., Colaço, A., Creemers, M., Cristobo, J., Federwisch, L., Franke,
1084 A., Gavriilidou, A., Hethke, A., Kenchington, E., Mienis, F., Mills, S., Riesgo, A., Ríos, P., Roberts, E. M., Sipkema, D., Pita,
1085 L., Schupp, P. J., Xavier, J., Rapp, H. T., and Hentschel, U.: Biodiversity, environmental drivers, and sustainability of the
1086 global deep-sea sponge microbiome, *Nat. Commun.*, 13, <https://doi.org/10.1038/s41467-022-32684-4>, 2022.

1087 Cahoon, L. B.: The role of benthic microalgae in neritic ecosystems, in: *Oceanography and Marine Biology*, vol. 37, CRC
1088 Press, 40, 1999.

1089 Calvert, S. E.: Silica Balance in the Ocean and Diagenesis, *Nature*, 219, 919–920, <https://doi.org/10.1038/219919a0>, 1968.

1090 Cardinal, D., Alleman, L. Y., Dehairs, F., Savoye, N., Trull, T. W., and André, L.: Relevance of silicon isotopes to Si-nutrient
1091 utilization and Si-source assessment in Antarctic waters, *Glob. Biogeochem. Cycles*, 19, 2004GB002364,
1092 <https://doi.org/10.1029/2004GB002364>, 2005.

1093 Carvajal-Landinez, F. M., Helenes, J., and Murcia, L.-A. G.: Quantitative biostratigraphy and paleoecology of Neogene
1094 tropical dinoflagellate cysts, *J. South Am. Earth Sci.*, 134, 104776, <https://doi.org/10.1016/j.jsames.2023.104776>, 2024.

1095 Cassarino, L., Hendry, K. R., Henley, S. F., MacDonald, E., Arndt, S., Freitas, F. S., Pike, J., and Firing, Y. L.: Sedimentary
1096 Nutrient Supply in Productive Hot Spots off the West Antarctic Peninsula Revealed by Silicon Isotopes, *Glob. Biogeochem.*
1097 *Cycles*, 34, <https://doi.org/10.1029/2019gb006486>, 2020.

1098 Cassarino, L., Curnow, P., and Hendry, K. R.: A biomimetic peptide has no effect on the isotopic fractionation during in vitro
1099 silica precipitation, *Sci. Rep.*, 11, 9698, <https://doi.org/10.1038/s41598-021-88881-6>, 2021.

1100 Chadwick, M., Allen, C. S., Sime, L. C., Crosta, X., and Hillenbrand, C.-D.: Reconstructing Antarctic winter sea-ice extent
1101 during Marine Isotope Stage 5e, *Clim. Past*, 18, 129–146, <https://doi.org/10.5194/cp-18-129-2022>, 2022.

1102 Chang, F. H. and Gall, M.: Autecology, pigment composition and toxicology of *Dictyocha octonaria* (Dictyochophyceae,
1103 Ochrophyta) from Wellington Harbor, New Zealand, *Phycol. Res.*, 64, 65–71, <https://doi.org/10.1111/pre.12122>, 2016.

1104 Chang, F. H., McVeagh, M., Gall, M., and Smith, P.: Chattonella globosa is a member of Dictyochophyceae: reassignment to
1105 Vicicitus gen. nov., based on molecular phylogeny, pigment composition, morphology and life history, *Phycologia*, 51, 403–
1106 420, <https://doi.org/10.2216/10-104.1>, 2012.

1107 Chang, F. H., Sutherland, J., and Bradford-Grieve, J.: Taxonomic revision of Dictyochaes (Dictyochophyceae) based on
1108 morphological, ultrastructural, biochemical and molecular data, *Phycol. Res.*, 65, 235–247, <https://doi.org/10.1111/pre.12181>,
1109 2017a.

1110 Chang, S., Feng, Q., Clausen, S., and Zhang, L.: Sponge spicules from the lower Cambrian in the Yanjiahe Formation, South
1111 China: The earliest biomineralizing sponge record, *Palaeogeogr. Palaeoclimatol. Palaeoecol.*, 474, 36–44,
1112 <https://doi.org/10.1016/j.palaeo.2016.06.032>, 2017b.

1113 Chang, S., Zhang, L., Clausen, S., Bottjer, D. J., and Feng, Q.: The Ediacaran-Cambrian rise of siliceous sponges and
1114 development of modern oceanic ecosystems, *Precambrian Res.*, 333, 105438,
1115 <https://doi.org/10.1016/j.precamres.2019.105438>, 2019.

1116 Chen, C., Feng, Q., Algeo, T. J., Zhang, L., Chang, S., and Li, M.: New sponge spicules from the Ediacaran-Cambrian
1117 transition in deep-water facies of South China, *Palaeogeogr. Palaeoclimatol. Palaeoecol.*, 627, 111714,
1118 <https://doi.org/10.1016/j.palaeo.2023.111714>, 2023.

1119 Chepurnov, V. A., Mann, D. G., Vyverman, W., Sabbe, K., and Danielidis, D. B.: Sexual Reproduction, mating system, and
1120 protoplast dynamics of *Seminavis* (Bacillariophyceae), *J. Phycol.*, 38, 1004–1019, <https://doi.org/10.1046/j.1529-8817.2002.t01-1-01233.x>, 2002.

1122 Cho, H.-M., Kim, G., Kwon, E. Y., Moosdorf, N., Garcia-Orellana, J., and Santos, I. R.: Radium tracing nutrient inputs through
1123 submarine groundwater discharge in the global ocean, *Sci. Rep.*, 8, 2439, <https://doi.org/10.1038/s41598-018-20806-2>, 2018.

1124 Chong, L. S., Berelson, W. M., McManus, J., Hammond, D. E., Rollins, N. E., and Yager, P. L.: Carbon and biogenic silica
1125 export influenced by the Amazon River Plume: Patterns of remineralization in deep-sea sediments, *Deep Sea Res. Part*
1126 *Oceanogr. Res. Pap.*, 85, 124–137, <https://doi.org/10.1016/j.dsr.2013.12.007>, 2014.

1127 Chu, J., Maldonado, M., Yahel, G., and Leys, S.: Glass sponge reefs as a silicon sink, *Mar. Ecol. Prog. Ser.*, 441, 1–14,
1128 <https://doi.org/10.3354/meps09381>, 2011.

1129 Churakova, Y., Aguilera, A., Charalampous, E., Conley, D. J., Lundin, D., Pinhassi, J., and Farnelid, H.: Biogenic silica
1130 accumulation in picoeukaryotes: Novel players in the marine silica cycle, *Environ. Microbiol. Rep.*, 15, 282–290,
1131 <https://doi.org/10.1111/1758-2229.13144>, 2023.

1132 Civel-Mazens, M., Cortese, G., Crosta, X., Lawler, K. A., Lowe, V., Ikehara, M., and Itaki, T.: New Southern Ocean transfer
1133 function for subsurface temperature prediction using radiolarian assemblages, *Mar. Micropaleontol.*, 178, 102198,
1134 <https://doi.org/10.1016/j.marmicro.2022.102198>, 2023.

1135 Civel-Mazens, M., Crosta, X., Cortese, G., Lowe, V., Itaki, T., Ikehara, M., and Kohfeld, K.: Subantarctic jet migrations
1136 regulate vertical mixing in the Southern Indian, *Earth Planet. Sci. Lett.*, 642, 118877,
1137 <https://doi.org/10.1016/j.epsl.2024.118877>, 2024.

1138 Closset, I., McNair, H. M., Brzezinski, M. A., Krause, J. W., Thamtrakoln, K., and Jones, J. L.: Diatom response to alterations
1139 in upwelling and nutrient dynamics associated with climate forcing in the California Current System, *Limnol. Oceanogr.*, 66,
1140 1578–1593, <https://doi.org/10.1002/lno.11705>, 2021.

1141 Closset, I., Brzezinski, M. A., Cardinal, D., Dapoigny, A., Jones, J. L., and Robinson, R. S.: A silicon isotopic perspective on
1142 the contribution of diagenesis to the sedimentary silicon budget in the Southern Ocean, *Geochim. Cosmochim. Acta*, 327, 298–
1143 313, <https://doi.org/10.1016/j.gca.2022.04.010>, 2022.

1144 Conley, D. J.: Terrestrial ecosystems and the global biogeochemical silica cycle, *Glob. Biogeochem. Cycles*, 16,
1145 <https://doi.org/10.1029/2002gb001894>, 2002.

1146 Conley, D. J. and Carey, J. C.: Silica cycling over geologic time, *Nat. Geosci.*, 8, 431–432, <https://doi.org/10.1038/ngeo2454>,
1147 2015.

1148 Conley, D. J., Frings, P. J., Fontorbe, G., Clymans, W., Stadmark, J., Hendry, K. R., Marron, A. O., and De La Rocha, C. L.:
1149 Biosilicification Drives a Decline of Dissolved Si in the Oceans through Geologic Time, *Front. Mar. Sci.*, 4, 397,
1150 <https://doi.org/10.3389/fmars.2017.00397>, 2017.

1151 Cooke, J. and Leishman, M. R.: Consistent alleviation of abiotic stress with silicon addition: a meta-analysis, *Funct. Ecol.*, 30,
1152 1340–1357, <https://doi.org/10.1111/1365-2435.12713>, 2016.

1153 Cornelis, J. and Delvaux, B.: Soil processes drive the biological silicon feedback loop, *Funct. Ecol.*, 30, 1298–1310,
1154 <https://doi.org/10.1111/1365-2435.12704>, 2016.

1155 Crosta, X. and Koç, N.: Diatoms: From Micropaleontology to Isotope Geochemistry, in: *Developments in Marine Geology*,
1156 vol. 1, edited by: Hillaire-Marcel, C. and De Vernal, A., Elsevier, 327–369, [https://doi.org/10.1016/S1572-5480\(07\)01013-5](https://doi.org/10.1016/S1572-5480(07)01013-5),
1157 2007.

1158 Crosta, X. and Shemesh, A.: Reconciling down core anticorrelation of diatom carbon and nitrogen isotopic ratios from the
1159 Southern Ocean, *Paleoceanography*, 17, <https://doi.org/10.1029/2000PA000565>, 2002.

1160 Crosta, X., Etourneau, J., Orme, L. C., Dalaiden, Q., Campagne, P., Swingedouw, D., Goosse, H., Massé, G., Miettinen, A.,
1161 McKay, R. M., Dunbar, R. B., Escutia, C., and Ikehara, M.: Multi-decadal trends in Antarctic sea-ice extent driven by ENSO–
1162 SAM over the last 2,000 years, *Nat. Geosci.*, 14, 156–160, <https://doi.org/10.1038/s41561-021-00697-1>, 2021.

1163 Cumming, B. F., Wilson, S. E., and Smol, J. P.: Paleolimnological potential of chrysophyte cysts and scales and of sponge
1164 spicules as indicators of lake salinity, *Int. J. Salt Lake Res.*, 2, 87–92, <https://doi.org/10.1007/BF02905055>, 1993.

1165 Currie, H. A. and Perry, C. C.: Silica in Plants: Biological, Biochemical and Chemical Studies, *Ann. Bot.*, 100, 1383–1389,
1166 <https://doi.org/10.1093/aob/mcm247>, 2007.

1167 De Freitas Oliveira, M. R., da Costa, C., and Benedito, E.: Trends and gaps in scientific production on freshwater sponges,
1168 *Oecologia Aust.*, 24, 61–75, <https://doi.org/10.4257/oeco.2020.2401.05>, 2020.

1169 De Goeij, J. M., Van Oevelen, D., Vermeij, M. J. A., Osinga, R., Middelburg, J. J., De Goeij, A. F. P. M., and Admiraal, W.:
1170 Surviving in a Marine Desert: The Sponge Loop Retains Resources Within Coral Reefs, *Science*, 342, 108–110,
1171 <https://doi.org/10.1126/science.1241981>, 2013.

1172 De La Rocha, C. L., Brzezinski, M. A., and DeNiro, M. J.: Fractionation of silicon isotopes by marine diatoms during biogenic
1173 silica formation, *Geochim. Cosmochim. Acta*, 61, 5051–5056, [https://doi.org/10.1016/S0016-7037\(97\)00300-1](https://doi.org/10.1016/S0016-7037(97)00300-1), 1997.

1174 De La Rocha, C. L., Brzezinski, M. A., DeNiro, M. J., and Shemesh, A.: Silicon-isotope composition of diatoms as an indicator
1175 of past oceanic change, *Nature*, 395, 680–683, <https://doi.org/10.1038/27174>, 1998.

1176 De Tommasi, E., Gielis, J., and Rogato, A.: Diatom Frustule Morphogenesis and Function: a Multidisciplinary Survey, *Mar.*
1177 *Genomics*, 35, 1–18, <https://doi.org/10.1016/j.margen.2017.07.001>, 2017.

1178 De Wever, P., Dumitrica, P., Caulet, J. P., Nigrini, C., and Caridroit, M.: Radiolarians in the Sedimentary Record, 0 ed., Gordan
1179 and Breach Science Publishers, <https://doi.org/10.1201/9781482283181>, 2001.

1180 Decelle, J., Veronesi, G., LeKieffre, C., Gallet, B., Chevalier, F., Stryhanyuk, H., Marro, S., Ravanel, S., Tucoulou, R.,
1181 Schieber, N., Finazzi, G., Schwab, Y., and Musat, N.: Subcellular architecture and metabolic connection in the planktonic
1182 photosymbiosis between Collodaria (radiolarians) and their microalgae, *Environ. Microbiol.*, 23, 6569–6586,
1183 <https://doi.org/10.1111/1462-2920.15766>, 2021.

1184 Demarest, M. S., Brzezinski, M. A., and Beucher, C. P.: Fractionation of silicon isotopes during biogenic silica dissolution,
1185 *Geochim. Cosmochim. Acta*, 73, 5572–5583, <https://doi.org/10.1016/j.gca.2009.06.019>, 2009.

1186 DeMaster, D. J.: The supply and accumulation of silica in the marine environment, *Geochim. Cosmochim. Acta*, 45, 1715–
1187 1732, [https://doi.org/10.1016/0016-7037\(81\)90006-5](https://doi.org/10.1016/0016-7037(81)90006-5), 1981.

1188 DeMaster, D. J.: The Diagenesis of Biogenic Silica: Chemical Transformations Occurring in the Water Column, Seabed, and
1189 Crust, *Treatise Geochem.*, 7, 407, <https://doi.org/10.1016/B0-08-043751-6/07095-X>, 2003.

1190 DeMaster, D. J.: The Global Marine Silica Budget: Sources and Sinks, in: *Encyclopedia of Ocean Sciences*, vol. 1, edited by:
1191 Cochran, J. K., Bokuniewicz, H. J., and Yager, P. L., Elsevier, 473–483, [https://doi.org/10.1016/b978-0-12-409548-9.10799-](https://doi.org/10.1016/b978-0-12-409548-9.10799-7)
1192 7, 2019.

1193 Deshmukh, R., Sonah, H., and Belanger, R. R.: New evidence defining the evolutionary path of aquaporins regulating silicon
1194 uptake in land plants, *J. Exp. Bot.*, 71, 6775–6788, <https://doi.org/10.1093/jxb/eraa342>, 2020.

1195 Doering, K., Erdem, Z., Ehlert, C., Fleury, S., Frank, M., and Schneider, R.: Changes in diatom productivity and upwelling
1196 intensity off Peru since the Last Glacial Maximum: Response to basin-scale atmospheric and oceanic forcing,
1197 *Paleoceanography*, 31, 1453–1473, <https://doi.org/10.1002/2016PA002936>, 2016.

1198 Doering, K., Ehlert, C., Pahnke, K., Frank, M., Schneider, R., and Grasse, P.: Silicon Isotope Signatures of Radiolaria Reveal
1199 Taxon-Specific Differences in Isotope Fractionation, *Front. Mar. Sci.*, 8, <https://doi.org/10.3389/fmars.2021.666896>, 2021.

1200 Dumitrica, P.: Double skeletons of silicoflagellates: Their reciprocal position and taxonomical and paleobiological values,
1201 *Rev. Micropaléontologie*, 57, 57–74, <https://doi.org/10.1016/j.revmic.2014.04.001>, 2014.

1202 Durak, G. M., Taylor, A. R., Walker, C. E., Probert, I., De Vargas, C., Audic, S., Schroeder, D., Brownlee, C., and Wheeler,
1203 G. L.: A role for diatom-like silicon transporters in calcifying coccolithophores, *Nat. Commun.*, 7, 10543,
1204 <https://doi.org/10.1038/ncomms10543>, 2016.

1205 Durbin, E. G.: Studies on the autecology of the marine diatom *Thalassiosira nordenskiöldii* II. The influence of cell size
1206 on growth rate, and carbon, nitrogen, chlorophyll *a* and silica content, *J. Phycol.*, 13, 150–155, [https://doi.org/10.1111/j.1529-](https://doi.org/10.1111/j.1529-8817.1977.tb02904.x)
1207 8817.1977.tb02904.x, 1977.

1208 Durkin, C. A., Koester, J. A., Bender, S. J., and Armbrust, E. V.: The evolution of silicon transporters in diatoms, *J. Phycol.*,
1209 52, 716–731, <https://doi.org/10.1111/jpy.12441>, 2016.

1210 Eckford-Soper, L. and Daugbjerg, N.: The ichthyotoxic genus *Pseudochattonella* (Dictyochophyceae): Distribution, toxicity,
1211 enumeration, ecological impact, succession and life history – A review, *Harmful Algae*, 58, 51–58,
1212 <https://doi.org/10.1016/j.hal.2016.08.002>, 2016.

1213 Egan, K. E., Rickaby, R. E. M., Leng, M. J., Hendry, K. R., Hermoso, M., Sloane, H. J., Bostock, H., and Halliday, A. N.:
1214 Diatom silicon isotopes as a proxy for silicic acid utilisation: A Southern Ocean core top calibration, *Geochim. Cosmochim.*
1215 *Acta*, 96, 174–192, <https://doi.org/10.1016/j.gca.2012.08.002>, 2012.

1216 Ehler, C., Doering, K., Wallmann, K., Scholz, F., Sommer, S., Grasse, P., Geilert, S., and Frank, M.: Stable silicon isotope
1217 signatures of marine pore waters – Biogenic opal dissolution versus authigenic clay mineral formation, *Geochim. Cosmochim.*
1218 *Acta*, 191, 102–117, <https://doi.org/10.1016/j.gca.2016.07.022>, 2016.

1219 Ehrenberg: Ueber das Massenverhältniss der jetzt lebenden Kiesel-Infusorien und über ein neues Infusorien-Conglomerat als
1220 Polirschiefer von Jastraba in Ungarn, *Ann. Phys.*, 117, 555–558, <https://doi.org/10.1002/andp.18371170712>, 1837.

1221 Ehrlich, H., Deutzmann, R., Brunner, E., Cappellini, E., Koon, H., Solazzo, C., Yang, Y., Ashford, D., Thomas-Oates, J.,
1222 Lubeck, M., Baessmann, C., Langrock, T., Hoffmann, R., Wörheide, G., Reitner, J., Simon, P., Tsurkan, M., Ereskovsky, A.
1223 V., Kurek, D., Bazhenov, V. V., Hunoldt, S., Mertig, M., Vyalikh, D. V., Molodtsov, S. L., Kummer, K., Worch, H., Smetacek,
1224 V., and Collins, M. J.: Mineralization of the metre-long biosilica structures of glass sponges is templated on hydroxylated
1225 collagen, *Nat. Chem.*, 2, 1084–1088, <https://doi.org/10.1038/nchem.899>, 2010.

1226 Eicken, H.: From the Microscopic, to the Macroscopic, to the Regional Scale: Growth, Microstructure and Properties of Sea
1227 Ice, in: *Sea Ice: An Introduction to its Physics, Chemistry, Biology and Geology*, edited by: Thomas, D. N. and Dieckmann,
1228 G. S., Wiley, 22–81, <https://doi.org/10.1002/9780470757161.ch2>, 2003.

1229 Esenkulova, S., Sutherland, B. J. G., Tabata, A., Haigh, N., Pearce, C. M., and Miller, K. M.: Comparing metabarcoding and
1230 morphological approaches to identify phytoplankton taxa associated with harmful algal blooms, *Facets*, 5, 784–811,
1231 <https://doi.org/10.1139/facets-2020-0025>, 2020.

1232 Fabre, S., Jeandel, C., Zambardi, T., Roustan, M., and Almar, R.: An Overlooked Silica Source of the Modern Oceans: Are
1233 Sandy Beaches the Key?, *Front. Earth Sci.*, 7, <https://doi.org/10.3389/feart.2019.00231>, 2019.

1234 Fagerness, V. L.: The spring bloom of the silicoflagellate *Dictyocha speculum* in East Sound, Washington, with respect to
1235 certain environmental factors, 1984.

1236 Falkowski, P. G., Katz, M. E., Knoll, A. H., Quigg, A., Raven, J. A., Schofield, O., and Taylor, F. J. R.: The Evolution of
1237 Modern Eukaryotic Phytoplankton, *Science*, 305, 354–360, <https://doi.org/10.1126/science.1095964>, 2004.

1238 Falkowski, P. G., Fenchel, T., and Delong, E. F.: The Microbial Engines That Drive Earth’s Biogeochemical Cycles, *Science*,
1239 320, 1034–1039, <https://doi.org/10.1126/science.1153213>, 2008.

1240 Farooq, M. A. and Dietz, K.-J.: Silicon as Versatile Player in Plant and Human Biology: Overlooked and Poorly Understood,
1241 *Front. Plant Sci.*, 6, <https://doi.org/10.3389/fpls.2015.00994>, 2015.

1242 Faure, E., Not, F., Benoiston, A.-S., Labadie, K., Bittner, L., and Ayata, S.-D.: Mixotrophic protists display contrasted
1243 biogeographies in the global ocean, *ISME J.*, 13, 1072–1083, <https://doi.org/10.1038/s41396-018-0340-5>, 2019.

1244 Ferguson, A. and Davis, A.: Heart of glass: spicule armament and physical defense in temperate reef sponges, *Mar. Ecol. Prog.*
1245 *Ser.*, 372, 77–86, <https://doi.org/10.3354/meps07680>, 2008.

1246 Fernandez, N. M., Bouchez, J., Derry, L. A., Chorover, J., Gaillardet, J., Giesbrecht, I., Fries, D., and Druhan, J. L.: Resiliency
1247 of Silica Export Signatures When Low Order Streams Are Subject to Storm Events, *J. Geophys. Res. Biogeosciences*, 127,
1248 <https://doi.org/10.1029/2021jg006660>, 2022.

1249 Field, C. B., Behrenfeld, M. J., Randerson, J. T., and Falkowski, P.: Primary Production of the Biosphere: Integrating
1250 Terrestrial and Oceanic Components, *Science*, 281, 237–240, <https://doi.org/10.1126/science.281.5374.237>, 1998.

1251 Flombaum, P., Wang, W.-L., Primeau, F. W., and Martiny, A. C.: Global picophytoplankton niche partitioning predicts overall
1252 positive response to ocean warming, *Nat. Geosci.*, 13, 116–120, <https://doi.org/10.1038/s41561-019-0524-2>, 2020.

1253 Flynn, K. J. and Martin-Jézéquel, V.: Modelling Si-N-limited growth of diatoms, *J. Plankton Res.*, 22, 447–472,
1254 <https://doi.org/10.1093/plankt/22.3.447>, 2000.

1255 Folkers, M. and Rombouts, T.: Sponges Revealed: A Synthesis of Their Overlooked Ecological Functions Within Aquatic
1256 Ecosystems, in: *YOUMARES 9 - The Oceans: Our Research, Our Future*, edited by: Jungblut, S., Liebich, V., and Bode-
1257 Dalby, M., Springer International Publishing, Cham, 181–193, https://doi.org/10.1007/978-3-030-20389-4_9, 2020.

1258 Fontorbe, G., Frings, P. J., De La Rocha, C. L., Hendry, K. R., and Conley, D. J.: A silicon depleted North Atlantic since the
1259 Palaeogene: Evidence from sponge and radiolarian silicon isotopes, *Earth Planet. Sci. Lett.*, 453, 67–77,
1260 <https://doi.org/10.1016/j.epsl.2016.08.006>, 2016.

1261 Fontorbe, G., Frings, P. J., De La Rocha, C. L., Hendry, K. R., Carstensen, J., and Conley, D. J.: Enrichment of dissolved silica
1262 in the deep equatorial Pacific during the Eocene-Oligocene, *Paleoceanography*, 32, 848–863,
1263 <https://doi.org/10.1002/2017PA003090>, 2017.

1264 Fortey, R. A. and Holdsworth, B. K.: The oldest known well-preserved Radiolaria, *Boll. Della Soc. Paleontol. Ital.*, 10, 35–
1265 41, 1971.

1266 Frings, P. J., Clymans, W., Fontorbe, G., De La Rocha, C. L., and Conley, D. J.: The continental Si cycle and its impact on the
1267 ocean Si isotope budget, *Chem. Geol.*, 425, 12–36, <https://doi.org/10.1016/j.chemgeo.2016.01.020>, 2016.

1268 Frings, P. J., Schubring, F., Oelze, M., and Von Blanckenburg, F.: Quantifying biotic and abiotic Si fluxes in the Critical Zone
1269 with Ge/Si ratios along a gradient of erosion rates, *Am. J. Sci.*, 321, 1204–1245, <https://doi.org/10.2475/08.2021.03>, 2021.

1270 Frings, P. J., Panizzo, V. N., Sutton, J. N., and Ehlert, C.: Diatom silicon isotope ratios in Quaternary research: Where do we
1271 stand?, *Quat. Sci. Rev.*, 344, 108966, <https://doi.org/10.1016/j.quascirev.2024.108966>, 2024.

1272 Fripiat, F., Cardinal, D., Tison, J.-L., Worby, A., and André, L.: Diatom-induced silicon isotopic fractionation in Antarctic sea
1273 ice, *J. Geophys. Res. Biogeosciences*, 112, <https://doi.org/10.1029/2006JG000244>, 2007.

1274 Fripiat, F., Tison, J.-L., André, L., Notz, D., and Delille, B.: Biogenic silica recycling in sea ice inferred from Si-isotopes:
1275 constraints from Arctic winter first-year sea ice, *Biogeochemistry*, 119, 25–33, <https://doi.org/10.1007/s10533-013-9911-8>,
1276 2014.

1277 Fuhrman, J. A.: Marine viruses and their biogeochemical and ecological effects, *Nature*, 399, 541–548,
1278 <https://doi.org/10.1038/21119>, 1999.

1279 Gaino, E., Scoccia, F., Piersanti, S., Rebora, M., Bellucci, L. G., and Ludovisi, A.: Spicule records of *Ephydatia fluviatilis* as
1280 a proxy for hydrological and environmental changes in the shallow Lake Trasimeno (Umbria, Italy), *Hydrobiologia*, 679, 139–
1281 153, <https://doi.org/10.1007/s10750-011-0861-7>, 2012.

1282 Geilert, S., Grasse, P., Doering, K., Wallmann, K., Ehlert, C., Scholz, F., Frank, M., Schmidt, M., and Hensen, C.: Impact of
1283 ambient conditions on the Si isotope fractionation in marine pore fluids during early diagenesis, [https://doi.org/10.5194/bg-](https://doi.org/10.5194/bg-2019-481)
1284 2019-481, 8 January 2020.

1285 Geilert, S., Frick, D. A., Garbe-Schönberg, D., Scholz, F., Sommer, S., Grasse, P., Vogt, C., and Dale, A. W.: Coastal El Niño
1286 triggers rapid marine silicate alteration on the seafloor, *Nat. Commun.*, 14, <https://doi.org/10.1038/s41467-023-37186-5>, 2023.

1287 Gentil, J., Hempel, F., Moog, D., Zauner, S., and Maier, U. G.: Review: origin of complex algae by secondary endosymbiosis:
1288 a journey through time, *J. Soil Sci. Plant Nutr.*, 254, 1835–1843, <https://doi.org/10.1007/s00709-017-1098-8>, 2017.

1289 Gereá, M., Saad, J., Izaguirre, I., Queimaliños, C., Gasol, J., and Unrein, F.: Presence, abundance and bacterivory of the
1290 mixotrophic algae *Pseudopedinella* (Dictyochophyceae) in freshwater environments, *Aquat. Microb. Ecol.*, 76, 219–232,
1291 <https://doi.org/10.3354/ame01780>, 2016.

1292 Ghobara, M. M., Ghobara, M. M., Mazumder, N., Vinayak, V., Reissig, L., Gebeshuber, I. C., Tiffany, M. A., Gordon, R., and
1293 Gordon, R.: On Light and Diatoms: A Photonics and Photobiology Review, in: *Diatoms: Fundamentals and Applications*, John
1294 Wiley & Sons, Ltd, 129–189, <https://doi.org/10.1002/9781119370741.ch7>, 2019.

1295 Giesbrecht, K. E. and Varela, D. E.: Summertime Biogenic Silica Production and Silicon Limitation in the Pacific Arctic
1296 Region From 2006 to 2016, *Glob. Biogeochem. Cycles*, 35, e2020GB006629, <https://doi.org/10.1029/2020GB006629>, 2021.

1297 Görlich, S., Pawolski, D., Zlotnikov, I., and Kröger, N.: Control of biosilica morphology and mechanical performance by the
1298 conserved diatom gene *Silicanin-1*, *Commun. Biol.*, 2, <https://doi.org/10.1038/s42003-019-0436-0>, 2019.

1299 Gouretski, V. V. and Koltermann, K. P.: WOCE - Global Hydrographic Climatology: A Technical Report, Bundesamt für
1300 Seeschifffahrt und Hydrographie (BSH), Hamburg & Rostock, <https://doi.org/10.57802/azf1-r757>, 2004.

1301 Gouvêa, L., Fragkopoulou, E., B. Araújo, M., Serrão, E. A., and Assis, J.: Seagrass Biodiversity Under the Latest-Generation
1302 Scenarios of Projected Climate Change, *J. Biogeogr.*, 52, 172–185, <https://doi.org/10.1111/jbi.15021>, 2024.

1303 Grasse, P., Closset, I., Jones, J. L., Geilert, S., and Brzezinski, M. A.: Controls on Dissolved Silicon Isotopes Along the U.S.
1304 GEOTRACES Eastern Pacific Zonal Transect (GP16), *Glob. Biogeochem. Cycles*, 34, e2020GB006538,
1305 <https://doi.org/10.1029/2020GB006538>, 2020.

1306 Grenne, T. and Slack, J. F.: Paleozoic and Mesozoic silica-rich seawater: Evidence from hematitic chert (jasper) deposits,
1307 *Geology*, 31, 319, [https://doi.org/10.1130/0091-7613\(2003\)031%253C0319:pamsrs%253E2.0.co;2](https://doi.org/10.1130/0091-7613(2003)031%253C0319:pamsrs%253E2.0.co;2), 2003.

1308 Gutierrez-Rodriguez, A., Stukel, M. R., Lopes dos Santos, A., Biard, T., Scharek, R., Vaultot, D., Landry, M. R., and Not, F.:
1309 High contribution of Rhizaria (Radiolaria) to vertical export in the California Current Ecosystem revealed by DNA
1310 metabarcoding, *ISME J.*, 13, 964–976, <https://doi.org/10.1038/s41396-018-0322-7>, 2019.

1311 Haeckel, E.: Report on the Radiolaria collected by H.M.S. Challenger during the years 1873-1876, *Zoology*, 18, 1–1803, 1887.

1312 Halbach, L., Vihtakari, M., Duarte, P., Everett, A., Granskog, M. A., Hop, H., Kauko, H. M., Kristiansen, S., Myhre, P. I.,
1313 Pavlov, A. K., Pramanik, A., Tatarek, A., Torsvik, T., Wiktor, J. M., Wold, A., Wulff, A., Steen, H., and Assmy, P.: Tidewater
1314 Glaciers and Bedrock Characteristics Control the Phytoplankton Growth Environment in a Fjord in the Arctic, *Front. Mar.*
1315 *Sci.*, 6, <https://doi.org/10.3389/fmars.2019.00254>, 2019.

1316 Hamm, C. E., Merkel, R., Springer, O., Jurkojc, P., Maier, C., Prechtel, K., and Smetacek, V.: Architecture and material
1317 properties of diatom shells provide effective mechanical protection, *Nature*, 421, 841–843,
1318 <https://doi.org/10.1038/nature01416>, 2003.

1319 Harper, H. E. and Knoll, A. H.: Silica, diatoms, and Cenozoic radiolarian evolution, *Geology*, 3, 175,
1320 [https://doi.org/10.1130/0091-7613\(1975\)3%253C175:sdacre%253E2.0.co;2](https://doi.org/10.1130/0091-7613(1975)3%253C175:sdacre%253E2.0.co;2), 1975.

1321 Harrison, F. W.: Sponges (Porifera: Spongillidae), in: *Pollution Ecology of Freshwater Invertebrates*, edited by: Hart, C. W.
1322 and Fuller, S. L. H., Academic Press New York, New York, 29–66, 1974.

1323 Hartley, S. E. and DeGabriel, J. L.: The ecology of herbivore-induced silicon defences in grasses, *Funct. Ecol.*, 30, 1311–1322,
1324 <https://doi.org/10.1111/1365-2435.12706>, 2016.

1325 Hatton, J. E., Hendry, K. R., Hawkings, J. R., Wadham, J. L., Kohler, T. J., Stibal, M., Beaton, A. D., Bagshaw, E. A., and
1326 Telling, J.: Investigation of subglacial weathering under the Greenland Ice Sheet using silicon isotopes, *Geochim. Cosmochim.*
1327 *Acta*, 247, 191–206, <https://doi.org/10.1016/j.gca.2018.12.033>, 2019a.

1328 Hatton, J. E., Hendry, K. R., Hawkings, J. R., Wadham, J. L., Opfergelt, S., Kohler, T. J., Yde, J. C., Stibal, M., and Žárský,
1329 J. D.: Silicon isotopes in Arctic and sub-Arctic glacial meltwaters: the role of subglacial weathering in the silicon cycle, *Proc.*
1330 *R. Soc. Math. Phys. Eng. Sci.*, 475, 20190098, <https://doi.org/10.1098/rspa.2019.0098>, 2019b.

1331 Hatton, J. E., Hendry, K. R., Hawkings, J. R., Wadham, J. L., Benning, L. G., Blukis, R., Roddatis, V., Ng, H. C., and Wang,
1332 T.: Physical weathering by glaciers enhances silicon mobilisation and isotopic fractionation, *Geochem. Perspect. Lett.*, 7–12,
1333 <https://doi.org/10.7185/geochemlet.2126>, 2021.

1334 Hatton, J. E., Ng, H. C., Meire, L., Woodward, E. M. S., Leng, M. J., Coath, C. D., Stuart-Lee, A., Wang, T., Annett, A. L.,
1335 and Hendry, K. R.: Silicon Isotopes Highlight the Role of Glaciated Fjords in Modifying Coastal Waters, *J. Geophys. Res.*
1336 *Biogeosciences*, 128, <https://doi.org/10.1029/2022jg007242>, 2023.

1337 Hawkings, J. R., Wadham, J. L., Benning, L. G., Hendry, K. R., Tranter, M., Tedstone, A., Nienow, P., and Raiswell, R.: Ice
1338 sheets as a missing source of silica to the polar oceans, *Nat. Commun.*, 8, <https://doi.org/10.1038/ncomms14198>, 2017.

1339 Hawkings, J. R., Hatton, J. E., Hendry, K. R., De Souza, G. F., Wadham, J. L., Ivanovic, R., Kohler, T. J., Stibal, M., Beaton,
1340 A., Lamarche-Gagnon, G., Tedstone, A., Hain, M. P., Bagshaw, E., Pike, J., and Tranter, M.: The silicon cycle impacted by
1341 past ice sheets, *Nat. Commun.*, 9, <https://doi.org/10.1038/s41467-018-05689-1>, 2018.

1342 Hendry, K. R. and Robinson, L. F.: The relationship between silicon isotope fractionation in sponges and silicic acid
1343 concentration: Modern and core-top studies of biogenic opal, *Geochim. Cosmochim. Acta*, 81, 1–12,
1344 <https://doi.org/10.1016/j.gca.2011.12.010>, 2012.

1345 Hendry, K. R., Georg, R. B., Rickaby, R. E. M., Robinson, L. F., and Halliday, A. N.: Deep ocean nutrients during the Last
1346 Glacial Maximum deduced from sponge silicon isotopic compositions, *Earth Planet. Sci. Lett.*, 292, 290–300,
1347 <https://doi.org/10.1016/j.epsl.2010.02.005>, 2010.

1348 Hendry, K. R., Swann, G. E. A., Leng, M. J., Sloane, H. J., Goodwin, C., Berman, J., and Maldonado, M.: Silica stable isotopes
1349 and silicification in a carnivorous sponge *Asbestopluma* sp., *Biogeosciences Discuss.*, 11, 16573–16597,
1350 <https://doi.org/10.5194/bgd-11-16573-2014>, 2014.

1351 Hendry, K. R., Marron, A. O., Vincent, F., Conley, D. J., Gehlen, M., Ibarbalz, F. M., Quéguiner, B., and Bowler, C.:
1352 Competition between Silicifiers and Non-silicifiers in the Past and Present Ocean and Its Evolutionary Impacts, *Front. Mar.*
1353 *Sci.*, 5, 22, <https://doi.org/10.3389/fmars.2018.00022>, 2018.

1354 Hendry, K. R., Sales De Freitas, F., Arndt, S., Beaton, A., Friberg, L., Hatton, J. E., Hawkings, J. R., Jones, R. L., Krause, J.
1355 W., Meire, L., Ng, H. C., Pryer, H., Tingey, S., Van De Velde, S. J., Wadham, J., Wang, T., and Woodward, E. M. S.: Insights
1356 into silicon cycling from ice sheet to coastal ocean from isotope geochemistry, *Commun. Earth Environ.*, 6,
1357 <https://doi.org/10.1038/s43247-025-02264-7>, 2025.

1358 Heneghan, R. F., Holloway-Brown, J., Gasol, J. M., Herndl, G. J., Morán, X. A. G., and Galbraith, E. D.: The global
1359 distribution and climate resilience of marine heterotrophic prokaryotes, *Nat. Commun.*, 15, [https://doi.org/10.1038/s41467-](https://doi.org/10.1038/s41467-024-50635-z)
1360 024-50635-z, 2024.

1361 Henriksen, P., Knipschildt, F., Moestrup, Ø., and Thomsen, H. A.: Autecology, life history and toxicology of the
1362 silicoflagellate *Dictyocha speculum* (Silicoflagellata, Dictyochophyceae), *Phycologia*, 32, 29–39,
1363 <https://doi.org/10.2216/i0031-8884-32-1-29.1>, 1993.

1364 Herman, P. M. J., Hemminga, M. A., Nienhuis, P. H., Verschuure, J. M., and Wessel, E. G. J.: Wax and wane of eelgrass
1365 *Zostera marina* and water column silicon levels, *Mar. Ecol. Prog. Ser.*, 144, 303–307, <https://doi.org/10.3354/meps144303>,
1366 1996.

1367 Hernández-Almeida, I., Cortese, G., Yu, P. -S., Chen, M. -T., and Kucera, M.: Environmental determinants of radiolarian
1368 assemblages in the western Pacific since the last deglaciation, *Paleoceanography*, 32, 830–847,
1369 <https://doi.org/10.1002/2017PA003159>, 2017.

1370 Hernández-Becerril, D. U. and Bravo-Sierra, E.: Planktonic Silicoflagellates (Dictyochophyceae) from the Mexican Pacific
1371 Ocean, *Bot. Mar.*, 44, <https://doi.org/10.1515/bot.2001.050>, 2001.

1372 Hervé, V., Derr, J., Douady, S., Quinet, M., Moisan, L., and Lopez, P. J.: Multiparametric Analyses Reveal the pH-Dependence
1373 of Silicon Biomineralization in Diatoms, *PLOS ONE*, 7, e46722, <https://doi.org/10.1371/journal.pone.0046722>, 2012.

1374 Hiebert, T. C., Thompson, A. W., and Sutherland, K. R.: Diverse microbial prey in the guts of gelatinous grazers revealed by
1375 microscopy, *Mar. Biol.*, 172, <https://doi.org/10.1007/s00227-025-04615-6>, 2025.

1376 Hildebrand, M. and Lerch, S. J. L.: Diatom silica biomineralization: Parallel development of approaches and understanding,
1377 *Semin. Cell Dev. Biol.*, 46, 27–35, <https://doi.org/10.1016/j.semcdb.2015.06.007>, 2015.

1378 Hildebrand, M., Volcani, B. E., Gassmann, W., and Schroeder, J. I.: A gene family of silicon transporters, *Nature*, 385, 688–
1379 689, <https://doi.org/10.1038/385688b0>, 1997.

1380 Hildebrand, M., Lerch, S. J. L., and Shrestha, R. P.: Understanding Diatom Cell Wall Silicification—Moving Forward, *Front.*
1381 *Mar. Sci.*, 5, <https://doi.org/10.3389/fmars.2018.00125>, 2018.

1382 Hirota, R., Hata, Y., Ikeda, T., Ishida, T., and Kuroda, A.: The Silicon Layer Supports Acid Resistance of *Bacillus cereus*
1383 Spores, *J. Bacteriol.*, 192, 111–116, <https://doi.org/10.1128/jb.00954-09>, 2010.

1384 Hobbie, J. E., Daley, R. J., and Jasper, S.: Use of nuclepore filters for counting bacteria by fluorescence microscopy, *Appl.*
1385 *Environ. Microbiol.*, 33, 1225–1228, <https://doi.org/10.1128/aem.33.5.1225-1228.1977>, 1977.

1386 Hodell, D. A., Kanfoush, S. L., Shemesh, A., Crosta, X., Charles, C. D., and Guilderson, T. P.: Abrupt Cooling of Antarctic
1387 Surface Waters and Sea Ice Expansion in the South Atlantic Sector of the Southern Ocean at 5000 cal yr B.P., *Quat. Res.*, 56,
1388 191–198, <https://doi.org/10.1006/qres.2001.2252>, 2001.

1389 Hodson, M. J., White, P. J., Mead, A., and Broadley, M. R.: Phylogenetic Variation in the Silicon Composition of Plants, *Ann.*
1390 *Bot.*, 96, 1027–1046, <https://doi.org/10.1093/aob/mci255>, 2005.

1391 Hong, W.-L., Sun, X., Torres, M. E., Huang, T.-H., and Pickering, R. A.: The role of silicate alteration in regulating marine
1392 carbon cycling, *Chem. Geol.*, 684, 122769, <https://doi.org/10.1016/j.chemgeo.2025.122769>, 2025.

1393 Hooper, J. N. A. and Van Soest, R. W. M.: *Systema Porifera. A Guide to the Classification of Sponges*, in: *Systema Porifera*,
1394 Springer US, Boston, MA, 1–7, https://doi.org/10.1007/978-1-4615-0747-5_1, 2002.

1395 Hopwood, M. J., Carroll, D., Dunse, T., Hodson, A., Holding, J. M., Iriarte, J. L., Ribeiro, S., Achterberg, E. P., Cantoni, C.,
1396 Carlson, D. F., Chierici, M., Clarke, J. S., Cozzi, S., Fransson, A., Juul-Pedersen, T., Winding, M. H. S., and Meire, L.: Review
1397 article: How does glacier discharge affect marine biogeochemistry and primary production in the Arctic?, *The Cryosphere*, 14,
1398 1347–1383, <https://doi.org/10.5194/tc-14-1347-2020>, 2020.

1399 Hopwood, M. J., Carroll, D., Gu, Y., Huang, X., Krause, J., Cozzi, S., Cantoni, C., Gastelu Barcena, M. F., Carroll, S., and
1400 Körtzinger, A.: A Close Look at Dissolved Silica Dynamics in Disko Bay, West Greenland, *Glob. Biogeochem. Cycles*, 39,
1401 <https://doi.org/10.1029/2023gb008080>, 2025.

1402 Hou, Y., Baronas, J., Kemeny, P., Bouchez, J., Geirsdóttir, Á., Miller, G., and Torres, M.: Glacially enhanced silicate
1403 weathering revealed by Holocene lake records, <https://doi.org/10.31223/X5RM73>, 8 February 2025.

1404 Ignatiades, L.: The Relationship of the Seasonality of Silicoflagellates to Certain Environmental Factors, *Bot. Mar.*, 13,
1405 <https://doi.org/10.1515/botm.1970.13.1.44>, 1970.

1406 Iler, R. K.: The chemistry of silica, Solubility, Polymerization, *Colloid Surf. Prop. Biochem.*, 866, 1979.

1407 Inagaki, F., Motomura, Y., and Ogata, S.: Microbial silica deposition in geothermal hot waters, *Appl. Microbiol. Biotechnol.*,
1408 60, 605–611, <https://doi.org/10.1007/s00253-002-1100-y>, 2003.

1409 Isson, T. T. and Planavsky, N. J.: Reverse weathering as a long-term stabilizer of marine pH and planetary climate, *Nature*,
1410 560, 471–475, <https://doi.org/10.1038/s41586-018-0408-4>, 2018.

1411 Iwai, M., Motoyama, I., Lin, W., Takashima, R., Yamada, Y., and Eguchi, N.: Diatom and Radiolarian Biostratigraphy in the
1412 Vicinity of the 2011 Tohoku Earthquake Source Fault in IODP Hole 343- C0019E of JFAST, *Isl. Arc*, 34, e70009,
1413 <https://doi.org/10.1111/iar.70009>, 2025.

1414 Jeong, Y. and Lee, J.: Comparative analysis of organelle genomes provides conflicting evidence between morphological
1415 similarity and phylogenetic relationship in diatoms, *Front. Mar. Sci.*, 10, <https://doi.org/10.3389/fmars.2023.1283893>, 2024.

1416 Jewson, D. H.: Size reduction, reproductive strategy and the life cycle of a centric diatom, *Philos. Trans. R. Soc. Lond.*, 336,
1417 191–213, <https://doi.org/10.1098/rstb.1992.0056>, 1997.

1418 Jin, X., Gruber, N., Dunne, J. P., Sarmiento, J. L., and Armstrong, R. A.: Diagnosing the contribution of phytoplankton
1419 functional groups to the production and export of particulate organic carbon, CaCO₃, and opal from global nutrient and
1420 alkalinity distributions, *Glob. Biogeochem. Cycles*, 20, <https://doi.org/10.1029/2005gb002532>, 2006.

1421 Jochem, F. and Babenerd, B.: Naked Dictyocha speculum – a new type of phytoplankton bloom in the Western Baltic, *Mar.*
1422 *Biol.*, 103, 373–379, <https://doi.org/10.1007/bf00397272>, 1989.

1423 Johnson, S. N., Waterman, J. M., Hartley, S. E., Cooke, J., Ryalls, J. M. W., Lagisz, M., and Nakagawa, S.: Plant Silicon
1424 Defences Suppress Herbivore Performance, but Mode of Feeding Is Key, *Ecol. Lett.*, 27, e14519,
1425 <https://doi.org/10.1111/ele.14519>, 2024.

1426 Jordan, R. and McCartney, K.: *Stephanocha* nom. nov., a replacement name for the illegitimate silicoflagellate genus
1427 *Distephanus* Stöhr., *Phytotaxa*, 201, 177–187, 2015.

1428 Jumper, J., Evans, R., Pritzel, A., Green, T., Figurnov, M., Ronneberger, O., Tunyasuvunakool, K., Bates, R., Žídek, A.,
1429 Potapenko, A., Bridgland, A., Meyer, C., Kohl, S. A. A., Ballard, A. J., Cowie, A., Romera-Paredes, B., Nikolov, S., Jain, R.,
1430 Adler, J., Back, T., Petersen, S., Reiman, D., Clancy, E., Zielinski, M., Steinegger, M., Pacholska, M., Berghammer, T.,
1431 Bodenstein, S., Silver, D., Vinyals, O., Senior, A. W., Kavukcuoglu, K., Kohli, P., and Hassabis, D.: Highly accurate protein
1432 structure prediction with AlphaFold, *Nature*, 596, 583–589, <https://doi.org/10.1038/s41586-021-03819-2>, 2021.

1433 Jurkowska, A. and Świerczewska-Gładysz, E.: The evolution of the marine Si cycle in the Archean-Palaeozoic - an overlooked
1434 Si source?, *Earth-Sci. Rev.*, 248, 104629, <https://doi.org/10.1016/j.earscirev.2023.104629>, 2024.

1435 Kemp, A. E. S., Pearce, R. B., Grigorov, I., Rance, J., Lange, C. B., Quilty, P., and Salter, I.: Production of giant marine
1436 diatoms and their export at oceanic frontal zones: Implications for Si and C flux from stratified oceans, *Glob. Biogeochem.*
1437 *Cycles*, 20, 2006GB002698, <https://doi.org/10.1029/2006GB002698>, 2006.

1438 Kidder, D. L. and Tomescu, I.: Biogenic chert and the Ordovician silica cycle, *Palaeogeogr. Palaeoclimatol. Palaeoecol.*, 458,
1439 29–38, <https://doi.org/10.1016/j.palaeo.2015.10.013>, 2016.

1440 Kim, H. H., Laufkötter, C., Lovato, T., Doney, S. C., and Ducklow, H. W.: Projected 21st-century changes in marine
1441 heterotrophic bacteria under climate change, *Front. Microbiol.*, 14, <https://doi.org/10.3389/fmicb.2023.1049579>, 2023.

1442 Klitgaard, A. B.: The fauna associated with outer shelf and upper slope sponges (Porifera, Demospongiae) at the Faroe Islands,
1443 northeastern Atlantic, *Sarsia*, 80, 1–22, <https://doi.org/10.1080/00364827.1995.10413574>, 1995.

1444 Knight, M. J., Senior, L., Nancolas, B., Ratcliffe, S., and Curnow, P.: Direct evidence of the molecular basis for biological
1445 silicon transport, *Nat. Commun.*, 7, 11926, <https://doi.org/10.1038/ncomms11926>, 2016.

1446 Knight, M. J., Hardy, B. J., Wheeler, G. L., and Curnow, P.: Computational modelling of diatom silicic acid transporters
1447 predicts a conserved fold with implications for their function and evolution, *Biochim. Biophys. Acta BBA - Biomembr.*, 1865,
1448 184056, <https://doi.org/10.1016/j.bbamem.2022.184056>, 2023.

1449 Koltun, V. M.: Spicule analysis and its application in geology: *Izvestiya Akademii Nauk SSR, Seriya Geol.*, 4, 73–77, 1960.

1450 Kotzsch, A., Gröger, P., Pawolski, D., Bomans, P. H. H., Sommerdijk, N. A. J. M., Schlierf, M., and Kröger, N.: Silicanin-1
1451 is a conserved diatom membrane protein involved in silica biomineralization, *BMC Biol.*, 15, <https://doi.org/10.1186/s12915-017-0400-8>, 2017.

1453 Krause, J. W., Nelson, D. M., and Brzezinski, M. A.: Biogenic silica production and the diatom contribution to primary
1454 production and nitrate uptake in the eastern equatorial Pacific Ocean, *Deep Sea Res. Part II Top. Stud. Oceanogr.*, 58, 434–
1455 448, <https://doi.org/10.1016/j.dsr2.2010.08.010>, 2011.

1456 Krause, J. W., Brzezinski, M. A., Baines, S. B., Collier, J. L., Twining, B. S., and Ohnemus, D. C.: Picoplankton contribution
1457 to biogenic silica stocks and production rates in the Sargasso Sea, *Glob. Biogeochem. Cycles*, 31, 762–774,
1458 <https://doi.org/10.1002/2017gb005619>, 2017.

1459 Krause, J. W., Schulz, I. K., Rowe, K. A., Dobbins, W., Winding, M. H. S., Sejr, M. K., Duarte, C. M., and Agustí, S.: Silicic
1460 acid limitation drives bloom termination and potential carbon sequestration in an Arctic bloom, *Sci. Rep.*, 9, 8149,
1461 <https://doi.org/10.1038/s41598-019-44587-4>, 2019.

1462 Kristiansen, S., Farbrot, T., and Naustvoll, L.-J.: Production of biogenic silica by spring diatoms, *Limnol. Oceanogr.*, 45, 472–
1463 478, <https://doi.org/10.4319/lo.2000.45.2.0472>, 2000.

1464 Kröger, N., Deutzmann, R., and Sumper, M.: Polycationic Peptides from Diatom Biosilica That Direct Silica Nanosphere
1465 Formation, *Science*, 286, 1129–1132, <https://doi.org/10.1126/science.286.5442.1129>, 1999.

1466 Kröger, N., Lorenz, S., Brunner, E., and Sumper, M.: Self-Assembly of Highly Phosphorylated Silaffins and Their Function
1467 in Biosilica Morphogenesis, *Science*, 298, 584–586, <https://doi.org/10.1126/science.1076221>, 2002.

1468 Kuerten, S., Parolin, M., Assine, M. L., and McGlue, M. M.: Sponge spicules indicate Holocene environmental changes on
1469 the Nabileque River floodplain, southern Pantanal, Brazil, *J. Paleolimnol.*, 49, 171–183, [https://doi.org/10.1007/s10933-012-](https://doi.org/10.1007/s10933-012-9652-z)
1470 9652-z, 2013.

1471 Kumar, S., Milstein, Y., Bami, Y., Elbaum, M., and Elbaum, R.: Mechanism of silica deposition in sorghum silica cells, *New*
1472 *Phytol.*, 213, 791–798, <https://doi.org/10.1111/nph.14173>, 2017a.

1473 Kumar, S., Soukup, M., and Elbaum, R.: Silicification in Grasses: Variation between Different Cell Types, *Front. Plant Sci.*,
1474 8, <https://doi.org/10.3389/fpls.2017.00438>, 2017b.

1475 Kumar, S., Rechav, K., Kaplan-Ashiri, I., and Gal, A.: Imaging and quantifying homeostatic levels of intracellular silicon in
1476 diatoms, *Sci. Adv.*, 6, eaaz7554, <https://doi.org/10.1126/sciadv.aaz7554>, 2020a.

1477 Kumar, S., Adiram-Filiba, N., Blum, S., Sanchez-Lopez, J. A., Tzfadia, O., Omid, A., Volpin, H., Heifetz, Y., Goobes, G., and
1478 Elbaum, R.: Siliplant1 protein precipitates silica in sorghum silica cells, *J. Exp. Bot.*, 71, 6830–6843,
1479 <https://doi.org/10.1093/jxb/eraa258>, 2020b.

1480 Kumar, S., Natalio, F., and Elbaum, R.: Protein-driven biomineralization: Comparing silica formation in grass silica cells to
1481 other biomineralization processes, *J. Struct. Biol.*, 213, 107665, <https://doi.org/10.1016/j.jsb.2020.107665>, 2021.

1482 Kuwata, A., Yamada, K., Ichinomiya, M., Yoshikawa, S., Tragin, M., Vaultot, D., and Lopes dos Santos, A.: Bolidophyceae,
1483 a Sister Picoplanktonic Group of Diatoms – A Review, *Front. Mar. Sci.*, 5, <https://doi.org/10.3389/fmars.2018.00370>, 2018.

1484 Laget, M., Drago, L., Panaiotis, T., Kiko, R., Stemmann, L., Rogge, A., Llopis-Monferrer, N., Leynaert, A., Irisson, J.-O., and
1485 Biard, T.: Global census of the significance of giant mesopelagic protists to the marine carbon and silicon cycles, *Nat.*
1486 *Commun.*, 15, 3341, <https://doi.org/10.1038/s41467-024-47651-4>, 2024.

1487 Lalonde, S. V., Konhauser, K. O., Reysenbach, A.-L., and Ferris, F. G.: The experimental silicification of Aquificales and
1488 their role in hot spring sinter formation, *Geobiology*, 3, 41–52, <https://doi.org/10.1111/j.1472-4669.2005.00042.x>, 2005.

1489 Lampitt, R. S., Briggs, N., Cael, B. B., Espinola, B., Hélaouët, P., Henson, S. A., Norrbin, F., Pebody, C. A., and Smeed, D.:
1490 Deep ocean particle flux in the Northeast Atlantic over the past 30 years: carbon sequestration is controlled by ecosystem
1491 structure in the upper ocean, *Front. Earth Sci.*, 11, <https://doi.org/10.3389/feart.2023.1176196>, 2023.

1492 Laruelle, G. G., Roubex, V., Sferratore, A., Brodherr, B., Ciuffa, D., Conley, D. J., Dürr, H. H., Garnier, J., Lancelot, C., Le
1493 Thi Phuong, Q., Meunier, J. -D., Meybeck, M., Michalopoulos, P., Moriceau, B., Ni Longphui, S., Loucaides, S., Papush, L.,
1494 Presti, M., Ragueneau, O., Regnier, P., Saccone, L., Slomp, C. P., Spiteri, C., and Van Cappellen, P.: Anthropogenic
1495 perturbations of the silicon cycle at the global scale: Key role of the land-ocean transition, *Glob. Biogeochem. Cycles*, 23, 1–
1496 17, <https://doi.org/10.1029/2008GB003267>, 2009.

1497 Läubli, C., Gaviria-Lugo, N., Bernhardt, A., Wittmann, H., Sachse, D., Mohtadi, M., Lückge, A., and Frings, P. J.: Constraints
1498 on the Role of Marine Authigenic Clay Formation in Determining Seawater Lithium Isotope Composition, *Geochem. Geophys.*
1499 *Geosystems*, 26, e2024GC012099, <https://doi.org/10.1029/2024GC012099>, 2025.

1500 Le Quéré, C., Harrison, S. P., Prentice, I. C., Buitenhuis, E. T., Aumont, O., Bopp, L., Claustre, H., Cotrim Da Cunha, L.,
1501 Geider, R., Giraud, X., Klaas, C., Kohfeld, K. E., Legendre, L., Manizza, M., Platt, T., Rivkin, R. B., Sathyendranath, S., Uitz,
1502 J., Watson, A. J., and Wolf-Gladrow, D.: Ecosystem dynamics based on plankton functional types for global ocean
1503 biogeochemistry models, *Glob. Change Biol.*, 11, 2016–2040, <https://doi.org/10.1111/j.1365-2486.2005.1004.x>, 2005.

1504 Leblanc, K. and Hutchins, D. A.: New applications of a biogenic silica deposition fluorophore in the study of oceanic diatoms,
1505 *Limnol. Oceanogr. Methods*, 3, 462–476, <https://doi.org/10.4319/lom.2005.3.462>, 2005.

1506 Leventer, A., Dunbar, R. B., and DeMaster, D. J.: Diatom Evidence for Late Holocene Climatic Events in Granite Harbor,
1507 Antarctica, *Paleoceanography*, 8, 373–386, <https://doi.org/10.1029/93PA00561>, 1993.

1508 Leventer, A., Domack, E., Dunbar, R., Pike, J., Stickley, C., Maddison, E., Brachfeld, S., Manley, P., and McClennen, C.:
1509 Marine sediment record from the East Antarctic margin reveals dynamics of ice sheet recession, *GSA Today*, 16, 4,
1510 <https://doi.org/10.1130/GSAT01612A.1>, 2006.

1511 Leys, S. P. and Lauzon, N. R. J.: Hexactinellid sponge ecology: growth rates and seasonality in deep water sponges, *J. Exp.*
1512 *Mar. Biol. Ecol.*, 230, 111–129, [https://doi.org/10.1016/S0022-0981\(98\)00088-4](https://doi.org/10.1016/S0022-0981(98)00088-4), 1998.

1513 Li, J., Zhang, K., Ke, Z., Liu, J., Tan, Y., Chen, Z., and Liu, H.: Composition and genetic diversity of picoeukaryotes in the
1514 northeastern South China Sea during the Luzon winter bloom, *Reg. Stud. Mar. Sci.*, 57, 102752,
1515 <https://doi.org/10.1016/j.rsma.2022.102752>, 2023.

1516 Liang, Y., Hua, H., Zhu, Y.-G., Zhang, J., Cheng, C., and Römheld, V.: Importance of plant species and external silicon
1517 concentration to active silicon uptake and transport, *New Phytol.*, 172, 63–72, <https://doi.org/10.1111/j.1469-8137.2006.01797.x>, 2006.

1519 Likhoshway, Ye. V., Masyukova, Yu. A., Sherbakova, T. A., Petrova, D. P., and Grachev, M. A.: Detection of the gene
1520 responsible for silicic acid transport in chrysophycean algae, *Dokl. Biol. Sci.*, 408, 256–260,
1521 <https://doi.org/10.1134/S001249660603015X>, 2006.

1522 Litchman, E.: Trait-Based Diatom Ecology, in: *The Molecular Life of Diatoms*, edited by: Falciatore, A. and Mock, T.,
1523 Springer International Publishing, Cham, 3–27, https://doi.org/10.1007/978-3-030-92499-7_1, 2022.

1524 Livage, J.: Bioinspired nanostructured materials, *Comptes Rendus Chim.*, 21, 969–973,
1525 <https://doi.org/10.1016/j.crci.2018.08.001>, 2018.

1526 Llopis Monferrer, N., Boltovskoy, D., Tréguer, P., Sandin, M. M., Not, F., and Leynaert, A.: Estimating Biogenic Silica
1527 Production of Rhizaria in the Global Ocean, *Glob. Biogeochem. Cycles*, 34, <https://doi.org/10.1029/2019gb006286>, 2020.

1528 Llopis Monferrer, N., Romac, S., Laget, M., Nakamura, Y., Biard, T., and Sandin, M. M.: Is the Gelatinous Matrix of
1529 Nassellaria (Radiolaria) a Strategy for Coping With Oligotrophy?, *Environ. Microbiol.*, 27, e70098,
1530 <https://doi.org/10.1111/1462-2920.70098>, 2025.

1531 Lohman, K. E.: The ubiquitous diatom—a brief survey of the present state of knowledge, *Am. J. Sci.*, 258, 180–191, 1960.

1532 López-Acosta, M., Leynaert, A., and Maldonado, M.: Silicon consumption in two shallow-water sponges with contrasting
1533 biological features: Si consumption by sponges, *Limnol. Oceanogr.*, 61, 2139–2150, <https://doi.org/10.1002/lno.10359>, 2016.

1534 López-Acosta, M., Leynaert, A., Grall, J., and Maldonado, M.: Silicon consumption kinetics by marine sponges: An
1535 assessment of their role at the ecosystem level, *Limnol. Oceanogr.*, 63, 2508–2522, <https://doi.org/10.1002/lno.10956>, 2018.

1536 López-Acosta, M., Maldonado, M., Grall, J., Ehrhold, A., Sitjà, C., Galobart, C., Pérez, F. F., and Leynaert, A.: Sponge
 1537 contribution to the silicon cycle of a diatom-rich shallow bay, *Limnol. Oceanogr.*, 67, 2431–2447,
 1538 <https://doi.org/10.1002/Ino.12211>, 2022.

1539 Loucaides, S., Michalopoulos, P., Presti, M., Koning, E., Behrends, T., and Van Cappellen, P.: Seawater-mediated interactions
 1540 between diatomaceous silica and terrigenous sediments: Results from long-term incubation experiments, *Chem. Geol.*, 270,
 1541 68–79, <https://doi.org/10.1016/j.chemgeo.2009.11.006>, 2010.

1542 Łukowiak, M.: Fossil and modern sponge fauna of southern Australia and adjacent regions compared: interpretation,
 1543 evolutionary and biogeographic significance of the late Eocene ‘soft’ sponges, *Contrib. Zool.*, 85, 13–35,
 1544 <https://doi.org/10.1163/18759866-08501002>, 2016.

1545 Luo, M., Li, W., Geilert, S., Dale, A. W., Song, Z., and Chen, D.: Active Silica Diagenesis in the Deepest Hadal Trench
 1546 Sediments, *Geophys. Res. Lett.*, 49, e2022GL099365, <https://doi.org/10.1029/2022GL099365>, 2022.

1547 Luo, M., Zheng, M., Wallmann, K., Dale, A. W., Strasser, M., Torres, M. E., Koelling, M., Riedinger, N., März, C., Rasbury,
 1548 T., Bao, R., Itaki, T., Ikehara, K., Johnson, J. E., Bellanova, P., Nakamura, Y., Yu, M., Xie, J., and Chen, D.: Rapid burial and
 1549 intense degradation of organic matter drive active silicate weathering in the subsurface sediments of the ocean’s deepest realm,
 1550 *Geology*, 53, 636–641, <https://doi.org/10.1130/G53131.1>, 2025.

1551 Maavara, T., Dürr, H. H., and Van Cappellen, P.: Worldwide retention of nutrient silicon by river damming: From sparse data
 1552 set to global estimate, *Glob. Biogeochem. Cycles*, 28, 842–855, <https://doi.org/10.1002/2014gb004875>, 2014.

1553 Mackenzie, F. T. and Garrels, R. M.: Chemical mass balance between rivers and oceans, *Am. J. Sci.*, 264, 507–525,
 1554 <https://doi.org/10.2475/ajs.264.7.507>, 1966.

1555 Mackie, G. O. and Singla, C. L.: Studies on hexactinellid sponges. I. Histology of *Rhabdocalyptus dawsoni* (Lambe, 1873),
 1556 *Philos. Trans. R. Soc. Lond. B Biol. Sci.*, 301, 365–400, <https://doi.org/10.1098/rstb.1983.0028>, 1997.

1557 Maddison, E. J., Pike, J., Leventer, A., Dunbar, R., Brachfeld, S., Domack, E. W., Manley, P., and McClennen, C.: Post-glacial
 1558 seasonal diatom record of the Mertz Glacier Polynya, East Antarctica, *Mar. Micropaleontol.*, 60, 66–88,
 1559 <https://doi.org/10.1016/j.marmicro.2006.03.001>, 2006.

1560 Maldonado, M. and Abdul Wahab, M. A.: Phylum Porifera, in: *Atlas of Marine Invertebrate Larvae*, edited by: Boyle, M. J.,
 1561 Young, C. M., and Sewell, M. A., Elsevier Science & Technology, Chantilly, 626, 2025.

1562 Maldonado, M. and Hendry, K. R.: Revisiting the silicon isotopic signal of sponge skeletons and its implications, *Limnol.*
 1563 *Oceanogr.*, Ino.70138, <https://doi.org/10.1002/Ino.70138>, 2025.

1564 Maldonado, M. and Riesgo, A.: Reproduction in Porifera: a synoptic overview, *Treballs de la Societat Catalana de Biologia*,
 1565 24–49 pp., 2008.

1566 Maldonado, M., Navarro, L., Grasa, A., Gonzalez, A., and Vaquerizo, I.: Silicon uptake by sponges: a twist to understanding
 1567 nutrient cycling on continental margins, *Sci. Rep.*, 1, <https://doi.org/10.1038/srep00030>, 2011.

1568 Maldonado, M., Ribes, M., and Van Duyl, F. C.: Nutrient Fluxes Through Sponges: biology, budgets, and ecological
 1569 implications, *Adv. Mar. Biol.*, 62, 113–182, <https://doi.org/10.1016/b978-0-12-394283-8.00003-5>, 2012.

1570 Maldonado, M., Aguilar, R., Bannister, R. J., Bell, J. J., Conway, K. W., Dayton, P. K., Díaz, C., Gutt, J., Kelly, M.,
 1571 Kenchington, E. L. R., Leys, S. P., Pomponi, S. A., Rapp, H. T., Rützler, K., Tendal, O. S., Vacelet, J., and Young, C. M.:

1572 Sponge Grounds as Key Marine Habitats: A Synthetic Review of Types, Structure, Functional Roles, and Conservation
1573 Concerns, in: *Marine Animal Forests: The Ecology of Benthic Biodiversity Hotspots*, vol. 1, edited by: Rossi, S., Bramanti,
1574 L., Gori, A., and Orejas Saco del Valle, C., Springer International Publishing, Cham, 145–184, [https://doi.org/10.1007/978-3-](https://doi.org/10.1007/978-3-319-17001-5_24-1)
1575 319-17001-5_24-1, 2017.

1576 Maldonado, M., López-Acosta, M., Sitjà, C., García-Puig, M., Galobart, C., Ercilla, G., and Leynaert, A.: Sponge skeletons as
1577 an important sink of silicon in the global oceans, *Nat. Geosci.*, 12, 815–822, <https://doi.org/10.1038/s41561-019-0430-7>, 2019.

1578 Maldonado, M., López-Acosta, M., Beazley, L., Kenchington, E., Koutsouveli, V., and Riesgo, A.: Cooperation between
1579 passive and active silicon transporters clarifies the ecophysiology and evolution of biosilicification in sponges, *Sci. Adv.*, 6,
1580 eaba9322, <https://doi.org/10.1126/sciadv.aba9322>, 2020.

1581 Maldonado, M., Beazley, L., López-Acosta, M., Kenchington, E., Casault, B., Hanz, U., and Mienis, F.: Massive silicon
1582 utilization facilitated by a benthic-pelagic coupled feedback sustains deep-sea sponge aggregations, *Limnol. Oceanogr.*, 66,
1583 366–391, <https://doi.org/10.1002/lno.11610>, 2021.

1584 Maldonado, M., López-Acosta, M., Abalde, S., Martos, I., Ehrlich, H., and Leynaert, A.: On the dissolution of sponge silica:
1585 Assessing variability and biogeochemical implications, *Front. Mar. Sci.*, 9, <https://doi.org/10.3389/fmars.2022.1005068>, 2022.

1586 Malinverno, E.: Extant morphotypes of *Distephanus speculum* (Silicoflagellata) from the Australian sector of the Southern
1587 Ocean: Morphology, morphometry and biogeography, *Mar. Micropaleontol.*, 77, 154–174,
1588 <https://doi.org/10.1016/j.marmicro.2010.09.002>, 2010.

1589 Maliva, R. G., Knoll, A. H., and Siever, R.: Secular Change in Chert Distribution: A Reflection of Evolving Biological
1590 Participation in the Silica Cycle, *PALAIOS*, 4, 519, <https://doi.org/10.2307/3514743>, 1989.

1591 Maliva, R. G., Knoll, A. H., and Simonson, B. M.: Secular change in the Precambrian silica cycle: Insights from chert
1592 petrology, *Geol. Soc. Am. Bull.*, 117, 835–845, <https://doi.org/10.1130/b25555.1>, 2005.

1593 Maniscalco, M. A., Brzezinski, M. A., Lampe, R. H., Cohen, N. R., McNair, H. M., Ellis, K. A., Brown, M., Till, C. P.,
1594 Twining, B. S., Bruland, K. W., Marchetti, A., and Thamatrakoln, K.: Diminished carbon and nitrate assimilation drive changes
1595 in diatom elemental stoichiometry independent of silicification in an iron-limited assemblage, *ISME Commun.*, 2, 57,
1596 <https://doi.org/10.1038/s43705-022-00136-1>, 2022.

1597 Mann, D. G. and Vanormelingen, P.: An Inordinate Fondness? The Number, Distributions, and Origins of Diatom Species, *J.*
1598 *Eukaryot. Microbiol.*, 60, 414–420, <https://doi.org/10.1111/jeu.12047>, 2013.

1599 Marron, A., Cassarino, L., Hatton, J., Curnow, P., and Hendry, K. R.: Technical note: The silicon isotopic composition of
1600 choanoflagellates: implications for a mechanistic understanding of isotopic fractionation during biosilicification,
1601 *Biogeosciences*, 16, 4805–4813, <https://doi.org/10.5194/bg-16-4805-2019>, 2019.

1602 Marron, A. O., Alston, M. J., Heavens, D., Akam, M., Caccamo, M., Holland, P. W. H., and Walker, G.: A family of diatom-
1603 like silicon transporters in the siliceous loricate choanoflagellates, *Proc. R. Soc. B Biol. Sci.*, 280, 20122543,
1604 <https://doi.org/10.1098/rspb.2012.2543>, 2013.

1605 Marron, A. O., Ratcliffe, S., Wheeler, G. L., Goldstein, R. E., King, N., Not, F., De Vargas, C., and Richter, D. J.: The Evolution
1606 of Silicon Transport in Eukaryotes, *Mol. Biol. Evol.*, 33, 3226–3248, <https://doi.org/10.1093/molbev/msw209>, 2016.

1607 Martin-Jézéquel, V., Hildebrand, M., and Brzezinski, M. A.: Silicon metabolism in diatoms: implications for growth, *J.*
1608 *Phycol.*, 36, 821–840, <https://doi.org/10.1046/j.1529-8817.2000.00019.x>, 2000.

1609 Massey, F. P., Ennos, A. R., and Hartley, S. E.: Silica in grasses as a defence against insect herbivores: contrasting effects on
1610 folivores and a phloem feeder, *J. Anim. Ecol.*, 75, 595–603, <https://doi.org/10.1111/j.1365-2656.2006.01082.x>, 2006.

1611 Mavromatis, V., Rinder, T., Prokushkin, A. S., Pokrovsky, O. S., Korets, M. A., Chmeleff, J., and Oelkers, E. H.: The effect
1612 of permafrost, vegetation, and lithology on Mg and Si isotope composition of the Yenisey River and its tributaries at the end
1613 of the spring flood, *Geochim. Cosmochim. Acta*, 191, 32–46, <https://doi.org/10.1016/j.gca.2016.07.003>, 2016.

1614 Mayzel, B., Aram, L., Varsano, N., Wolf, S. G., and Gal, A.: Structural evidence for extracellular silica formation by diatoms,
1615 *Nat. Commun.*, 12, <https://doi.org/10.1038/s41467-021-24944-6>, 2021.

1616 McCartney, K., Churchill, S., and Woestendiek, L.: Silicoflagellates and Ebridians from Leg 138, Eastern Equatorial Pacific,
1617 *Proc. Ocean Drill. Program*, <https://doi.org/10.2973/odp.proc.sr.138.108.1995>, 1995.

1618 McCartney, K., Witkowski, J., Jordan, R. W., Daugbjerg, N., Malinverno, E., Van Wezel, R., Kano, H., Abe, K., Scott, F.,
1619 Schweizer, M., Young, J. R., Hallegraeff, G. M., and Shiozawa, A.: Fine structure of silicoflagellate double skeletons, *Mar.*
1620 *Micropaleontol.*, 113, 10–19, <https://doi.org/10.1016/j.marmicro.2014.08.006>, 2014.

1621 McCartney, K., Witkowski, J., and Szaruga, A.: Palaeocene–early Eocene southern subtropical to subpolar silicoflagellate
1622 biostratigraphy, *Acta Geol. Pol.*, 68, 219–248, 2018.

1623 McCartney, K., Witkowski, J., Jordan, R. W., Abe, K., Januszkiewicz, A., Wróbel, R., Bąk, M., and Soeding, E.:
1624 Silicoflagellate evolution through the Cenozoic, *Mar. Micropaleontol.*, 172, 102108,
1625 <https://doi.org/10.1016/j.marmicro.2022.102108>, 2022.

1626 McCutchin, C. A., Edgar, K. J., Chen, C.-L., and Dove, P. M.: Silica–Biomacromolecule Interactions: Toward a Mechanistic
1627 Understanding of Silicification, *Biomacromolecules*, 26, 43–84, <https://doi.org/10.1021/acs.biomac.4c00674>, 2025.

1628 McGrath, E. C., Woods, L., Jompa, J., Haris, A., and Bell, J. J.: Growth and longevity in giant barrel sponges: Redwoods of
1629 the reef or Pines in the Indo-Pacific?, *Sci. Rep.*, 8, <https://doi.org/10.1038/s41598-018-33294-1>, 2018.

1630 McKenzie, L., Nordlund, L. M., Jones, B. L., Cullen-Unsworth, L. C., Roelfsema, C. M., and Unsworth, R.: The global
1631 distribution of seagrass meadows, *Environ. Res. Lett.*, 15, 074041, <https://doi.org/10.1088/1748-9326/ab7d06>, 2020.

1632 McManus, J., Hammond, D. E., Berelson, W. M., Kilgore, T. E., Demaster, D. J., Ragueneau, O. G., and Collier, R. W.: Early
1633 diagenesis of biogenic opal: Dissolution rates, kinetics, and paleoceanographic implications, *Deep Sea Res. Part II Top. Stud.*
1634 *Oceanogr.*, 42, 871–903, [https://doi.org/10.1016/0967-0645\(95\)00035-o](https://doi.org/10.1016/0967-0645(95)00035-o), 1995.

1635 McMurray, S. E., Blum, J. E., and Pawlik, J. R.: Redwood of the reef: growth and age of the giant barrel sponge *Xestospongia*
1636 *muta* in the Florida Keys, *Mar. Biol.*, 155, 159–171, <https://doi.org/10.1007/s00227-008-1014-z>, 2008.

1637 McNair, H. M., Brzezinski, M. A., and Krause, J. W.: Quantifying diatom silicification with the fluorescent dye, PDMPO,
1638 *Limnol. Oceanogr. Methods*, 13, 587–599, <https://doi.org/10.1002/lom3.10049>, 2015.

1639 McNair, H. M., Brzezinski, M. A., and Krause, J. W.: Diatom populations in an upwelling environment decrease silica content
1640 to avoid growth limitation, *Environ. Microbiol.*, 20, 4184–4193, <https://doi.org/10.1111/1462-2920.14431>, 2018.

1641 Meire, L., Meire, P., Struyf, E., Krawczyk, D. W., Arendt, K. E., Yde, J. C., Juul Pedersen, T., Hopwood, M. J., Rysgaard, S.,
1642 and Meysman, F. J. R.: High export of dissolved silica from the Greenland Ice Sheet, *Geophys. Res. Lett.*, 43, 9173–9182,
1643 <https://doi.org/10.1002/2016gl070191>, 2016.

1644 Meister, P., Alexandre, A., Bailey, H., Barker, P., Biskaborn, B. K., Broadman, E., Cartier, R., Chaplign, B., Couapel, M.,
1645 Dean, J. R., Diekmann, B., Harding, P., Henderson, A. C. G., Hernandez, A., Herzs Schuh, U., Kostrova, S. S., Lacey, J., Leng,
1646 M. J., Lücke, A., Mackay, A. W., Magyari, E. K., Narancic, B., Porchier, C., Rosqvist, G., Shemesh, A., Sonzogni, C., Swann,
1647 G. E. A., Sylvestre, F., and Meyer, H.: A global compilation of diatom silica oxygen isotope records from lake sediment –
1648 trends and implications for climate reconstruction, *Clim. Past*, 20, 363–392, <https://doi.org/10.5194/cp-20-363-2024>, 2024.

1649 Michalopoulos, P. and Aller, R. C.: Rapid Clay Mineral Formation in Amazon Delta Sediments: Reverse Weathering and
1650 Oceanic Elemental Cycles, *Science*, 270, 614–617, <https://doi.org/10.1126/science.270.5236.614>, 1995.

1651 Michalopoulos, P. and Aller, R. C.: Early diagenesis of biogenic silica in the Amazon delta: alteration, authigenic clay
1652 formation, and storage, *Geochim. Cosmochim. Acta*, 68, 1061–1085, <https://doi.org/10.1016/j.gca.2003.07.018>, 2004.

1653 Michalopoulos, P., Aller, R. C., and Reeder, R. J.: Conversion of diatoms to clays during early diagenesis in tropical,
1654 continental shelf muds, *Geology*, 28, 1095–1098, [https://doi.org/10.1130/0091-7613\(2000\)028%253C1095:codtcd%253E2.3.co;2](https://doi.org/10.1130/0091-7613(2000)028%253C1095:codtcd%253E2.3.co;2), 2000.

1656 Mirdita, M., Schütze, K., Moriwaki, Y., Heo, L., Ovchinnikov, S., and Steinegger, M.: ColabFold: making protein folding
1657 accessible to all, *Nat. Methods*, 19, 679–682, <https://doi.org/10.1038/s41592-022-01488-1>, 2022.

1658 Mitani-Ueno, N., Yamaji, N., Huang, S., Yoshioka, Y., Miyaji, T., and Ma, J. F.: A silicon transporter gene required for healthy
1659 growth of rice on land, *Nat. Commun.*, 14, 6522, <https://doi.org/10.1038/s41467-023-42180-y>, 2023.

1660 Moestrup, Ø. and Thomsen, H. A.: Dictyocha speculum (Silicoflagellata, Dictyochophyceae). Studies on armoured and
1661 unarmoured stages, *Biol. Skr. Det K. Dan. Vidensk. Selsk.*, 37, 1–57, 1990.

1662 Molina-Cruz, A.: Holocene palaeo-oceanography of the northern Iceland Sea, indicated by Radiolaria and sponge spicules, *J.*
1663 *Quat. Sci.*, 6, 303–312, <https://doi.org/10.1002/jqs.3390060405>, 1991.

1664 Morais, L., Fairchild, T. R., Lahr, D. J. G., Rudnitzki, I. D., Schopf, J. W., Garcia, A. K., Kudryavtsev, A. B., and Romero, G.
1665 R.: Carbonaceous and siliceous Neoproterozoic vase-shaped microfossils (Urucum Formation, Brazil) and the question of
1666 early protistan biomineralization, *J. Paleontol.*, 91, 393–406, <https://doi.org/10.1017/jpa.2017.16>, 2017.

1667 Morozov, A. A. and Galachyants, Y. P.: Diatom genes originating from red and green algae: Implications for the secondary
1668 endosymbiosis models, *Mar. Genomics*, 45, 72–78, <https://doi.org/10.1016/j.margen.2019.02.003>, 2019.

1669 Mouget, J.-L., Gastineau, R., Davidovich, O., Gaudin, P., and Davidovich, N. A.: Light is a key factor in triggering sexual
1670 reproduction in the pennate diatom *Haslea ostrearia*: Light induction of sexual reproduction in diatoms, *FEMS Microbiol.*
1671 *Ecol.*, 69, 194–201, <https://doi.org/10.1111/j.1574-6941.2009.00700.x>, 2009.

1672 Müller, W. E. G., Boreiko, A., Wang, X., Belikov, S. I., Wiens, M., Grebenjuk, V. A., Schloßmacher, U., and Schröder, H. C.:
1673 Silicateins, the major biosilica forming enzymes present in demosponges: Protein analysis and phylogenetic relationship, *Gene*,
1674 395, 62–71, <https://doi.org/10.1016/j.gene.2007.02.014>, 2007.

1675 Müller, W. E. G., Mugnaioli, E., Schröder, H. C., Schloßmacher, U., Giovine, M., Kolb, U., and Wang, X.: Hierarchical
1676 composition of the axial filament from spicules of the siliceous sponge *Suberites domuncula*: from biosilica-synthesizing
1677 nanofibrils to structure- and morphology-guiding triangular stems, *Cell Tissue Res.*, 351, 49–58,
1678 <https://doi.org/10.1007/s00441-012-1519-0>, 2013.

1679 Murray, D. and Schrader, H.: Distribution of silicoflagellates in plankton and core top samples from the Gulf of California,
1680 *Mar. Micropaleontol.*, 7, 517–539, [https://doi.org/10.1016/0377-8398\(83\)90013-0](https://doi.org/10.1016/0377-8398(83)90013-0), 1983.

1681 Naidoo-Bagwell, A. A., Monteiro, F. M., Hendry, K. R., Burgan, S., Wilson, J. D., Ward, B. A., Ridgwell, A., and Conley, D.
1682 J.: A diatom extension to the cGEnIE Earth system model – EcoGEnIE 1.1, *Geosci. Model Dev.*, 17, 1729–1748,
1683 <https://doi.org/10.5194/gmd-17-1729-2024>, 2024.

1684 Nakagawa Y., Endo Y., and Taki K.: Contributions of heterotrophic and autotrophic prey to the diet of euphausiid, *Euphausia*
1685 *pacifica* in the coastal waters off northeastern Japan, *Polar Biosci.*, 15, 52–65, <https://doi.org/10.15094/00006183>, 2002.

1686 Nakamura, Y., Tuji, A., Kimoto, K., Yamaguchi, A., Hori, R. S., and Suzuki, N.: Ecology, Morphology, Phylogeny and
1687 Taxonomic Revision of Giant Radiolarians, *Orodaria* ord. nov. (Radiolaria; Rhizaria; SAR), *Protist*, 172, 125808,
1688 <https://doi.org/10.1016/j.protis.2021.125808>, 2021.

1689 Nakov, T., Beaulieu, J. M., and Alverson, A. J.: Accelerated diversification is related to life history and locomotion in a
1690 hyperdiverse lineage of microbial eukaryotes (Diatoms, Bacillariophyta), *New Phytol.*, 219, 462–473,
1691 <https://doi.org/10.1111/nph.15137>, 2018.

1692 Nantke, C. K. M., Frings, P. J., Stadmark, J., Czymzik, M., and Conley, D. J.: Correction to: Si cycling in transition zones: a
1693 study of Si isotopes and biogenic silica accumulation in the Chesapeake Bay through the Holocene, *Biogeochemistry*, 146,
1694 171–171, <https://doi.org/10.1007/s10533-019-00618-w>, 2019.

1695 Naumova, E. Yu., Zaidykov, I. Yu., Tauson, V. L., and Likhoshway, Y. V.: Features of the Fine Structure and SI Content of
1696 the Mandibular Gnathobase of Four Freshwater Species of *Epischura* (Copepoda: Calanoida), *J. Crustac. Biol.*, 35, 741–746,
1697 <https://doi.org/10.1163/1937240X-00002385>, 2015.

1698 Nawaz, M. A., Azeem, F., Zakharenko, A. M., Lin, X., Atif, R. M., Baloch, F. S., Chan, T.-F., Chung, G., Ham, J., Sun, S.,
1699 and Golokhvast, K. S.: In-silico Exploration of Channel Type and Efflux Silicon Transporters and Silicification Proteins in 80
1700 Sequenced Viridiplantae Genomes, *Plants*, 9, 1612, <https://doi.org/10.3390/plants9111612>, 2020.

1701 Nelson, D. M. and Goering, J. J.: A stable isotope tracer method to measure silicic acid uptake by marine phytoplankton, *Anal.*
1702 *Biochem.*, 78, 139–147, [https://doi.org/10.1016/0003-2697\(77\)90017-3](https://doi.org/10.1016/0003-2697(77)90017-3), 1977.

1703 Nelson, D. M., Tréguer, P., Brzezinski, M. A., Leynaert, A., and Quéguiner, B.: Production and dissolution of biogenic silica
1704 in the ocean: Revised global estimates, comparison with regional data and relationship to biogenic sedimentation, *Glob.*
1705 *Biogeochem. Cycles*, 9, 359–372, <https://doi.org/10.1029/95gb01070>, 1995.

1706 Neuweiler, F., Larmagnat, S., Molson, J., and Fortin-Morin, F.: Sponge Spicules, Silicification, and Sequence Stratigraphy, *J.*
1707 *Sediment. Res.*, 84, 1107–1119, <https://doi.org/10.2110/jsr.2014.86>, 2014.

1708 Ng, H. C., Cassarino, L., Pickering, R. A., Woodward, E. M. S., Hammond, S. J., and Hendry, K. R.: Sediment efflux of silicon
1709 on the Greenland margin and implications for the marine silicon cycle, *Earth Planet. Sci. Lett.*, 529, 115877,
1710 <https://doi.org/10.1016/j.epsl.2019.115877>, 2020.

1711 Ng, H. C., Hawkings, J. R., Bertrand, S., Summers, B. A., Sieber, M., Conway, T. M., Freitas, F. S., Ward, J. P. J., Pryer, H.
1712 V., Wadham, J. L., Arndt, S., and Hendry, K. R.: Benthic Dissolved Silicon and Iron Cycling at Glaciated Patagonian Fjord
1713 Heads, *Glob. Biogeochem. Cycles*, 36, <https://doi.org/10.1029/2022gb007493>, 2022.

1714 Ng, H. C., Hendry, K. R., Ward, R., Woodward, E. M. S., Leng, M. J., Pickering, R. A., and Krause, J. W.: Detrital Input
1715 Sustains Diatom Production off a Glaciated Arctic Coast, *Geophys. Res. Lett.*, 51, e2024GL108324,
1716 <https://doi.org/10.1029/2024GL108324>, 2024.

1717 Nikolaev, S. I., Berney, C., Fahrni, J. F., Bolivar, I., Polet, S., Mylnikov, A. P., Aleshin, V. V., Petrov, N. B., and Pawlowski,
 1718 J.: The twilight of Heliozoa and rise of Rhizaria, an emerging supergroup of amoeboid eukaryotes, *Proc. Natl. Acad. Sci.*, 101,
 1719 8066–8071, <https://doi.org/10.1073/pnas.0308602101>, 2004.

1720 Ogane, K., Tuji, A., Suzuki, N., Kurihara, T., and Matsuoka, A.: First application of PDMPO to examine silicification in
 1721 polycystine Radiolaria, *Plankton Benthos Res.*, 4, 89–94, <https://doi.org/10.3800/pbr.4.89>, 2009.

1722 Ohnemus, D. C., Rauschenberg, S., Krause, J. W., Brzezinski, M. A., Collier, J. L., Geraci-Yee, S., Baines, S. B., and Twining,
 1723 B. S.: Silicon content of individual cells of *Synechococcus* from the North Atlantic Ocean, *Mar. Chem.*, 187, 16–24,
 1724 <https://doi.org/10.1016/j.marchem.2016.10.003>, 2016.

1725 Oksman, M., Juggins, S., Miettinen, A., Witkowski, A., and Weckström, K.: The biogeography and ecology of common diatom
 1726 species in the northern North Atlantic, and their implications for paleoceanographic reconstructions, *Mar. Micropaleontol.*,
 1727 148, 1–28, <https://doi.org/10.1016/j.marmicro.2019.02.002>, 2019.

1728 Olofsson, M., Robertson, E. K., Edler, L., Arneborg, L., Whitehouse, M. J., and Ploug, H.: Nitrate and ammonium fluxes to
 1729 diatoms and dinoflagellates at a single cell level in mixed field communities in the sea, *Sci. Rep.*, 9, 1424,
 1730 <https://doi.org/10.1038/s41598-018-38059-4>, 2019.

1731 Onodera, J., Watanabe, E., Nishino, S., and Harada, N.: Distribution and vertical fluxes of silicoflagellates, ebridians, and the
 1732 endoskeletal dinoflagellate *Actiniscus* in the western Arctic Ocean, *Polar Biol.*, 39, 327–341, <https://doi.org/10.1007/s00300-015-1784-y>, 2016.

1734 Opfergelt, S., Gaspard, F., Hirst, C., Monin, L., Juhls, B., Morgenstern, A., Angelopoulos, M., and Overduin, P. P.: Frazil ice
 1735 changes winter biogeochemical processes in the Lena River, *Commun. Earth Environ.*, 5, [https://doi.org/10.1038/s43247-024-](https://doi.org/10.1038/s43247-024-01884-9)
 1736 01884-9, 2024.

1737 Otero-Ferrer, J. L., Cermeño, P., Bode, A., Fernández-Castro, B., Gasol, J. M., Morán, X. A. G., Maraño, E., Moreira-Coello,
 1738 V., Varela, M. M., Villamaña, M., and Mouriño-Carballido, B.: Factors controlling the community structure of picoplankton
 1739 in contrasting marine environments, *Biogeosciences*, 15, 6199–6220, <https://doi.org/10.5194/bg-15-6199-2018>, 2018.

1740 Ou, Q., Xu, H., Zhang, Z., Ma, J., and Pan, K.: Effects of ambient silicic acid concentration on the physiology of marine
 1741 cyanobacterial *Synechococcus*, *Mar. Environ. Res.*, 209, 107220, <https://doi.org/10.1016/j.marenvres.2025.107220>, 2025.

1742 Painting, S. J., Lucas, M. I., Peterson, W. T., Brown, P. C., Hutchings, L., and Mitchell-Innes, B. A.: Dynamics of
 1743 bacterioplankton, phytoplankton and mesozooplankton communities during the development of an upwelling plume in the
 1744 southern Benguela, *Mar. Ecol. Prog. Ser.*, 100, 35–53, 1993.

1745 Pančić, M., Torres, R. R., Almeda, R., and Kiørboe, T.: Silicified cell walls as a defensive trait in diatoms, *Proc. R. Soc. B*
 1746 *Biol. Sci.*, 286, 20190184, <https://doi.org/10.1098/rspb.2019.0184>, 2019.

1747 Passmore, A. J., Jarman, S. N., Swadling, K. M., Kawaguchi, S., McMinn, A., and Nicol, S.: DNA as a Dietary Biomarker in
 1748 Antarctic Krill, *Euphausia superba*, *Mar. Biotechnol.*, 8, 686–696, <https://doi.org/10.1007/s10126-005-6088-8>, 2006.

1749 Pasternak, A. F. and Schnack-Schiel, S. B.: Seasonal feeding patterns of the dominant Antarctic copepods *Calanus propinquus*
 1750 and *Calanoides acutus* in the Weddell Sea, *Polar Biol.*, 24, 771–784, <https://doi.org/10.1007/s003000100283>, 2001.

1751 Perry, E. C. and Lefticariu, L.: Formation and Geochemistry of Precambrian Cherts, in: *Treatise on Geochemistry*, Elsevier,
 1752 1–21, <https://doi.org/10.1016/B0-08-043751-6/07138-3>, 2007.

1753 Petrucciani, A., Chaerle, P., and Norici, A.: Diatoms Versus Copepods: Could Frustule Traits Have a Role in Avoiding
1754 Predation?, *Front. Mar. Sci.*, 8, <https://doi.org/10.3389/fmars.2021.804960>, 2022a.

1755 Petrucciani, A., Knoll, A. H., and Norici, A.: Si decline and diatom evolution: Insights from physiological experiments, *Front.*
1756 *Mar. Sci.*, 9, 924452, <https://doi.org/10.3389/fmars.2022.924452>, 2022b.

1757 Petrucciani, A., Moretti, P., Ortore, M. G., and Norici, A.: Integrative effects of morphology, silicification, and light on diatom
1758 vertical movements, *Front. Plant Sci.*, 14, <https://doi.org/10.3389/fpls.2023.1143998>, 2023.

1759 Phoenix, V. R., Adams, D. G., and Konhauser, K. O.: Cyanobacterial viability during hydrothermal biomineralisation, *Chem.*
1760 *Geol.*, 169, 329–338, [https://doi.org/10.1016/S0009-2541\(00\)00212-6](https://doi.org/10.1016/S0009-2541(00)00212-6), 2000.

1761 Pike, J. and Kemp, A. E. S.: Early Holocene decadal-scale ocean variability recorded in Gulf of California laminated sediments,
1762 *Paleoceanography*, 12, 227–238, <https://doi.org/10.1029/96PA03132>, 1997.

1763 Pisera, A. and Sáez, A.: Paleoenvironmental significance of a new species of freshwater sponge from the Late Miocene
1764 Quillagua Formation (N Chile), *J. South Am. Earth Sci.*, 15, 847–852, [https://doi.org/10.1016/S0895-9811\(03\)00012-9](https://doi.org/10.1016/S0895-9811(03)00012-9), 2003.

1765 Pokrovsky, O. S., Reynolds, B. C., Prokushkin, A. S., Schott, J., and Viers, J.: Silicon isotope variations in Central Siberian
1766 rivers during basalt weathering in permafrost-dominated larch forests, *Chem. Geol.*, 355, 103–116,
1767 <https://doi.org/10.1016/j.chemgeo.2013.07.016>, 2013.

1768 Pondaven, P., Gallinari, M., Chollet, S., Bucciarelli, E., Sarthou, G., Schultes, S., and Jean, F.: Grazing-induced Changes in
1769 Cell Wall Silicification in a Marine Diatom, *Protist*, 158, 21–28, <https://doi.org/10.1016/j.protis.2006.09.002>, 2007.

1770 Porter, S. M. and Knoll, A. H.: Testate amoebae in the Neoproterozoic Era: evidence from vase-shaped microfossils in the
1771 Chuar Group, Grand Canyon, *Paleobiology*, 26, 360–385, [https://doi.org/10.1666/0094-8373\(2000\)026%253C0360:taitne%253E2.0.co;2](https://doi.org/10.1666/0094-8373(2000)026%253C0360:taitne%253E2.0.co;2), 2000.

1773 Presti, M. and Michalopoulos, P.: Estimating the contribution of the authigenic mineral component to the long-term reactive
1774 silica accumulation on the western shelf of the Mississippi River Delta, *Cont. Shelf Res.*, 28, 823–838,
1775 <https://doi.org/10.1016/j.csr.2007.12.015>, 2008.

1776 Preston, C. M., Durkin, C. A., and Yamahara, K. M.: DNA metabarcoding reveals organisms contributing to particulate matter
1777 flux to abyssal depths in the North East Pacific ocean, *Deep Sea Res. Part II Top. Stud. Oceanogr.*, 173, 104708,
1778 <https://doi.org/10.1016/j.dsr2.2019.104708>, 2020.

1779 Pryer, H. V., Hawkings, J. R., Wadham, J. L., Robinson, L. F., Hendry, K. R., Hatton, J. E., Kellerman, A. M., Bertrand, S.,
1780 Gill-Olivas, B., Marshall, M. G., Brooker, R. A., Daneri, G., and Häussermann, V.: The Influence of Glacial Cover on Riverine
1781 Silicon and Iron Exports in Chilean Patagonia, *Glob. Biogeochem. Cycles*, 34, <https://doi.org/10.1029/2020gb006611>, 2020.

1782 Ragueneau, O., Schultes, S., Bidle, K., Claquin, P., and Moriceau, B.: Si and C interactions in the world ocean: Importance of
1783 ecological processes and implications for the role of diatoms in the biological pump, *Glob. Biogeochem. Cycles*, 20,
1784 <https://doi.org/10.1029/2006GB002688>, 2006.

1785 Rahman, S., Aller, R. C., and Cochran, J. K.: The Missing Silica Sink: Revisiting the Marine Sedimentary Si Cycle Using
1786 Cosmogenic ³²Si, *Glob. Biogeochem. Cycles*, 31, 1559–1578, <https://doi.org/10.1002/2017gb005746>, 2017.

1787 Rahman, S., Tamborski, J. J., Charette, M. A., and Cochran, J. K.: Dissolved silica in the subterranean estuary and the impact
1788 of submarine groundwater discharge on the global marine silica budget, *Mar. Chem.*, 208, 29–42,
1789 <https://doi.org/10.1016/j.marchem.2018.11.006>, 2019.

1790 Ran, L., Wiesner, M. G., Liang, Y., Liang, W., Zhang, L., Yang, Z., Li, H., and Chen, J.: Differential dissolution of biogenic
1791 silica significantly affects the utility of sediment diatoms as paleoceanographic proxies, *Limnol. Oceanogr.*, 69, 467–481,
1792 <https://doi.org/10.1002/lno.12492>, 2024.

1793 Ran, X., Wu, W., Song, Z., Wang, H., Chen, H., Yao, Q., Xin, M., Liu, P., and Yu, Z.: Decadal change in dissolved silicate
1794 concentration and flux in the Changjiang (Yangtze) River, *Sci. Total Environ.*, 839, 156266,
1795 <https://doi.org/10.1016/j.scitotenv.2022.156266>, 2022.

1796 Ratcliffe, S., Meyer, E. M., Walker, C. E., Knight, M., McNair, H. M., Matson, P. G., Iglesias-Rodriguez, D., Brzezinski, M.,
1797 Langer, G., Sadekov, A., Greaves, M., Brownlee, C., Curnow, P., Taylor, A. R., and Wheeler, G. L.: Characterization of the
1798 molecular mechanisms of silicon uptake in coccolithophores, *Env. Microbiol.*, 25, 315–330, [https://doi.org/10.1111/1462-](https://doi.org/10.1111/1462-2920.16280)
1799 2920.16280, 2023a.

1800 Ratcliffe, S., Meyer, E. M., Walker, C. E., Knight, M., McNair, H. M., Matson, P. G., Iglesias-Rodriguez, D., Brzezinski, M.,
1801 Langer, G., Sadekov, A., Greaves, M., Brownlee, C., Curnow, P., Taylor, A. R., and Wheeler, G. L.: Characterization of the
1802 molecular mechanisms of silicon uptake in coccolithophores, *Environ. Microbiol.*, 25, 315–330, [https://doi.org/10.1111/1462-](https://doi.org/10.1111/1462-2920.16280)
1803 2920.16280, 2023b.

1804 Raven, J.: Blue carbon: past, present and future, with emphasis on macroalgae, *Biol. Lett.*, 14, 20180336,
1805 <https://doi.org/10.1098/rsbl.2018.0336>, 2018.

1806 Ray, N., Al-Haj, A., Maguire, T., Henning, M., and Fulweiler, R.: Coastal silicon cycling amplified by oyster aquaculture,
1807 *Mar. Ecol. Prog. Ser.*, 673, 29–41, <https://doi.org/10.3354/meps13803>, 2021.

1808 Riesgo, A., Maldonado, M., López-Legentil, S., and Giribet, G.: A Proposal for the Evolution of Cathepsin and Silicatein in
1809 Sponges, *J. Mol. Evol.*, 80, 278–291, <https://doi.org/10.1007/s00239-015-9682-z>, 2015.

1810 Rigual-Hernández, A. S., Trull, T. W., Bray, S. G., and Armand, L. K.: The fate of diatom valves in the Subantarctic and Polar
1811 Frontal Zones of the Southern Ocean: Sediment trap versus surface sediment assemblages, *Palaeogeogr. Palaeoclimatol.*
1812 *Palaeoecol.*, 457, 129–143, <https://doi.org/10.1016/j.palaeo.2016.06.004>, 2016.

1813 Rzos, I., Frada, M. J., Bittner, L., and Not, F.: Life cycle strategies in free-living unicellular eukaryotes: Diversity, evolution,
1814 and current molecular tools to unravel the private life of microorganisms, *J. Eukaryot. Microbiol.*, 71, e13052,
1815 <https://doi.org/10.1111/jeu.13052>, 2024.

1816 Robinson, R. S., Moore, T. C., Erhardt, A. M., and Scher, H. D.: Evidence for changes in subsurface circulation in the late
1817 Eocene equatorial Pacific from radiolarian-bound nitrogen isotope values, *Paleoceanography*, 30, 912–922,
1818 <https://doi.org/10.1002/2015PA002777>, 2015.

1819 Robinson, R. S., Jones, C. A., Kelly, R. P., Love, A., Closset, I., Rafter, P. A., and Brzezinski, M.: A Test of the Diatom-
1820 Bound Paleoproxy: Tracing the Isotopic Composition of Nutrient-Nitrogen Into Southern Ocean Particles and Sediments,
1821 *Glob. Biogeochem. Cycles*, 34, e2019GB006508, <https://doi.org/10.1029/2019GB006508>, 2020.

1822 Rohde, S. and Schupp, P. J.: Allocation of chemical and structural defenses in the sponge *Melophlus sarasinorum*, *J. Exp. Mar.*
1823 *Biol. Ecol.*, 399, 76–83, <https://doi.org/10.1016/j.jembe.2011.01.012>, 2011.

1824 Rong, B., Zhang, L., Liu, Z., Bai, W., Gu, W., Wei, X., Hou, W., and Ge, C.: Role of phytoliths in carbon stabilization of
1825 *Zostera marina* L. plants: One unreported mechanism of carbon sequestration in eelgrass beds, *Estuar. Coast. Shelf Sci.*, 301,
1826 108751, <https://doi.org/10.1016/j.ecss.2024.108751>, 2024.

1827 Roseby, Z. A., Smith, J. A., Hillenbrand, C.-D., Allen, C. S., Leventer, A., Hogan, K., Cartigny, M. J. B., Rosenheim, B. E.,
1828 Kuhn, G., and Larter, R. D.: History of Anvers-Hugo Trough, western Antarctic Peninsula shelf, since the Last Glacial
1829 Maximum. Part II: Palaeo-productivity and palaeoceanographic changes during the Last Glacial Transition, *Quat. Sci. Rev.*,
1830 294, 107503, <https://doi.org/10.1016/j.quascirev.2022.107503>, 2022.

1831 Roth, J., Gallinari, M., Schoelynck, J., Hernán, G., Máñez-Crespo, J., Ricart, A. M., and López-Acosta, M.: Chemical
1832 determination of silica in seagrass leaves reveals two operational silica pools in *Zostera marina*, *Biogeochemistry*, 168,
1833 <https://doi.org/10.1007/s10533-024-01189-1>, 2025.

1834 Round, F. E., Crawford, R. M., and Mann, D. G.: *Diatoms: Biology and Morphology of the Genera*, Cambridge University
1835 Press, 768 pp., 1990.

1836 Ryderheim, F., Grønning, J., and Kiørboe, T.: Thicker shells reduce copepod grazing on diatoms, *Limnol. Oceanogr. Lett.*, 7,
1837 435–442, <https://doi.org/10.1002/lol2.10243>, 2022.

1838 Sancetta, C.: Seasonal occurrence of silicoflagellate morphologies in different environments of the eastern Pacific Ocean, *Mar.*
1839 *Micropaleontol.*, 16, 285–291, [https://doi.org/10.1016/0377-8398\(90\)90007-9](https://doi.org/10.1016/0377-8398(90)90007-9), 1990.

1840 Santos, I. R., Chen, X., Lecher, A. L., Sawyer, A. H., Moosdorf, N., Rodellas, V., Tamborski, J., Cho, H.-M., Dimova, N.,
1841 Sugimoto, R., Bonaglia, S., Li, H., Hajati, M.-C., and Li, L.: Submarine groundwater discharge impacts on coastal nutrient
1842 biogeochemistry, *Nat. Rev. Earth Environ.*, 2, 307–323, <https://doi.org/10.1038/s43017-021-00152-0>, 2021.

1843 Schiller, J.: Die planktonischen Vegetationen des Adriatischen Meeres, *Arch Protistenkd*, 53, 59–123, 1925.

1844 Schneider-Mor, A., Yam, R., Bianchi, C., Kunz-Pirrung, M., Gersonde, R., and Shemesh, A.: Diatom stable isotopes, sea ice
1845 presence and sea surface temperature records of the past 640 ka in the Atlantic sector of the Southern Ocean, *Geophys. Res.*
1846 *Lett.*, 32, 2005GL022543, <https://doi.org/10.1029/2005GL022543>, 2005.

1847 Schoelynck, J. and Struyf, E.: Silicon in aquatic vegetation, *Funct. Ecol.*, 30, 1323–1330, [https://doi.org/10.1111/1365-](https://doi.org/10.1111/1365-2435.12614)
1848 2435.12614, 2016.

1849 Schoelynck, J., Bal, K., Puijalon, S., Meire, P., and Struyf, E.: Hydrodynamically mediated macrophyte silica dynamics, *Plant*
1850 *Biol.*, 14, 997–1005, <https://doi.org/10.1111/j.1438-8677.2012.00583.x>, 2012.

1851 Schröder, H. C., Brandt, D., Schloßmacher, U., Wang, X., Tahir, M. N., Tremel, W., Belikov, S. I., and Müller, W. E. G.:
1852 Enzymatic production of biosilica glass using enzymes from sponges: basic aspects and application in nanobiotechnology
1853 (material sciences and medicine), *Naturwissenschaften*, 94, 339–359, <https://doi.org/10.1007/s00114-006-0192-0>, 2007.

1854 Schröder, H.-C., Perović-Ottstadt, S., Rothenberger, M., Wiens, M., Schwertner, H., Batel, R., Korzhev, M., Müller, I. M., and
1855 Müller, W. E. G.: Silica transport in the demosponge *Suberites domuncula* : fluorescence emission analysis using the PDMPO
1856 probe and cloning of a potential transporter, *Biochem. J.*, 381, 665–673, <https://doi.org/10.1042/BJ20040463>, 2004.

1857 Sekiguchi, H., Moriya, M., Nakayama, T., and Inouye, I.: Vestigial Chloroplasts in Heterotrophic Stramenopiles *Pteridomonas*
1858 *danica* and *Ciliophrys infusionum* (Dictyochophyceae), *Protist*, 153, 157–167, <https://doi.org/10.1078/1434-4610-00094>,
1859 2002.

1860 Sheath, R. and Wehr, J.: Freshwater Algae of North America, Elsevier, <https://doi.org/10.1016/b978-0-12-741550-5.x5000-4>,
1861 2003.

1862 Shemesh, A., Rietti-Shati, M., Rioual, P., Battarbee, R., De Beaulieu, J., Reille, M., Andrieu, V., and Svobodova, H.: An
1863 oxygen isotope record of lacustrine opal from a European Maar indicates climatic stability during the Last Interglacial,
1864 Geophys. Res. Lett., 28, 2305–2308, <https://doi.org/10.1029/2000GL012720>, 2001.

1865 Shimizu, K., Cha, J., Stucky, G. D., and Morse, D. E.: Silicatein α : Cathepsin L-like protein in sponge biosilica, Proc. Natl.
1866 Acad. Sci., 95, 6234–6238, <https://doi.org/10.1073/pnas.95.11.6234>, 1998.

1867 Shimizu, K., Amo, Y. D., Brzezinski, M. A., Stucky, G. D., and Morse, D. E.: A novel fluorescent silica tracer for biological
1868 silicification studies, Chem. Biol., 8, 1051–1060, [https://doi.org/10.1016/S1074-5521\(01\)00072-2](https://doi.org/10.1016/S1074-5521(01)00072-2), 2001.

1869 Shimizu, K., Amano, T., Bari, Md. R., Weaver, J. C., Arima, J., and Mori, N.: Glassin, a histidine-rich protein from the siliceous
1870 skeletal system of the marine sponge *Euplectella*, directs silica polycondensation, Proc. Natl. Acad. Sci., 112, 11449–
1871 11454, <https://doi.org/10.1073/pnas.1506968112>, 2015.

1872 Shimizu, K., Nishi, M., Sakate, Y., Kawanami, H., Bito, T., Arima, J., Leria, L., and Maldonado, M.: Silica-associated proteins
1873 from hexactinellid sponges support an alternative evolutionary scenario for biomineralization in Porifera, Nat. Commun., 15,
1874 <https://doi.org/10.1038/s41467-023-44226-7>, 2024.

1875 Shrestha, R. P., Tesson, B., Norden-Krichmar, T., Federowicz, S., Hildebrand, M., and Allen, A. E.: Whole transcriptome
1876 analysis of the silicon response of the diatom *Thalassiosira pseudonana*, BMC Genomics, 13, <https://doi.org/10.1186/1471-2164-13-499>, 2012.

1878 Sieradzki, E. T., Ignacio-Espinoza, J. C., Needham, D. M., Fichot, E. B., and Fuhrman, J. A.: Dynamic marine viral infections
1879 and major contribution to photosynthetic processes shown by spatiotemporal picoplankton metatranscriptomes, Nat.
1880 Commun., 10, 1169, <https://doi.org/10.1038/s41467-019-09106-z>, 2019.

1881 Siever, R.: Silica in the oceans: biological-geochemical interplay, in: Scientists on Gaia, edited by: S. H., S. and P. J., B., MIT
1882 Press, Cambridge, 287–295, 1991.

1883 Siever, R.: The silica cycle in the Precambrian, Geochim. Cosmochim. Acta, 56, 3265–3272, [https://doi.org/10.1016/0016-7037\(92\)90303-z](https://doi.org/10.1016/0016-7037(92)90303-z), 1992.

1885 Silva, P. C.: Algae. A Taxonomic Survey. Fasc. 1, Phycologia, 21, 192–194, <https://doi.org/10.2216/i0031-8884-21-2-192.1>,
1886 1982.

1887 Sim-Smith, C., Ellwood, M., and Kelly, M.: Sponges as Proxies for Past Climate Change Events, in: Climate Change, Ocean
1888 Acidification and Sponges: Impacts Across Multiple Levels of Organization, edited by: Carballo, J. L. and Bell, J. J., Springer
1889 International Publishing, Cham, 49–78, https://doi.org/10.1007/978-3-319-59008-0_3, 2017.

1890 Sperling, E. A., Robinson, J. M., Pisani, D., and Peterson, K. J.: Where’s the glass? Biomarkers, molecular clocks, and
1891 microRNAs suggest a 200-Myr missing Precambrian fossil record of siliceous sponge spicules, Geobiology, 8, 24–36,
1892 <https://doi.org/10.1111/j.1472-4669.2009.00225.x>, 2010.

1893 Struyf, E. and Conley, D. J.: Emerging understanding of the ecosystem silica filter, Biogeochemistry, 107, 9–18,
1894 <https://doi.org/10.1007/s10533-011-9590-2>, 2012.

- 1895 Struyf, E., Smis, A., Van Damme, S., Meire, P., and Conley, D. J.: The Global Biogeochemical Silicon Cycle, *Silicon*, 1, 207–
1896 213, <https://doi.org/10.1007/s12633-010-9035-x>, 2009.
- 1897 Strydom, S., McCallum, R., Lafratta, A., Webster, C. L., O’Dea, C. M., Said, N. E., Dunham, N., Inostroza, K., Salinas, C.,
1898 Billingham, S., Phelps, C. M., Campbell, C., Gorham, C., Bernasconi, R., Frouws, A. M., Werner, A., Vitelli, F., Puigcorb ,
1899 V., D’Cruz, A., McMahon, K. M., Robinson, J., Huggett, M. J., McNamara, S., Hyndes, G. A., and Serrano, O.: Global dataset
1900 on seagrass meadow structure, biomass and production, *Earth Syst. Sci. Data*, 15, 511–519, [https://doi.org/10.5194/essd-15-](https://doi.org/10.5194/essd-15-511-2023)
1901 511-2023, 2023.
- 1902 Stukel, M. R., Biard, T., Krause, J., and Ohman, M. D.: Large Phaeodaria in the twilight zone: Their role in the carbon cycle,
1903 *Limnol. Oceanogr.*, 63, 2579–2594, <https://doi.org/10.1002/lno.10961>, 2018.
- 1904 Su, Y., Lundholm, N., and Ellegaard, M.: The effect of different light regimes on diatom frustule silicon concentration, *Algal*
1905 *Res.*, 29, 36–40, <https://doi.org/10.1016/j.algal.2017.11.014>, 2018.
- 1906 Sun, X., M rth, C.-M., Porcelli, D., Kutscher, L., Hirst, C., Murphy, M. J., Maximov, T., Petrov, R. E., Humborg, C., Schmitt,
1907 M., and Andersson, P. S.: Stable silicon isotopic compositions of the Lena River and its tributaries: Implications for silicon
1908 delivery to the Arctic Ocean, *Geochim. Cosmochim. Acta*, 241, 120–133, <https://doi.org/10.1016/j.gca.2018.08.044>, 2018.
- 1909 Sutton, J. N., Varela, D. E., Brzezinski, M. A., and Beucher, C.: Species-dependent silicon isotope fractionation in unialgal
1910 cultures of marine diatoms, AGU Fall Meeting Abstracts, ADS Bibcode: 2011AGUFMPP51B1831S, PP51B-1831, 2011.
- 1911 Sutton, J. N., Varela, D. E., Brzezinski, M. A., and Beucher, C. P.: Species-dependent silicon isotope fractionation by marine
1912 diatoms, *Geochim. Cosmochim. Acta*, 104, 300–309, <https://doi.org/10.1016/j.gca.2012.10.057>, 2013.
- 1913 Suzuki, N. and Not, F.: Biology and Ecology of Radiolaria, in: *Marine Protists: Diversity and Dynamics*, edited by: Ohtsuka,
1914 S., Suzaki, T., Horiguchi, T., Suzuki, N., and Not, F., Springer Japan, Tokyo, 179–222, [https://doi.org/10.1007/978-4-431-](https://doi.org/10.1007/978-4-431-55130-0_8)
1915 55130-0_8, 2015.
- 1916 Swann, G. E. A., Leng, M. J., Juschus, O., Melles, M., Brigham-Grette, J., and Sloane, H. J.: A combined oxygen and silicon
1917 diatom isotope record of Late Quaternary change in Lake El’gygytyn, North East Siberia, *Quat. Sci. Rev.*, 29, 774–786,
1918 <https://doi.org/10.1016/j.quascirev.2009.11.024>, 2010.
- 1919 Taguchi, S. and Laws, E. A.: Application of a single-cell isolation technique to studies of carbon assimilation by the subtropical
1920 silicoflagellate *Dictyocha perlae vis*, *Mar. Ecol. Prog. Ser.*, 23, 251–255, 1985a.
- 1921 Taguchi, S. and Laws, E. A.: Application of a single-cell isolation technique to studies of carbon assimilation by the subtropical
1922 silicoflagellate *Dictyocha perlaevis*, *Mar. Ecol. Prog. Ser.*, 23, 251–255, 1985b.
- 1923 Takahashi, K.: Radiolaria: Sinking population, standing stock, and production rate, *Mar. Micropaleontol.*, 8, 171–181,
1924 [https://doi.org/10.1016/0377-8398\(83\)90022-1](https://doi.org/10.1016/0377-8398(83)90022-1), 1983.
- 1925 Takahashi, K.: Silicoflagellates as productivity indicators: Evidence from long temporal and spatial flux variability responding
1926 to hydrography in the northeastern Pacific, *Glob. Biogeochem. Cycles*, 3, 43–61, <https://doi.org/10.1029/gb003i001p00043>,
1927 1989.
- 1928 Takahashi, K., Onodera, J., and Katsuki, K.: Significant populations of seven-sided *Distephanus* (Silicoflagellata) in the sea-
1929 ice covered environment of the central Arctic Ocean, summer 2004, *Micropaleontology*, 55, 313–325, 2009.

1930 Tesson, B., Lerch, S. J. L., and Hildebrand, M.: Characterization of a New Protein Family Associated With the Silica
 1931 Deposition Vesicle Membrane Enables Genetic Manipulation of Diatom Silica, *Sci. Rep.*, 7, [https://doi.org/10.1038/s41598-](https://doi.org/10.1038/s41598-017-13613-8)
 1932 017-13613-8, 2017.

1933 Thamatrakoln, K. and Hildebrand, M.: Silicon Uptake in Diatoms Revisited: A Model for Saturable and Nonsaturable Uptake
 1934 Kinetics and the Role of Silicon Transporters, *Plant Physiol.*, 146, 1397–1407, <https://doi.org/10.1104/pp.107.107094>, 2008.

1935 Thamatrakoln, K., Alverson, A. J., and Hildebrand, M.: Comparative sequence analysis of diatom silicon transporters: toward
 1936 a mechanistic model of silicon transport, *J. Phycol.*, 42, 822–834, <https://doi.org/10.1111/j.1529-8817.2006.00233.x>, 2006.

1937 de Tombeur, F., Turner, B. L., Laliberté, E., Lambers, H., Mahy, G., Faucon, M.-P., Zemunik, G., and Cornelis, J.-T.: Plants
 1938 sustain the terrestrial silicon cycle during ecosystem retrogression, *Science*, 369, 1245–1248,
 1939 <https://doi.org/10.1126/science.abc0393>, 2020.

1940 de Tombeur, F., Péliissier, R., Shihaan, A., Rahajaharilaza, K., Fort, F., Mahaut, L., Lemoine, T., Thorne, S. J., Hartley, S. E.,
 1941 Luquet, D., Fabre, D., Lambers, H., Morel, J.-B., Ballini, E., and Violle, C.: Growth–defence trade-off in rice: fast-growing
 1942 and acquisitive genotypes have lower expression of genes involved in immunity, *J. Exp. Bot.*, 74, 3094–3103,
 1943 <https://doi.org/10.1093/jxb/erad071>, 2023a.

1944 de Tombeur, F., Raven, J. A., Toussaint, A., Lambers, H., Cooke, J., Hartley, S. E., Johnson, S. N., Coq, S., Katz, O., Schaller,
 1945 J., and Violle, C.: Why do plants silicify?, *Trends Ecol. Evol.*, 38, 275–288, <https://doi.org/10.1016/j.tree.2022.11.002>, 2023b.

1946 de Tombeur, F., Plouzeau, L., Shaw, J., Hodson, M. J., Ranathunge, K., Kotula, J., Hayes, P. E., Tremblay, M., Coq, S., Stein,
 1947 M., Nakamura, R., Wright, I. J., Lambers, H., Violle, C., and Clode, P. L.: Anatomical and Trait Analyses Reveal a Silicon-
 1948 Carbon Trade-Off in the Epidermis of Sedges, *Plant Cell Environ.*, 48, 2396–2410, <https://doi.org/10.1111/pce.15307>, 2025.

1949 Torricella, F., Melis, R., Malinverno, E., Fontolan, G., Bussi, M., Capotondi, L., Del Carlo, P., Di Roberto, A., Geniram, A.,
 1950 Kuhn, G., Khim, B.-K., Morigi, C., Scateni, B., and Colizza, E.: Environmental and Oceanographic Conditions at the
 1951 Continental Margin of the Central Basin, Northwestern Ross Sea (Antarctica) Since the Last Glacial Maximum, *Geosciences*,
 1952 11, 155, <https://doi.org/10.3390/geosciences11040155>, 2021.

1953 Torricella, F., Gamboa Sojo, V. M., Gariboldi, K., Douss, N., Musco, M. E., Caricchi, C., Lucchi, R. G., Carbonara, K., and
 1954 Morigi, C.: Multiproxy investigation of the last 2,000 years BP marine paleoenvironmental record along the western
 1955 Spitsbergen margin, *Arct. Antarct. Alp. Res.*, 54, 562–583, <https://doi.org/10.1080/15230430.2022.2123859>, 2022.

1956 Torricella, F., Morigi, C., Gamboa-Sojo, V., Carbonara, K., Bronzo, L., and Lucchi, R. G.: Paleooceanographic changes along
 1957 the western Spitsbergen margin, evidence from planktic microfossil during the last 10 kyr BP, *Palaeogeogr. Palaeoclimatol.*
 1958 *Palaeoecol.*, 670, 112940, <https://doi.org/10.1016/j.palaeo.2025.112940>, 2025.

1959 Tréguer, P., Nelson, D. M., Van Bennekom, A. J., DeMaster, D. J., Leynaert, A., and Quéguiner, B.: The Silica Balance in the
 1960 World Ocean: A Reestimate, *Science*, 268, 375–379, <https://doi.org/10.1126/science.268.5209.375>, 1995.

1961 Tréguer, P., Bowler, C., Moriceau, B., Dutkiewicz, S., Gehlen, M., Aumont, O., Bittner, L., Dugdale, R., Finkel, Z., Iudicone,
 1962 D., Jahn, O., Guidi, L., Lasbleiz, M., Leblanc, K., Levy, M., and Pondaven, P.: Influence of diatom diversity on the ocean
 1963 biological carbon pump, *Nat. Geosci.*, 11, 27–37, <https://doi.org/10.1038/s41561-017-0028-x>, 2018.

1964 Tréguer, P. J.: The Southern Ocean silica cycle, *Comptes Rendus Géoscience*, 346, 279–286,
 1965 <https://doi.org/10.1016/j.crte.2014.07.003>, 2014.

- 1966 Tréguer, P. J. and De La Rocha, C. L.: The World Ocean Silica Cycle, *Annu. Rev. Mar. Sci.*, 5, 477–501,
1967 <https://doi.org/10.1146/annurev-marine-121211-172346>, 2013.
- 1968 Tréguer, P. J., Sutton, J. N., Brzezinski, M., Charette, M. A., Devries, T., Dutkiewicz, S., Ehlert, C., Hawkings, J., Leynaert,
1969 A., Liu, S. M., Llopió Monferrer, N., López-Acosta, M., Maldonado, M., Rahman, S., Ran, L., and Rouxel, O.: Reviews and
1970 syntheses: The biogeochemical cycle of silicon in the modern ocean, *Biogeosciences*, 18, 1269–1289,
1971 <https://doi.org/10.5194/bg-18-1269-2021>, 2021.
- 1972 Trower, E. J., Strauss, J. V., Sperling, E. A., and Fischer, W. W.: Isotopic analyses of Ordovician–Silurian siliceous skeletons
1973 indicate silica-depleted Paleozoic oceans, *Geobiology*, 19, 460–472, <https://doi.org/10.1111/gbi.12449>, 2021.
- 1974 Van Cappellen, P. and Qiu, L.: Biogenic silica dissolution in sediments of the Southern Ocean. I. Solubility, *Deep Sea Res.*
1975 Part II Top. *Stud. Oceanogr.*, 44, 1109–1128, [https://doi.org/10.1016/s0967-0645\(96\)00113-0](https://doi.org/10.1016/s0967-0645(96)00113-0), 1997.
- 1976 Van Cappellen, P., Dixit, S., and Van Beusekom, J.: Biogenic silica dissolution in the oceans: Reconciling experimental and
1977 field-based dissolution rates, *Glob. Biogeochem. Cycles*, 16, <https://doi.org/10.1029/2001gb001431>, 2002.
- 1978 Van Soest, R. W. M., Boury-Esnault, N., Vacelet, J., Dohrmann, M., Erpenbeck, D., De Voogd, N. J., Santodomingo, N.,
1979 Vanhoorne, B., Kelly, M., and Hooper, J. N. A.: Global Diversity of Sponges (Porifera), *PLoS ONE*, 7, e35105,
1980 <https://doi.org/10.1371/journal.pone.0035105>, 2012.
- 1981 Van Valkenburg, S. D. and Norris, R. E.: The Growth and Morphology of the Silicoflagellate *Dictyocha Fibula* Ehrenberg in
1982 Culture, *J. Phycol.*, 6, 48–54, <https://doi.org/10.1111/j.1529-8817.1970.tb02356.x>, 1970.
- 1983 Varela, D. E., Pride, C. J., and Brzezinski, M. A.: Biological fractionation of silicon isotopes in Southern Ocean surface waters,
1984 *Glob. Biogeochem. Cycles*, 18, <https://doi.org/10.1029/2003GB002140>, 2004.
- 1985 Vaultot, D., Eikrem, W., Viprey, M., and Moreau, H.: The diversity of small eukaryotic phytoplankton ($\leq 3 \mu\text{m}$) in marine
1986 ecosystems, *FEMS Microbiol. Rev.*, 32, 795–820, <https://doi.org/10.1111/j.1574-6976.2008.00121.x>, 2008.
- 1987 Visintini, N., Martiny, A. C., and Flombaum, P.: *Prochlorococcus*, *Synechococcus*, and picoeukaryotic phytoplankton
1988 abundances in the global ocean, *Limnol. Oceanogr. Lett.*, 6, 207–215, <https://doi.org/10.1002/lol2.10188>, 2021.
- 1989 Vonk, J. A., Smulders, F. O. H., Christianen, M. J. A., and Govers, L. L.: Seagrass leaf element content: A global overview,
1990 *Mar. Pollut. Bull.*, 134, 123–133, <https://doi.org/10.1016/j.marpolbul.2017.09.066>, 2018.
- 1991 de Voogd, N., Alvarez, B., Boury-Esnault, N., Cárdenas, P., Díaz, M.-C., Dohrmann, M., Downey, R., Goodwin, C., Hajdu,
1992 E., Hooper, J., Kelly, M., Klautau, M., Lim, S.-C., Manconi, R., Morrow, C., Pinheiro, U., Pisera, A., Ríos, P., Rützler, K.,
1993 Schönberg, C., Turner, T., Vacelet, J., van Soest, R., and Xavier, J.: World Porifera Database. Accessed at
1994 <https://www.marinespecies.org/porifera> on yyyy-mm-dd, <https://doi.org/10.14284/359>, 2025.
- 1995 Vrieling, E. G., Sun, Q., Tian, M., Kooyman, P. J., Gieskes, W. W. C., Van Santen, R. A., and Sommerdijk, N. A. J. M.:
1996 Salinity-dependent diatom biosilicification implies an important role of external ionic strength, *Proc. Natl. Acad. Sci.*, 104,
1997 10441–10446, <https://doi.org/10.1073/pnas.0608980104>, 2007.
- 1998 Wallmann, K., Geilert, S., and Scholz, F.: Chemical Alteration of Riverine Particles in Seawater and Marine Sediments: Effects
1999 on Seawater Composition and Atmospheric CO₂, *Am. J. Sci.*, 323, <https://doi.org/10.2475/001c.87455>, 2023.
- 2000 Wang, Q. and Danilov, S.: A Synthesis of the Upper Arctic Ocean Circulation During 2000–2019: Understanding the Roles
2001 of Wind Forcing and Sea Ice Decline, *Front. Mar. Sci.*, 9, <https://doi.org/10.3389/fmars.2022.863204>, 2022.

- 2002 Wang, X., Schloßmacher, U., Wiens, M., Batel, R., Schröder, H. C., and Müller, W. E. G.: Silicateins, silicatein interactors
2003 and cellular interplay in sponge skeletogenesis: formation of glass fiber-like spicules, *FEBS J.*, 279, 1721–1736,
2004 <https://doi.org/10.1111/j.1742-4658.2012.08533.x>, 2012.
- 2005 Ward, J. P. J., Hendry, K. R., Arndt, S., Faust, J. C., Freitas, F. S., Henley, S. F., Krause, J. W., März, C., Tessin, A. C., and
2006 Airs, R. L.: Benthic silicon cycling in the Arctic Barents Sea: a reaction–transport model study, *Biogeosciences*, 19, 3445–
2007 3467, <https://doi.org/10.5194/bg-19-3445-2022>, 2022.
- 2008 Wei, Y., Qu, K., Cui, Z., and Sun, J.: Picocyanobacteria—A non-negligible group for the export of biomineral silica to ocean
2009 depth, *J. Environ. Manage.*, 342, 118313, <https://doi.org/10.1016/j.jenvman.2023.118313>, 2023.
- 2010 Wenzl, S., Hett, R., Richthammer, P., and Sumper, M.: Silacidins: Highly Acidic Phosphopeptides from Diatom Shells Assist
2011 in Silica Precipitation In Vitro, *Angew. Chem. Int. Ed.*, 47, 1729–1732, <https://doi.org/10.1002/anie.200704994>, 2008.
- 2012 Wetzel, F., de Souza, G. F., and Reynolds, B. C.: What controls silicon isotope fractionation during dissolution of diatom
2013 opal?, *Geochim. Cosmochim. Acta*, 131, 128–137, <https://doi.org/10.1016/j.gca.2014.01.028>, 2014.
- 2014 Wild, B., Gerrits, R., and Bonneville, S.: The contribution of living organisms to rock weathering in the critical zone, *Npj*
2015 *Mater. Degrad.*, 6, <https://doi.org/10.1038/s41529-022-00312-7>, 2022.
- 2016 Wille, M., Sutton, J., Ellwood, M. J., Sambridge, M., Maher, W., Eggins, S., and Kelly, M.: Silicon isotopic fractionation in
2017 marine sponges: A new model for understanding silicon isotopic variations in sponges, *Earth Planet. Sci. Lett.*, 292, 281–289,
2018 <https://doi.org/10.1016/j.epsl.2010.01.036>, 2010.
- 2019 Williams, O. L., Kurtz, A. C., Eagle, M. J., Kroeger, K. D., Tamborski, J. J., and Carey, J. C.: Mechanisms and magnitude of
2020 dissolved silica release from a New England salt marsh, *Biogeochemistry*, 161, 251–271, <https://doi.org/10.1007/s10533-022-00976-y>, 2022.
- 2022 Wörheide, G., Dohrmann, M., Erpenbeck, D., Larroux, C., Maldonado, M., Voigt, O., Borchellini, C., and Lavrov, D. V.:
2023 Deep Phylogeny and Evolution of Sponges (Phylum Porifera), *Adv. Mar. Biol.*, 1–78, <https://doi.org/10.1016/B978-0-12-387787-1.00007-6>, 2012.
- 2025 Wu, X., Yang, S., Wallmann, K., Scholz, F., Dou, Y., Guo, J., and Xu, X.: Strong potassium uptake in surface sediments of
2026 the Changjiang River Estuary and the East China Sea: Implications for authigenic processes and the marine potassium budget,
2027 *Earth Planet. Sci. Lett.*, 657, 119292, <https://doi.org/10.1016/j.epsl.2025.119292>, 2025.
- 2028 Xu, H., Shi, Z., Zhang, X., Pang, M., Pan, K., and Liu, H.: Diatom frustules with different silica contents affect copepod
2029 grazing due to differences in the nanoscale mechanical properties, *Limnol. Oceanogr.*, 66, 3408–3420,
2030 <https://doi.org/10.1002/lno.11887>, 2021.
- 2031 Yacano, M. R., Foster, S. Q., Ray, N. E., Oczkowski, A., Raven, J. A., and Fulweiler, R. W.: Marine macroalgae are an
2032 overlooked sink of silicon in coastal systems, *New Phytol.*, 233, 2330–2336, <https://doi.org/10.1111/nph.17889>, 2021.
- 2033 Yager, J. A., West, A. J., Trower, E. J., Fischer, W. W., Ritterbush, K., Rosas, S., Bottjer, D. J., Celestian, A. J., Berelson, W.
2034 M., and Corsetti, F. A.: Evidence for Low Dissolved Silica in mid-Mesozoic Oceans, *Am. J. Sci.*, 325,
2035 <https://doi.org/10.2475/001c.122691>, 2025.
- 2036 Yamada, K., Yoshikawa, S., Ichinomiya, M., Kuwata, A., Kamiya, M., and Ohki, K.: Effects of Silicon-Limitation on Growth
2037 and Morphology of *Triparma laevis* NIES-2565 (Parnales, Heterokontophyta), *PLOS ONE*, 9, e103289,
2038 <https://doi.org/10.1371/journal.pone.0103289>, 2014.

2039 Zexer, N., Kumar, S., and Elbaum, R.: Silica deposition in plants: scaffolding the mineralization, *Ann. Bot.*, 131, 897–908,
2040 <https://doi.org/10.1093/aob/mcad056>, 2023.

2041 Zhang, L., Wang, R., Chen, M., Liu, J., Zeng, L., Xiang, R., and Zhang, Q.: Biogenic silica in surface sediments of the South
2042 China Sea: Controlling factors and paleoenvironmental implications, *Deep Sea Res. Part II Top. Stud. Oceanogr.*, 122, 142–
2043 152, <https://doi.org/10.1016/j.dsr2.2015.11.008>, 2015.

2044 Zhang, L., Suzuki, N., Nakamura, Y., and Tuji, A.: Modern shallow water radiolarians with photosynthetic microbiota in the
2045 western North Pacific, *Mar. Micropaleontol.*, 139, 1–27, <https://doi.org/10.1016/j.marmicro.2017.10.007>, 2018.

2046 Zhang, Z., Cao, Z., Grasse, P., Dai, M., Gao, L., Kuhnert, H., Gledhill, M., Chiessi, C. M., Doering, K., and Frank, M.:
2047 Dissolved silicon isotope dynamics in large river estuaries, *Geochim. Cosmochim. Acta*, 273, 367–382,
2048 <https://doi.org/10.1016/j.gca.2020.01.028>, 2020a.

2049 Zhang, Z., Sun, X., Dai, M., Cao, Z., Fontorbe, G., and Conley, D. J.: Impact of human disturbance on the biogeochemical
2050 silicon cycle in a coastal sea revealed by silicon isotopes, *Limnol. Oceanogr.*, 65, 515–528, <https://doi.org/10.1002/lno.11320>,
2051 2020b.

2052 Zhu, D., Liu, S. M., Leynaert, A., Tréguer, P., Ren, J., Schoelynck, J., Ma, Y., and Sutton, J. N.: Muddy sediments are an
2053 important potential source of silicon in coastal and continental margin zones, *Mar. Chem.*, 258, 104350,
2054 <https://doi.org/10.1016/j.marchem.2024.104350>, 2024.

2055 Zhu, T., Zhao, S., Xu, B., Liu, D., Cardenas, M. B., Yu, H., Zhang, Y., Chen, X., Xiao, K., Yi, L., Cho, H.-M., Liu, S., Zhang,
2056 Z., Lian, E., Burnett, W. C., Chen, G., Yu, Z., and Santos, I. R.: Large scale submarine groundwater discharge dominates
2057 nutrient inputs to China’s coast, *Nat. Commun.*, 16, 2932, <https://doi.org/10.1038/s41467-025-58103-y>, 2025.

2058 Ziegler, K., Chadwick, O. A., Brzezinski, M. A., and Kelly, E. F.: Natural variations of $\delta^{30}\text{Si}$ ratios during progressive basalt
2059 weathering, Hawaiian Islands, *Geochim. Cosmochim. Acta*, 69, 4597–4610, <https://doi.org/10.1016/j.gca.2005.05.008>, 2005.

2060

2061 **Author contributions.** All authors collaborated on the conception and writing of this manuscript. Author order was determined
2062 randomly using a Python script to reflect the equal contribution of all authors to the work. [Hence, neither the order of authors](#)
2063 [nor the role of corresponding authors is a reflection of their contribution to the work.](#)

2064

2065 **Acknowledgements.** The authors would like to thank the SILICAMICS (Biogeochemistry and Genomics of Silicification and
2066 Silicifiers) and IBIS (Isotopes in Biogenic Silica) communities for fostering such welcoming, open, and intellectually engaging
2067 environments during their 2024 conferences. The vibrant exchange of ideas and collaborative spirit at these events were
2068 instrumental in inspiring and shaping the conception of this manuscript.

2069

2070 **Financial support.** Félix de Tombeur received funding from the European Union’s Horizon 2020 research and innovation
2071 programme under the Marie Skłodowska-Curie grant agreement No. 101021641 (project SiliConomic). Alessandra Petrucciani
2072 received funding from the European Union’s Horizon research and innovation actions programme under grant agreement No.
2073 101083355 (project DESIRED). Natasha Bryan received funding from the Helmholtz Association through INSPIRES Project

2074 ‘Polar-Flow’-[\(2025\)](#). María López-Acosta received funding by a postdoctoral fellowship and project funded by the ‘Xunta de
2075 Galicia’ (IN606C-2023/001). Antonia U. Thielecke received funding from the Helmholtz Association through the Helmholtz
2076 Young Investigator group ‘Side-Effect’ (VH-NG-1600). Natalia Llopis Monferrer received funding from the European
2077 Union’s Horizon Europe research and innovation program under grant agreement No. 101064167 (MSCA postdoctoral
2078 fellowship Si-ORHIGENS). Dongdong Zhu was supported by the China Postdoctoral Science Foundation under Grant No.
2079 2024M753048, and the Qingdao Postdoctoral Grant (QDBSH20240202136).
2080

2081 Boxes

Box 1: Studying biosilicification and Si uptake: from molecular tools to radioisotope enrichment physiological experiments

Biosilicification is the molecular process by which organisms take up silicic acid and transform it into resistant, elastic biomaterials. The study of this process is crucial not only for understanding its biological and ecological significance, but also for unlocking sustainable solutions in material sciences. At the same time, insights gained at the molecular and cellular levels enhance our understanding of the marine Si cycle and improve the accuracy of global biogeochemical models. Recent advances in molecular and single-cell techniques are pushing the frontiers of this field. This toolbox highlights the key technologies currently used to investigate biosilicification.

A central focus in biosilicification research is the identification of molecular markers that signal the presence of this process. Among these, Si transporters are particularly informative. Due to their highly conserved (Hildebrand et al., 1997), these proteins are frequently identified using sequence similarity searches, hidden Markov models, and phylogenetic analyses to detect them in genome and transcriptome datasets (e.g. Durkin et al., 2016; Marron et al., 2016). Functional annotation and expression analyses can help confirm their roles in silicon transport and their regulation across different environmental conditions and taxa. However, silicon transporters are not necessarily the only proteins involved in this complex process. An indirect approach to studying silicification-related genes is to compare RNA transcript levels under limiting and excess silicate availability. By correlating the transcription of unknown genes with that of known silicifying proteins (e.g. Maniscalco et al., 2022; Thamtrakoln and Hildebrand, 2008), it is possible to identify potential candidates involved in silica metabolism. However, this approach is limited to the organisms that can be cultured or maintained in controlled conditions. Beyond genetic analyses, tools such as AlphaFold (Abramson et al., 2024; Mirdita et al., 2022) provide accurate structural predictions of proteins (Jumper et al., 2021). By modelling protein structures, it is possible to study active sites, binding interactions with silica precursors, and the molecular mechanisms driving silica deposition (Knight et al., 2023). Computational simulations and molecular docking further refine these insights by examining protein interactions with silicic acid and other biomolecules. In addition, structural alignment algorithms such as the Foldseek cluster (Barrio-

Hernandez et al., 2023) enable large-scale comparisons, helping to identify domain families and detect remote structural similarities, shedding light on protein function and evolution in diverse organisms. Integrating these predictive approaches with experimental techniques such as electron cryomicroscopy, X-ray crystallography, and biochemical assays strengthens structural interpretations, deepening our understanding of biomineralization processes.

There are also qualitative methods for studying silicification, such as the use of fluorescent compounds. More recent developments have used PDMPO ((2-(4-pyridyl)-5-[(4-(2-dimethylamino-ethylaminocarbamoyl)methoxy)-phenyl]oxazole) in sponges, diatoms, and siliceous Rhizaria (McNair et al., 2015; Ogane et al., 2009; Schröder et al., 2004). This compound is incorporated into newly polymerized bSi under acidic conditions and emits a strong green fluorescence allowing for single-cell and mortality-independent information on silicification and growth rates (Leblanc and Hutchins, 2005; McNair et al., 2015; Shimizu et al., 2001). While this technique is not fully quantitative, these fluorescent markers provide valuable insight into the silicification process, helping to determine the spatial and temporal patterns of silica deposition and offering a deeper understanding of biomineralization dynamics.

The study of radioisotopes and stable isotopes also provides valuable insights into the dynamics of silicification, including uptake mechanisms, intracellular processing, and environmental influences. Silicon stable isotope tracing (^{30}Si) has long been used to simultaneously quantify bSi production and dissolution in the ocean (Fripiat et al., 2007; Nelson and Goering, 1977). Despite the long sample preparation times and complex instrumental analysis required, they offer a powerful tool to understand and quantify nutrient uptake mechanisms, especially when used in conjunction with other stable isotopes such as carbon (^{13}C) or nitrogen (^{15}N -nitrate or ^{15}N -ammonium). Using secondary ion mass spectrometry, it is possible to obtain direct measurements of single cell uptake rates from the same sample (Olofsson et al., 2019). Beyond their use in ecosystem-scale studies, ^{30}Si has also been directly applied to investigate biosilicification pathways. [For instance, Marron et al. \(2019\) explored silicification in cultured choanoflagellates and highlighted potential similarities with sponge pathways, complementing mechanistic modelling of sponge Si isotope fractionation \(Wille et al., 2010; updated by Maldonado and Hendry, 2025\). In vitro experiments have also demonstrated the role of diatom proteins in fractionating Si isotopes, using the R5 peptide as a model for natural biomolecules involved in diatom silicification \(Cassarino et al., 2021\).](#)

Due to its easy applicability and increased sensitivity compared to stable isotopes, Si radioisotope tracing (^{32}Si) has gained increasing popularity in recent decades (Closset et al., 2021; Giesbrecht and Varela, 2021; Krause et al., 2019). It has been successfully applied to a variety of silicifying organisms, beginning with diatoms and later extended to others like Rhizaria (Llopis Monferrer et al., 2020). This technique may also be applicable to other organisms such as silicoflagellates and sponges, that can be maintained under controlled conditions.

Box 2: Siliceous microfossils as markers of past and present oceanic conditions

Siliceous microfossils are widely used to reconstruct past environments, from deep geological times to the recent past. Among these, radiolarians, diatoms, and dinoflagellate cysts are particularly valuable for biostratigraphic studies, especially in environments where carbonate fossils are scarce or poorly preserved (Barron et al., 2014; Carvajal-Landinez et al., 2024; Iwai et al., 2025). Siliceous microfossils also serve as proxies in palaeoclimatic reconstructions, providing insights into water masses and environmental parameters such as sea ice cover, sea surface temperature (SST), and marine productivity (Torricella et al., 2025).

Diatoms play a key role in palaeoceanographic and palaeoclimatic reconstructions, particularly at high latitudes, where carbonate preservation is poor. Their distribution is controlled by surface water parameters including light availability, salinity, nutrient levels, temperature, sea ice extent, and the concentration of dissolved silicic acid (Torricella et al., 2022). Benthic diatoms are also influenced by substrate type and water depth, typically flourishing at around 100 meters where sunlight still reaches the seafloor (Round et al., 1990). Because diatom species occupy well-defined ecological niches, their fossil assemblages can be used to infer past oceanographic variability. However, only about 1-10% of surface-dwelling diatoms are preserved in sediments. Their preservation is affected by silica dissolution during settling and at the seafloor, as well as by lateral transport, bioturbation, grazing, and diagenesis (e.g. Crosta and Koç, 2007; Ran et al., 2024). Despite these challenges, diatom assemblages provide crucial information on past surface ocean and climate conditions across a range of regions, including the Southern Ocean (e.g. Crosta et al., 2021), the Arctic (e.g. Oksman et al., 2019), and mid-latitudes (e.g. Bárcena et al., 2001). Exceptionally well-preserved, laminated diatom oozes — particularly those found in Southern Ocean coastal sites — enable high-resolution reconstructions of palaeoceanographic conditions (e.g. Alley et al., 2018; Leventer et al., 2006; Roseby et al., 2022). Seasonally laminated, diatom-rich sequences allow for annual-scale investigations of productivity and sedimentation processes (e.g. Leventer et al., 1993; Maddison et al., 2006; Pike and Kemp, 1997). In contrast, laminations formed by giant diatoms are often associated with specific oceanographic settings such as frontal systems and nutrient trapping, rather than seasonal cycles (Kemp et al., 2006). Stable isotope analyses have recently been applied to diatoms to strengthen palaeoenvironmental interpretations. Commonly measured isotopes include C and N in diatom-bound organic matter, as well as oxygen and Si in the siliceous frustules (Frings et al., 2024; Robinson et al., 2020; Swann et al., 2010). The oxygen isotope $\delta^{18}\text{O}$ provides information on ice volume, temperature, and regional oceanographic conditions (e.g. Hodell et al., 2001; Shemesh et al., 2001), while $\delta^{30}\text{Si}$ reflects the degree of dSi utilization by comparing uptake rates to ambient concentrations (Cardinal et al., 2005; De La Rocha et al., 1998; Varela et al., 2004). In addition, $\delta^{15}\text{N}$ and $\delta^{13}\text{C}$ serve as proxies for past ocean productivity (Crosta and Shemesh, 2002; Schneider-Mor et al., 2005).

Radiolarians, like diatoms, are widely employed in modern and palaeoceanographic studies due to their sensitivity to changes in SST, thermocline depth, nutrient availability, and water mass distribution (Hernández-Almeida et al., 2017; Zhang et al., 2015, 2018). Their siliceous skeletons are well preserved in sediments and form distinct assemblages that

record past temperature gradients, upwelling intensity, and ocean stratification (e.g. Civel-Mazens et al., 2024). Radiolarians can also serve as valuable palaeoceanographic proxies in regions where other silicifiers, such as diatoms, are rare or poorly preserved, particularly in certain deep-sea or oligotrophic sedimentary environments. Several studies have used both diatom and radiolarian assemblages to quantitatively estimate past sea temperature, salinity, and sea ice extent using transfer function techniques (Chadwick et al., 2022; Civel-Mazens et al., 2023; Crosta and Koç, 2007). These functions are based on three key datasets: (1) the modern species distributions in core-top sediments or water samples, (2) contemporary oceanographic parameters obtained from in situ measurements, and (3) fossil assemblages from sediment cores. A major limitation of this approach is the requirement for comprehensive coverage of all three datasets within the target study region.

Isotopic analyses can also be applied to radiolarians. The Si isotope $\delta^{30}\text{Si}$ is used to reconstruct past dSi concentrations (Doering et al., 2021), while $\delta^{18}\text{O}$ serves as a tracer for water temperature. Robinson et al. (2015) tested $\delta^{15}\text{N}$ measurements on radiolarian tests, finding that it reflects the isotopic composition of their food sources. However, $\delta^{15}\text{N}$ in radiolarians shows significant offsets compared to other siliceous microfossils, emphasizing the need to isolate radiolarian fractions carefully from other organisms. Abelmann et al. (2015) observed that $\delta^{18}\text{O}$ and $\delta^{30}\text{Si}$ from radiolarians and diatoms may not always align with changes in assemblages, but still offer valuable insights into silica uptake by different groups and changes in surface and subsurface water masses (down to ~ 400 m).

Silicoflagellates, though less abundant and less studied than diatoms and radiolarians, are still useful in micropalaeontology as proxies for palaeotemperature and palaeoceanographic reconstructions (e.g. McCartney et al., 2022; Rigual-Hernández et al., 2016; Torricella et al., 2021). Sponges also contribute to siliceous microfossil records, with their spicules commonly preserved in marine sediments. Although assigning isolated spicules to specific sponge taxa is often difficult and sponge-derived material may be scarce in some environments such as abyssal plains, they have been used to infer evolutionary, ecological, and environmental conditions (e.g. De Freitas Oliveira et al., 2020; Sim-Smith et al., 2017). Koltun (1960) first emphasized their utility in reconstructing salinity, temperature, and depth from sedimentary sequences. Sponge spicules now serve as valuable proxies for reconstructing a range of palaeoenvironmental conditions, including water flow regimes and velocities (Kuerten et al., 2013), pH (Pisera and Sáez, 2003), light availability (Harrison, 1974), temperature (Gaino et al., 2012), currents (Molina-Cruz, 1991), salinity (Cumming et al., 1993), and water depth (Łukowiak, 2016). Stable isotope analyses, particularly those focusing on $\delta^{30}\text{Si}$, are increasingly used on sponge silica to investigate Si cycling in ancient oceans (Egan et al., 2012). Sutton et al. (2011) demonstrated that $\delta^{30}\text{Si}$ in sponge spicules offers a more accurate and integrated view of whole-ocean Si cycling than surface-dominated diatom records alone.

In conclusion, siliceous microfossils offer a diverse and powerful set of tools for palaeoenvironmental and palaeoclimatic reconstruction in a range of marine environments. Each group contributes unique ecological and geochemical information: diatoms, silicoflagellates, and radiolarians are particularly valuable for deciphering past surface and subsurface oceanic

conditions, while sponge spicules provide complementary information on deeper water mass properties, benthic environments, and the Si cycle. Recent advances in stable isotope geochemistry have further expanded the potential of these microfossils, allowing for increasingly precise reconstructions of nutrient dynamics, temperature variations and Si utilisation.

2083

Box 3: Trait-based approaches to understand the functions of silicification: are diatoms and plants the same?

Why do species or families invest more in silicification than others? Does silicification involve trade-offs with key ecological strategies? What are the costs and benefits of silicification? In land plants, integrating Si concentrations in trait-based approaches has recently proved useful to answer those fundamental questions about Si utilization (de Tombeur et al., 2023b). The question arises as to whether the same approaches could be used in marine silicifiers such as diatoms. In plants, measuring organ-scale Si concentration is relatively easy and offers a reasonable proxy for the degree of silicification, which can then be linked to other functional traits (de Tombeur et al., 2023a, 2025). In diatoms, we hypothesize that it is probably more the shape of silica-based skeletons that is linked to specific functions and associated trade-offs, and less the bulk diatom Si concentrations per se. As such, using only diatom Si concentrations, as done in plants, may not be sufficient to infer specific functions associated with silicification given the large diversity of silicification patterns. Instead, diatom shapes should be involved in current trait-based frameworks. Beyond silicification, current trait-based approaches in diatoms mostly rely on metabolic traits (e.g. nutrient uptake rates; Ács et al., 2019; Litchman, 2022), and less on morphological and chemical traits that are reasonably easy to measure, as it the case in plants (e.g. leaf thickness, leaf area, leaf N concentration). This major difference explains why trait-based approaches to better understand the role and evolution of silicification will probably not follow the same paths for diatoms and plants. Maintaining a constant dialog between trait-based ecologists working on both types of silicifiers is, however, essential.

2084

Box 4: Silicon natural, stable isotopes as tracers of the marine silica cycle

In the natural environment, Si has three stable isotopes: ^{28}Si , ^{29}Si , and ^{30}Si . The natural isotopic composition, referred to as $\delta^{30}\text{Si}$ when expressed as the $^{30}\text{Si}/^{28}\text{Si}$ ratio relative to a reference standard, serves as a powerful tracer for elucidating the marine Si cycle by recording key processes such as biological uptake, dSi utilization, and diagenetic alteration. In the surface ocean, diatoms preferentially incorporate ^{28}Si when building their opaline frustules, leaving the residual dSi enriched in ^{30}Si (De La Rocha et al., 1997; Sutton et al., 2013). This isotopic fractionation (usually noted $^{30}\epsilon$ or $\Delta^{30}\text{Si}$) offers a window into dSi utilization: higher $\delta^{30}\text{Si}$ values in diatoms signal regions where Si is strongly depleted and efficiently used (Grasse et al., 2020). Consequently, measuring $\delta^{30}\text{Si}$ in sedimentary diatom frustules allows to reconstruct past shifts in nutrient availability and productivity, thereby shedding light on glacial-interglacial transitions and long-term variations in the Si cycle (e.g. De La Rocha et al., 1998; Doering et al., 2016; Egan et al., 2012).

In addition to diatoms, other silicifiers, such as sponges and radiolarians, provide complementary insights into Si cycling across various marine environments. Sponges, as benthic organisms, record Si isotope signatures from deeper water masses. Studies have demonstrated that isotopic fractionation in sponge spicules correlates closely with ambient dSi concentrations, and this relationship appears to be independent of factors like temperature, pH, salinity, or other nutrient levels (Hendry et al., 2010; Hendry and Robinson, 2012; Wille et al., 2010). However, a recent study suggests that the relationship between isotopic fractionation and dSi follows different trends in different sponge classes (Maldonado and Hendry, 2025). Radiolarians, on the other hand, are siliceous protozooplankton that inhabit both surface and deep waters unveiling the potential to reconstruct past dSi concentrations from different water depths (Fontorbe et al., 2016, 2017; Hendry et al., 2014). Current estimates of the isotopic fractionation of radiolarians rely on comparing $\delta^{30}\text{Si}$ values from radiolarians in surface sediments with those of the surrounding water mass (Abelmann et al., 2015; Doering et al., 2021).

Beyond these biological processes, $\delta^{30}\text{Si}$ is also a powerful tool for tracing terrestrial inputs and sedimentary recycling. Generally, silicate mineral weathering on land releases dSi with elevated $\delta^{30}\text{Si}$ compared to primary silicate minerals, due to the formation of isotopically light phases, such as secondary minerals in soils and biogenic phytoliths in vegetation (Baronas et al., 2018; Frings et al., 2021; Ziegler et al., 2005). Within marine sediments, the combined effects of bSi dissolution, silicate mineral dissolution, and authigenic clay formation are also reflected in the isotopic composition of porewaters and the buried silica pool (Closset et al., 2022; Ehlert et al., 2016; Geilert et al., 2020, 2023; Ng et al., 2022). Taken together, these processes underscore the versatility of $\delta^{30}\text{Si}$ as a geochemical tracer for both modern and ancient oceanic Si dynamics.

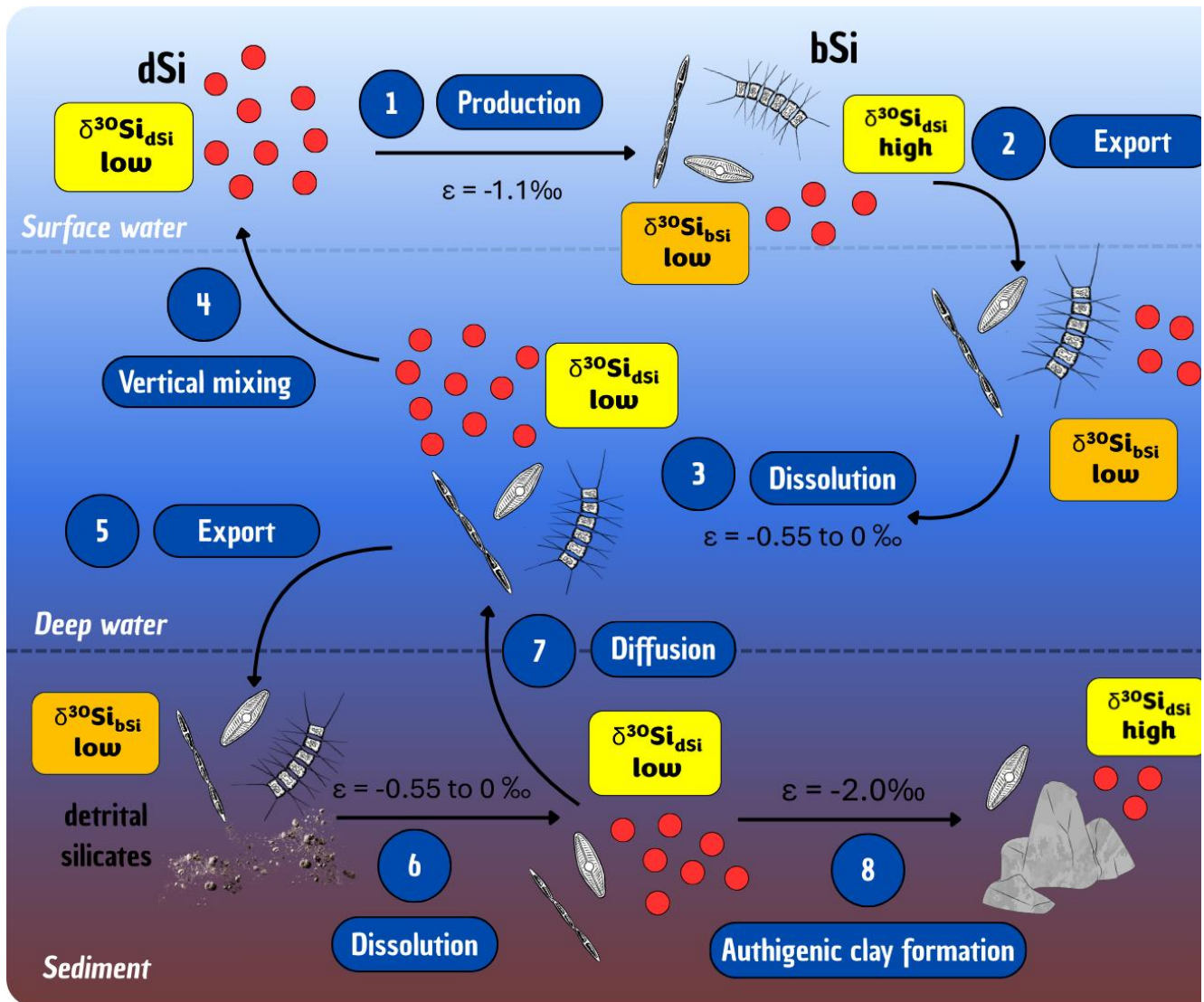


Figure 4. Schematics of the silicon (Si) cycle and isotope fractionation during various oceanic processes, using diatoms as a model for the biogenic silica (bSi) component. The dissolved silica (dSi) pool is depicted by red dots, with its isotopic composition represented by yellow squares. The bSi and detrital silicate pools are illustrated with representative symbols (diatoms, sediments, rocks), and their isotopic composition are shown as orange squares.

Various processes in the ocean affect isotopic fractionation throughout the Si cycle (Fig. 4). During the production of bSi, such as in the case of diatoms in surface waters, organisms preferentially incorporate lighter Si isotopes, raising the isotopic composition (high $\delta^{30}\text{Si}$ value) of the surrounding seawater. Simultaneously, the bSi itself becomes enriched in lighter Si isotopes (low $\delta^{30}\text{Si}$ value; Fig. 4 – 1). At the end of the productive season, the bSi, characterized by its lower $\delta^{30}\text{Si}$ value compared to dSi, is exported to deeper oceanic layers (Fig. 4 – 2). In the deep ocean, bSi undergoes gradual dissolution,

releasing its low $\delta^{30}\text{Si}$ signature back into the surrounding seawater. It remains uncertain whether this dissolution process actively fractionates Si isotopes — specifically, whether the release preferentially favours lighter Si isotopes (as proposed by Demarest et al., 2009) or not (as suggested by Wetzell et al., 2014). Nevertheless, the overall effect of this recycling process is the maintenance of a low $\delta^{30}\text{Si}$ signature in deep waters (**Fig. 4 – 3**). The light $\delta^{30}\text{Si}$ imprint from the deep waters is subsequently transported back to the surface through vertical mixing processes, particularly during winter periods or in upwelling regions, where it becomes available for uptake by new primary producers (**Fig. 4 – 4**). Simultaneously, the bSi that does not undergo further recycling within the water column settles and reaches the sediment (**Fig. 4 – 5**). Upon deposition in the sediment, bSi remains stored over extended timescales, during which it continues to undergo dissolution, releasing its light isotopic composition into the pore or interstitial waters (**Fig. 4 – 6**). These Si-rich pore waters with low $\delta^{30}\text{Si}$ value eventually diffuse back into the overlying bottom waters, contributing to the Si pool in the deeper ocean layers (**Fig. 4 – 7**). Under certain conditions, the dSi in pore waters may precipitate back into a mineral phase, forming authigenic clays. While the mechanisms underlying this process remain poorly understood, evidence suggests that it may involve isotopic fractionation, preferentially incorporating the lighter Si isotope into the newly formed clay minerals, thereby increasing the $\delta^{30}\text{Si}$ of the dissolved phase (**Fig. 4 – 8**).